Durham E-Theses

Electron trapping effects in cadmium sulphide

Cowell, T. A. T.

How to cite:

Cowell, T. A. T. (1968) *Electron trapping effects in cadmium sulphide*, Durham theses, Durham University. Available at Durham E-Theses Online: http://etheses.dur.ac.uk/8696/

Use policy

ELECTRON TRAPPING EFFECTS IN CADMIUM SULPHIDE

by

T. A. T. Cowell B.Sc.

Presented in candidature for the

degree of Doctor of Philosophy of

The University of Durham

August 1968.

TABLE OF CONTENTS

v

ELECTRON TRAPPING EFFECTS IN CADMIUM SULPHIDE

ABSTRACT

This work is an attempt to determine the origin and
behaviour of the defect centres in the forbidden gap of
cadmium sulphide. The methods of measurement used were
thermally stimulated current and infra-red luminescence
techniques. After introductory chapters on semiconductor
theory and the material, cadmium sulphide, the published
results on T.S.C. and infra-red luminescence measurements
are surveyed and analysed. Results are then given for a
series of samples with varying degrees of sulphur doping.
During the work, the need for a more accurate method of
T.S.C. curve analysis arose, and the curve fitting
technique was developed for this purpose. It was found
to have many advantages over existing techniques. The
combination of T.S.C. and infra-red techniques led to
the identification of the centres involved in the infra-
red luminescence. Important traps at 0.48, 0.62 and 0.84
eV below the conduction band are identified, and their
photochemical reactions with the luminescent centres
described. It is shown that the luminescent centres are
identical with the sensitising centres.

ACKNOWLEDGEMENTS

ELECTRONS IN CRYSTALS

1. Introduction

The II-VI compound cadmium sulphide has several possible applications. The most important of these is as a very sensitive radiation detector. Other possible applications include its use for solar batteries, acousto-electric amplification and electroluminescent lamps. Single crystals of cadmium sulphide can have values of resistivity varying over more than ten orders of magnitude, from 10^{12} to 10^{-1} ohm cm., depending upon the deviation from stoichiometry and purity of the samples. The photosensitivity and photo-response time can also vary greatly with purity. In order to have a useful device, it is therefore necessary to know what part the impurities play in controlling or causing the useful property, and also to be able to accurately control the purity of the sample. Any study of a useful property of a material must aim at understanding the mechanism that gives rise to that property. It must try to explain

what parts of the material are involved, and in what way these act. Furthermore, in order to control any property, an attempt must be made to understand the effect of any other constituents of the sample, such as impurity or lack of stoichiometry, upon the mechanism that gives rise to the useful phenomenon. It is the aim of this work to study the behaviour and origin of defects in cadmium sulphide, and the effect that these will have upon its useful properties.

To understand the interesting phenomena that can occur in cadmium sulphide and make it a material worth studying, it is necessary to discuss the behaviour of electrons in crystals in general, and in semiconductors in particular. There are two basic methods of approach to this problem, the tight binding model, and the band theory. The former considers the interaction between the extranuclear electrons as the individual atoms are gradually brought together to form a crystal. The discrete allowed electron energy levels then widen into allowed energy bands. On the other hand, the band theory, (1) (2) which is the method treated here, is concerned with the behaviour of electrons in the periodically changing potential of the crystal lattice.

2. The Band Theory

For the one dimensional case of an electron moving in the x-direction, in a potential V_x, the wave function describing its behaviour is a solution of the differential wave equation, known as Schrodinger's equation:-

$$\frac{\hbar^2}{2m} \frac{\partial^2 \psi}{\partial x^2} = (E - V_x)\psi \qquad \text{eq. 1.1}$$

where $\hbar = h/2\pi$, h = Planck's constant, m = the mass of the particle, and E = the energy of the electron.

In using this equation, the wave-particle duality of nature is assumed, since it is used to describe the behaviour of particles, electrons, in terms of a wavelength λ . This wavelength is related to the momentum of the particle p, by the de Broglie equation:-

$$p = h/\lambda \qquad \text{eq. 1.2}$$

A wave vector k can be defined such that:-

$$k = p/\hbar \qquad \text{eq. 1.3}$$

The principle of duality also allows the energy of the electron to be related to the angular frequency ω, by the expression:-

$$E = \hbar \omega \qquad \text{eq. 1.4}$$

Two important quantities that are associated with these equations are:-

1) the phase velocity $v_f = \omega/k$,   eq. 1.5

2) the group velocity $v_g = d\omega/dk = 1/\hbar . dE/dk$ eq. 1.6

The group velocity represents the velocity of propogation of a wave packet, or narrow band with angular frequencies centred around ω, and as such can be considered as the velocity of an individual electron.

In order to solve Schrödinger's equation, it is necessary to give some value to the potential V_x, in which the particle is moving. For a one dimensional system of periodic potential wells:-

$$V_x = V_{x+a} \qquad \text{eq. 1.7}$$

where a is the periodicity.

Bloch (3) showed that solutions of Schrödinger's equation for a potential of this form, are:-

$$\psi_k(x) = u_k(x) \exp(ikx) \qquad \text{eq. 1.8}$$

$u_k(x)$ is a periodic function of x, of period a, and k, the wave vector, is a constant, which can be used to label the state described by the wave function in eq. 1.8.

In order to obtain specific solutions to the wave equation, some assumptions must be made concerning the shape of the periodic potential. Krönig and Penney (4) investigated a periodic potential variation of the form of fig. 1.1, and then let b shrink to zero, with the
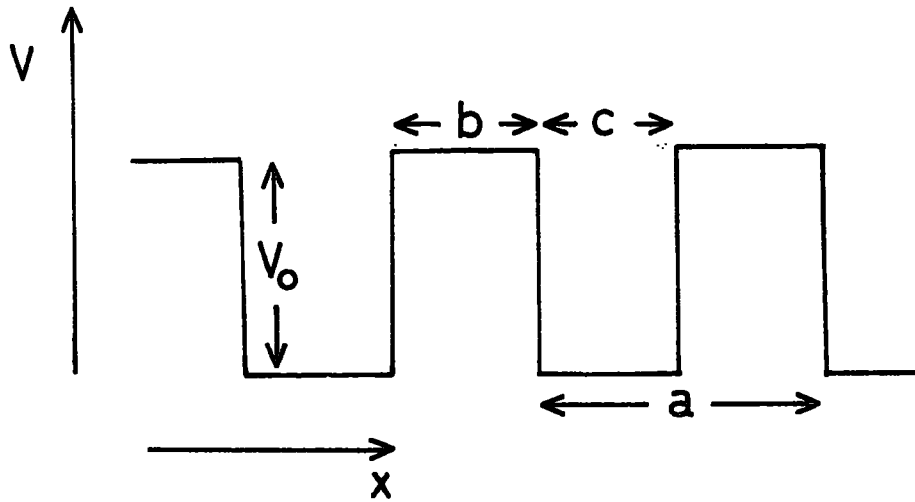
FIG. 1.1.

product $V_o b$ remaining constant = δ

The result of these assumptions is the requirement:-

$$\frac{m\delta a}{\hbar^2} \frac{\sin \alpha a}{\alpha a} + \cos \alpha a = \cos ka \qquad \text{eq. 1.9}$$

where $\alpha = \sqrt{\frac{2mE}{\hbar}}$

The magnitude of δ is a measure of the tightness of binding of the electrons to the atoms. If $\delta = 0$, i.e. $V = 0$, then $\alpha = k$. This is the free electron case, and therefore:-

$$E = \hbar^2 k^2 / 2m \qquad \text{eq. 1.10}$$

A plot of E against k is a parabola for an electron in free space, and there are no restrictions on the allowed values of E.

Fig. 1.2, is a plot of the left hand side of eq. 1.9, for $m \delta a / \hbar^2 = 1$. The values of cos ka, must lie between -1 and $+ 1$, and therefore the allowed values of αa, and thus E, consist of a series of allowed and forbidden bands. Fig. 1.2 shows that the point of transition between allowed and forbidden bands whenever $\alpha a = n\pi$, and for these cases eq. 1.9 reduces to:-

$$\cos \alpha a = \cos ka$$

Therefore transition occurs for values of $k = n\pi/a$. The corresponding plot of E, against k from eq. 1.9 is shown in fig. 1.3, with the parabola for the electron

$$\left(\frac{\sin \alpha a}{\alpha a} + \cos \alpha a \right)$$
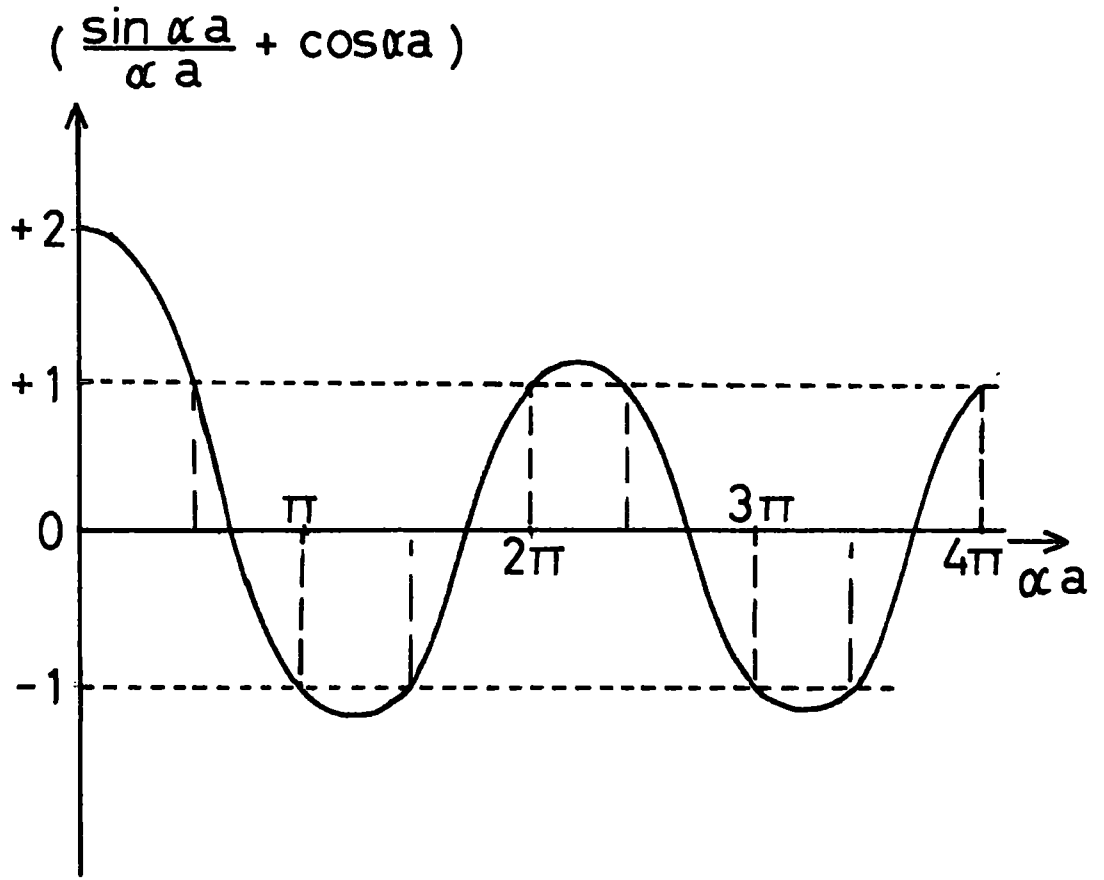
FIG. 1.2.
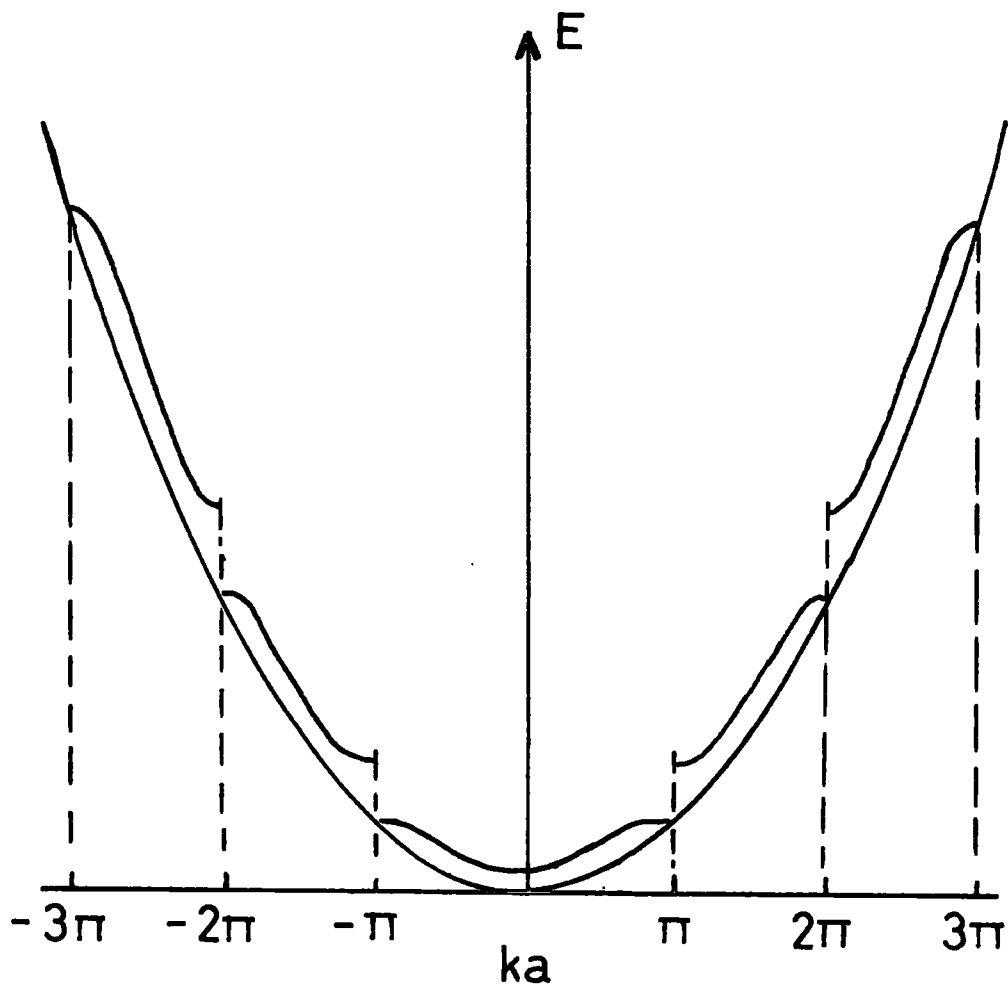
FIG. 1. 3.

in free space for comparison. If increments of $n\pi/a$ are added to k in eq. 1.3 it can be shown that the wave function is unchanged. For this reason, the whole of the E against k diagram can be plotted for values of k between $-\pi/a$ and $+\pi/a$, to give a reduced representation.

The result of the existence of the periodic crystal lattice is that the allowed electron energies are divided up into bands separated by gaps of forbidden energy.

Using eqs. 1.2 and 1.3, and the fact that transition between allowed and forbidden bands occurs for values of $k = n\pi/a$, it is seen that transition occurs for values of:-

$$n\lambda = 2a \qquad\qquad \text{eq. 1.11}$$

This is the value of energy, and thus wavelength, for which Bragg reflection of the electron takes place, according to the reflection law, $n\lambda = 2a\sin\theta$, for the special case of $\theta = \pi/2$.

3. Brillouin Zones

All the previous treatment has been concerned with behaviour in one dimension. In different directions, the periodicity of the lattice can be different, and so Bragg reflection will occur for different values of k. Therefore,

in order to obtain a complete picture of the way an electron will behave in a certain lattice, E must be known as a function of k in three dimensions. If the values of energy for which transition occurs are plotted against k in three dimensions, a model is obtained that consists of volumes of allowed and forbidden values of E in what is called k-space. These volumes are known as Brillouin zones. Their shape depends upon the crystal structure, and can be very complicated.

4. Insulators, Semiconductors and Metals

It is the outermost bands containing electrons that control the electrical properties of a solid. If the uppermost allowed band which contains electrons is completely full, then the electrons cannot absorb small amounts of energy from an applied electric field. The exclusion principle prevents the electrons from moving from one energy to another within the same band, as all the allowed states are completely occupied, and in order to enter the allowed band above it, it is necessary to absorb much larger energies. Because electrons in such a crystal cannot be accelerated by the applied field, the solid is an insulator. For conduction to occur, the electrons must be capable of accepting energy.

If the energy gap between the uppermost filled band and the next highest allowed band is small, of the order of 1 eV, then at room temperature electrons can absorb enough thermal energy to be excited from the top of the filled band, called the valence band, to the empty band above, the conduction band. Once in the conduction band the electron can contribute to electrical conduction, because only small energies are needed to move it between two states in the conduction band, and these states are now empty. More electrons are excited to the conduction band, the higher the temperature of the solid, so that electrical conductivity increases with temperature. Such a solid is an intrinsic semiconductor. The unoccupied state in k-space left in the valence band by the excitation of an electron to the conduction band, allows some contribution to be made to conduction by the electrons remaining in the valence band. There now exists a state to which adjacent electrons can be excited by relatively small energies. As an electron moves in one direction to occupy the vacant state, it leaves a vacant state behind, and the result is that the "hole" moves in the opposite direction. The collective movement of the electrons in the valence band can be considered as the movement of a

hole in the opposite direction. The hole behaves as a positive charge, of equal magnitude to the charge of the electron.

In metals the uppermost band containing electrons is only partially filled, so that the electrons can easily absorb small increases in energy, and thus contribute to conduction. In some anisotropic metals the band structure is different in different directions, and, although the top band should be empty, the valence band in one direction overlaps the conduction band in another. Some of the electrons from the valence band fill sites in the conduction band, as these are at a lower energy, and the crystal, by virtue of these partially filled bands; can conduct electricity. The difference between a metal and a semiconductor is that at absolute zero of temperature, the metal will have electrons in the conduction band so that the material can conduct, whilst the semiconductor, at this temperature has an empty conduction band and cannot conduct.

5.   Effective Mass

An electron in a crystal is subject to forces from the crystal lattice, as well as external forces, so that the equation of motion, $F = m.dv/dt$, cannot be applied

if F is the externally applied force only. For this reason it is convenient to define an effective mass, m*, that is found to obey this kind of relationship.

If a force F acts upon an electron, then the rate of change of momentum that it produces, is equal to that force. That is:-

$$F = dp/dt \qquad \text{eq. 1.12}$$

From eq. 1.3, $p= \hbar k$, and therefore:-

$$F = \hbar . dk/dt \qquad \text{eq. 1.13}$$

But from eq. 1.6, the group velocity is:-

$$v_g = 1/\hbar . \; dE/dk$$

If an effective mass, m*, is now defined such that:-

$$dv_g/dt = F/m* \qquad \text{eq. 1.14}$$

equation 1.14, can now be rewritten, using eqs. 1.6 and 1.13:-

$$\frac{F}{m*} = \frac{1}{\hbar} . \frac{d^2E}{dk^2} . \frac{dk}{dt} = \frac{F}{\hbar^2} . \frac{d^2E}{dk^2} \qquad \text{eq. 1.15}$$

This leads to the value of m*

$$m* = \hbar^2 / \frac{d^2E}{dk^2} \qquad \text{eq. 1.16}$$

From the E against k diagram it can be seen that near the top of a band m* will be negative, and near the bottom of the band it will be positive. The meaning of negative effective mass is that the acceleration produced

by a force is in the opposite direction to that force. This is another way of looking at the holes previously mentioned. Instead of considering electrons with negative charge and negative mass, one can think in terms of holes with positive charge and positive mass.

The effective mass is a parameter that allows one to consider electrons and holes as if they were free inside the lattice. It is an extremely useful concept, since it reduces to manageable terms the results of the very complex interactions of the charge carriers with the lattice.

In eq. 1.16, the effective mass has been deduced for simple spherical band surfaces. More generally it should be written in the form of a tensor:-

$$(1/m^*)_{\alpha,\beta} = \frac{1}{\hbar^2} \frac{d^2 E}{dk_\alpha \, dk_\beta} \quad (\alpha, \beta = x, y, z,) \quad \text{eq.1.17}$$

It can be seen that evaluation of m*, could give much information about the shape of the energy bands. The most direct way of measuring m* is by the method of cyclotron resonance. The equations of motion for an electron moving in a constant magnetic field of induction B along the z-axis are:-

$$\left.\begin{array}{l} m^* \dot{v}_x = -eBv_y \\ m^* \dot{v}_y = eBv_x \\ \dot{v}_z = 0 \end{array}\right\} \quad \text{eq. 1.18}$$

If v_z is initially zero, the particle describes a circle in the x-y plane, and:-

$$m*v^2/r = Bev \qquad \text{eq. 1.19}$$

where r is the radius of the circle. The electron describes the circle with frequency:-

$$\nu_c = Be/2 \,\pi\, m* \qquad \text{eq. 1.20}$$

which is independent of the radius of the circle. This frequency may be determined by the application of a small radio frequency field, and determination of the value of B at which resonance occurs. This gives directly a value of m*. (5) (6).

6. <u>Energy Levels in the Forbidden Gap</u>

If the periodicity of the crystal lattice is disturbed, then localised energy levels can be found in the forbidden gap. The main causes of cyrstal imperfections are:-

      a. impurities

      b. vacancies

      c. dislocations

      d. interstitial atoms

      e. the existence of a surface

If one considers a group I ion M^+ substituted for Cd^{++} in CdS, one has a localised site around which there is a lack of positive charge. The result of this will be to reduce the energy needed to remove an electron from a nearby S^{--} ion to the conduction band. This can be considered as a localised site just above the valence band by an amount equal to the decrease in energy needed to release an electron. Once this site has lost an electron to the conduction band it can easily accept an electron from the valence band since it is separated from it by only a small energy. Because it can so easily accept electrons from the valence band, this site is called an acceptor. When electrons are excited to such acceptor levels, holes remain in the valence band. The holes promote electrical conduction, and because the charge carriers are positively charged, the semiconductor is referred to as p-type.

Substitution of a cation M^{+++} for cadmium in CdS means that near the site one of the three valence electrons of the cation is very loosely bound to the spare positive charge of the ion. This exists as a site just below the conduction band, and is called a donor because the extra electron can easily be raised to that band. A semiconductor

containing donor centres is described as n-type.

Similar arguments can be used to show that the other types of crystal imperfection can produce discrete energy levels which lie in the forbidden gap.

Rather different localised levels in the forbidden gap are those due to excitons. An electron excited from the valence band to the conduction band has a coulombic attraction for the hole it leaves behind. The two can become bound together without recombining, and have allowed energy levels analogous to the levels of an electron around a hydrogen atom. Such an entity is an exciton, and it can lead to energy levels in the forbidden gap. These centres are different from the others, since normally the electrons and holes only determine the occupancy of a site, but in the case of excitons they are the cause of the energy levels. An electron in its ground state exists in the valence band of a semiconductor, so that if it becomes excited to form an exciton with the hole it leaves behind, then it will have an energy value within the forbidden gap. Between the lowest value of energy for the exciton, its ground state, and the conduction band, there will be an infinitive number of possible levels which approach the bottom of the conduction band in the same way as the electronic energy

levels in a hydrogen atom approach the energy value
of an electron in free space.

7. The Fermi Level

To determine the density of carriers in a band
with energies within the range E to E+dE, it is
necessary to know, firstly, the density of allowed
states, N(E)dE in that range, and secondly, the
probability of their being filled, f(E).

The number of carriers n per cm^3, between energies
E_1 and E_2 is then:-

$$n = \int_{E_2}^{E_1} f(E) \ N(E) \ dE \qquad \qquad eq. \ 1.21$$

The probability function f(E), is the Fermi-Dirac
distribution function:-

$$f(E) = \frac{1}{\exp(E - E_F)/kT + 1} \qquad \qquad eq. \ 1.22$$

where k = Boltzmann's constant, T = absolute
temperature and E_F is called the Fermi energy. If
$E = E_F$, $f(E) = \frac{1}{2}$, and therefore the Fermi energy can be
considered as the energy at which a state has an equal
chance of being empty or filled.

To be able to evaluate N(E) dE, it is necessary to
know the form of the appropriate part of the E against

k diagram. If one assumes that a cubic crystal has a conduction band minimum and a valence band maximum at k = 0, then for small values energy into either of these bands, it can be assumed that the shape of the E against k figure in three dimensions is spherical, and that the hole and electron effective masses are scalar. If the energy zero is taken as the bottom of the conduction band, and E_G is the width of the energy gap, then:-

$$N(E)dE = 2\pi(2m_e^*)^{3/2} h^{-3} E^{\frac{1}{2}} dE \qquad \text{eq. 1.23}$$

for the conduction band, where m_e^* is the electron effective mass. For the distribution of states in the valence band the appropriate expression is:-

$$N(E)dE = 2\pi(2m^*)^{3/2} h^{-3} (-E_G - E)^{\frac{1}{2}} dE \qquad \text{eq. 1.24}$$

To determine the concentration n, of electrons in the conduction band, eqs. 1.22 and 1.23 are substituted in eq. 1.21, and the limits zero and infinity are taken for the integral:-

$$n = 4\pi(2m_e^*)^{3/2} h^{-3} \int_0^\infty \frac{E^{\frac{1}{2}} dE}{\left[\exp(E - E_F)/kT\right]} \qquad \text{eq.1.25}$$

To obtain eq. 1.25 it was assumed that $(E - E_F) \gg kT$.

This means that:-

a. it is permitted to take eq. 1.23 as valid
   for all E,

b. infinity can be taken as the upper limit
   of the integral,

c. the Fermi-Dirac distribution reduces to
   the Boltzmann distribution:-

$$f(E) = \frac{1}{\exp\left[(E - E_F)/kT\right]} \qquad \text{eq. 1.26}$$

Integration of eq. 1.25 gives:-

$$n = N_c \exp\left[(E_F)/kT\right] \qquad \text{eq. 1.27}$$

and similarly for holes:-

$$p = N_v \exp\left[-(E_F + E_G)/kT\right] \qquad \text{eq. 1.28}$$

Where $N_{c,v} =$

$$2(2\pi m_{e,h} kT/h^2)^{3/2} \qquad \text{eq. 1.29}$$

and is the effective density of states in the
conduction (valence) band.

These equations define the position of the Fermi
level if p or n are known. For a semiconductor with
no donors or acceptors, which is an intrinsic semiconductor,
n = p, since holes and electrons are created in pairs, and
the Fermi level is given by:-

$$E_F = -E_G/2 + \frac{3kT}{4} \ln\left(m_h^*/m_e^*\right) \qquad \text{eq. 1.30}$$

As long as m_h^* is not very different from m_e^*, intrinsic semiconductors have a Fermi level near the centre of the forbidden gap. For materials containing impurities the Fermi level can be shifted either way. A semiconductor that is predominately n-type has a Fermi level nearer the conduction band. Since E_F is the only parameter of eqs. 1.27 and 1.28 that is not a property of the crystal lattice, the Fermi level defines the extent to which the material is n- or p-type. E can be eliminated from these two equations to give:-

$$n\,p = N_c N_v \exp(-E_G/kT) \qquad \text{eq. 1.31}$$

This expression holds true for all specimens of a given material. It means that the product np is a property of the material, and does not depend upon impurity concentrations.

8. Conductivity

Electrons and holes in an ideal lattice under the influence of a force F, would move unhindered according to eq. 1.13. This means that the carriers would oscillate around fixed centres whilst repeatedly crossing the Brillouin zone, leaving it, and reappearing at the other side. The result would be that no energy would be absorbed, and the direct current conductivity would be zero. Real

semiconductors contain defects and impurities that
spoil the regularity of the lattice, and these
irregularities cause carriers to lose their momentum
due to several mechanisms. Because of these defects,
the electrons can now absorb energy, and can therefore
contribute to conduction. The electrons have an average
drift velocity v_d which is equal to zero if no external
force is applied. In the presence of an external force,
the net drift velocity is produced which is equivalent
to a displaced distribution of carriers. In order to
give some quantitative value to the collision process
that allows the carrier to absorb energy, it is assumed
that the average time between collisions is a constant, τ .
This is called the relaxation time. This is equivalent
to saying that any disturbance from equilibrium dies out
exponentially, or:-

$$v_d(t) = v_d(0).\exp(-t/\tau) \qquad \text{eq. 1.32}$$

With a finite value of relaxation time, the equation
of motion in a constant electric field E_e, is:-

$$m^*(\, dv/dt + v_d/\tau \,) = eE_e \qquad \text{eq. 1.33}$$

The solution of this equation is:-

$$v_d = e \, \tau \, E_e/m^* \qquad \text{eq. 1.34}$$

- 19 -

The electric current density, j, is the electric charge carried through unit area in unit time. If n is the number of electrons per unit volume, then:-

$$j = nev_d \qquad \text{eq. 1.35}$$

This leads to:-

$$j = ne^2 E_e/m^* \qquad \text{eq. 1.36}$$

Electrical conductivity is defined by the equation:-

$$j = \sigma E_e \qquad \text{eq. 1.37}$$

Therefore the conductivity σ, is given by:-

$$\sigma = ne^2 \tau/m^* \qquad \text{eq. 1.38}$$

The conductivity is proportional to the charge density ne, and also to the time between collisions. The factor e/m^* enters because the acceleration in a field is proportional to the electronic charge, and inversely proportional to the mass m^*. A carrier mobility can be defined such that:-

$$\sigma = ne\mu \qquad \text{eq. 1.39}$$

where $\mu = e\tau/m^* \qquad \text{eq. 1.40}$

The mobility describes the contribution of the crystal lattice to the conductivity, since n can be a variable, but τ and m^* depend upon the properties of the sample. The mobility is defined as drift velocity

per unit electric field, since it can be rewritten in the form:-

$$\mu = v_d/E_e \qquad \text{eq. 1.41}$$

Eq. 1.39 applies to the conductivity due to one type of carrier only, the electron. To allow for the possibility of conduction by holes, this is rewritten:-

$$\sigma = ne\mu_e + pe\mu_p \qquad \text{eq. 1.42}$$

where p is the density of holes, and μ_p is called the hole mobility.

The effects that can cause carrier scattering, and therefore affect the value of mobility, include:-

    a.   thermal lattice vibrations

    b.   ionised impurities

    c.   dislocations and grain boundaries

    d.   other carriers

    e.   neutral impurities.

8.a.   Thermal Lattice Vibrations

As the carriers travel through the crystal at a
temperature above absolute zero, they have their
mobility reduced by interaction with the thermal
vibration of the lattice. The lattice can vibrate
in both acoustic and optical modes. For covalent
elemental semiconductors the interaction with the
acoustic mode is the most important factor effecting
the mobility. It is found that (7):-

$$\mu \propto T^{-3/2}/m*^{5/2} \qquad\qquad \text{eq. 1.43}$$

It can be seen this effect will be important
at higher temperatures.

For compound semiconductors, the movement of the
different constituent atoms cause dipoles in the
crystal that can interact strongly with the carriers.
The dependence of mobility upon temperature for
optical mode lattice scattering is found to be(8):-

$$\mu \propto \exp T / m*^{3/2} \qquad\qquad \text{eq. 1.44}$$

8.b.   Ionised Impurities

Large scattering effects can occur as a result of
charged impurity scattering. The importance of this
effect will obviously depend upon the density of the

impurities. The scattering due to this process gives
a mobility dependence upon temperature (9):-

$$\mu \propto T^{3/2}/m*^{\frac{1}{2}}$$
eq. 1.45

8.c. Dislocations and Grain Boundaries

The scattering caused by these defects that exist
on a larger than atomic scale are relative unimportant.
The temperature variation of mobility is found to be
linear.

8.d. Carrier-carrier Scattering

The scattering of carriers by other electrons and
holes is difficult to analyse because of screening
effects that occur at the high current densities at
which carrier carrier scattering is important. The
effect of the scattering upon the mobility will also
depend upon the mode of thermal scattering dominant
at lower carrier densities.

8.e. Neutral Impurities

Neutral impurity scattering is relatively
unimportant, and is found to be almost independent of
temperature.

The thermal vibration aspect of mobility will
be important at high temperatures, whilst the charged
impurity scattering will predominate at low temperatures.
The importance of dislocations at any temperature
depends upon their density. Neutral impurity
scattering shows very little temperature dependence,
and carrier-carrier scattering is only important at
very high carrier densities.

References for Chapter One

1. Smith R.A., 1961, Semiconductors, Cambridge
   University Press.

2. Bube R.H., 1960, Photoconductivity of Solids,
   J. Wiley & Sons, Inc.

3. Bloch F., 1928, Z. Phys., 52, 555

4. Kronig R. de L., Penney W.G., 1931, Proc. Roy.
   Soc., 130A, 499

5. Dorfman J.G., 1951, C.R. Acad. Sci. U.R.S.S.,
   81, 765.

6. Dresselhaus G., Kip A.F. & Kittel C., 1953,
   Phys. Rev. 92, 827

7. Bardeen F. & Shockley W., 1950, Phys. Rev.,
   77, 407.

8. Ehrenreich H., 1957, J. Phys. Chem. Sol.,
   2, 131

9. Brooks H., 1955, Advances in Electronics and
   Electron Physics, 7, 85

CHAPTER TWO

CADMIUM SULPHIDE

1. Introduction

        Cadmium sulphide is one of the group II-VI compounds
that are in general wide band gap semiconductors or semi-
insulators. Conduction in cadmium sulphide is nearly
always n-type. The only p-type conduction observed has
been in heavily doped samples in which it is thought
that conduction is in impurity bands in the forbidden
gap. The refractive index of cadmium sulphide is 2.6
at a wavelength of 5000 $\overset{o}{A}$, and its low frequency
dielectric constant is 11.6.

2. Band Gap of Cadmium Sulphide

        The band gap of a semiconducting or insulating
material can be measured by several basic methods.
These include the determination of the free carrier
density as a function of temperature, and the study of
photoconductivity, absorption or luminescence as a
function of incident wavelength. Cadmium sulphide is
found to give a value around 2.4 eV for all these

methods at room temperature (1)(2)(3). The temperature
variation of band gap E_G, is found to be of the form:-

$$E_G = E_{Go} - \left(5.2 \times 10^{-4} \times T\right) \qquad \text{eq. 2.1}$$

This variation is due to both the change in
temperature, and the expansion of the crystal due to
increased temperature (4)(5).

3. <u>Mobility and Effective Mass</u>

The electron mobility in cadmium sulphide is found
to depend strongly upon the purity of the sample, so
that higher values of mobility are continually being
quoted, as it becomes possible to produce purer specimens.
The temperature dependence of mobility suggests that the
principle scattering mechanisms are optical and piezo-
electric acoustic mode lattice scattering. Values of
mobility vary from 250 cm^2/ volt sec. at room temperature,
to 10^4 cm^2/ volt sec. at 44°K. (6)(7)(8). Zook and
Dexter (9) determined the ratio of the mobilities
parallel and perpendicular to the c-axis, μ_1/μ_3, and
found a value of 1.3 at 77°K. This anisotropy in
mobility also supports the idea that piezo-electric
scattering is one of the principle scattering mechanisms.

Hopfield and Thomas (10) determined an electron effective mass value of m* = $(0.204 \pm 0.010)m_e$, from a study of the exciton absorption and reflection spectra of cadmium sulphide. Piper and Marple (11) obtained a similar value, m* = $(0.22 \pm 0.01)m_e$, from a study of the free electron absorption in the infra-red spectrum. The structure of the conduction band minimum has thus been well established as being characterised by an effective mass m* = $0.21\ m_e$. There is some doubt as to whether this is isotropic or not, for although a fairly consistent small anisotropy has been found, it is generally less than the experimental error.

4. The Electro-acoustic Effect

The most important electron scattering mechanism in cadmium sulphide is piezo-electric acoustic mode lattice scattering. This means that the carriers are scattered by their interaction with the strong electric fields of piezo-electric origin. (12). If an electric field is applied to a crystal of cadmium sulphide, the sample obeys ohm's law at low fields. As the field is increased, the carriers interact more strongly with the

piezo-electric fields, and eventually a current
saturation is observed, when the carrier drift
velocity equals the acoustic wave velocity (13).
Instead of accelerating the carriers, the energy of
the applied field becomes ultrasonic energy, and
ultrasonic waves are seen to build up as the current
saturates. An acoustic wave flux is created. This
consists of a spectrum of frequencies, although only
a narrow band of this is observed, since the detecting
transducers are tuned to a single frequency. Instead
of allowing this flux to build up, Hutson et al. (14)
applied an ultrasonic signal to the sample, and observed
the effect of high drift fields upon it. It was found
the amplification of the acoustic signal could be
obtained for large applied fields. In this case the
drift field energy is transferred to the applied
ultrasonic signal, when the drift velocity of the
carriers becomes larger than the acoustic wave velocity.
Gains of 38 dB at 45 Mc/s were reported in a 7 cm.
length of cadmium sulphide. A radio frequency signal
is applied to the sample through a quartz transducer,
and the ultrasonic signal is detected by a second
transducer at the other end of the sample. Although

the ultrasonic signal amplification may be quite
large, the losses that occur in the transducers are
so great that overall amplification of the RF signal
is not possible. Work is being done on the possibility
of using evaporated films of cadmium sulphide as
transducers (15). These should show much greater
efficiency than the mechanically applied quartz
transducers used at present.

5. Cadmium Sulphide as a Photoconductor

Cadmium Sulphide is an extremely sensitive
photoconductor. (The mechanics of photoconductivity
in CdS is treated in Chapter Five). It is used in
some cameras as a light meter, and can be used for
X-ray and γ-ray detection. It can operate at high
enough power levels to be used directly in relay circuits
without amplification, and can thus be used for such
devices as simple burglar alarms and automatic headlight
dippers. A limitation in the use of CdS for radiation
detection is that it has a very slow response to X-rays
and γ-rays. It can, however, be used as a quantum
counter, since the material can be made to show current
spikes, corresponding to the passage of high energy

photons through the bulk of the device. Extremely small detectors can be produced, and as such can be used for medical purposes, e.g. there is a requirement for a sensitive probe, small enough to be placed inside the body, and left there, in order to monitor continuously the amount of radioactive material in any particular organ.

Cadmium sulphide can be treated to render it sensitive to infra-red radiation. Since it has a band gap of 2.4 eV, this seems surprising, but electrons can be excited to the conduction band by a two stage process. One excitation takes an electron from the valence band to a defect centre in the forbidden gap, and a second excitation can take it to the conduction band where it can be detected. The electrons excited to the conduction band by this process can, under some circumstances, recombine to give green band gap radiation. If such a mechanism could be properly controlled, it could be the basis of a very useful image converter, changing directly an infra-red signal to a visible output.

The disadvantages of cadmium sulphide as a photodetector are twofold. Firstly, although very high sensitivities are possible, these are accompanied by a pronounced increase in response time. Secondly, for very sensitive material it is found to be difficult to obtain good stability. The photoresponse is found to vary greatly both with time and with the illumination that the sample has received.

6. The Cadmium Sulphide Solar Cell

An evaporated film of cadmium sulphide on p-type copper sulphide forms a p-n junction that is the basis of a good photovoltaic cell. Efficiencies of 6% over quite large areas (50 cm^2) have been reported (16). Cadmium sulphide-silicon heterojunctions have also been used. Shirland (17) has written a review of the use of cadmium sulphide for solar cells, and has summarised the present state of the art, and future possibilities.

7. The Thin Film Transistor

The cadmium sulphide thin film transistor is a field effect transistor. It consists of a strip of cadmium sulphide, about ten microns wide evaporated on to a glass

substrate, with a contact evaporated on to either side (source and drain). The conductivity is modulated by a third electrode (gate). De Graaff and Koelmans (18) have constructed transistors with an input resistance of 10^4 megohms, covering an area of only 0.02 mm^2. Power amplification was found to be possible up to 200 Mc/s. At present, however, the spread in properties from device to device is too large for economic production. A second disadvantage of the device is that its properties tend to show hysteresis effects.

8. Cadmium Sulphide Laser

Electroluminescent cadmium sulphide emits radiation in the middle of the visible region of the spectrum. Since it is very desirable to have a solid state laser in the visible region, cadmium sulphide would seem a promising material to work on. However, because of the high density of electron traps that exist in cadmium sulphide, it is extremely difficult to obtain the population inversion that is needed for lasing action. Basov et al. have obtained lasing for both electron bombardment pumping (19) (200 keV electron beam, at 1 amp/cm^2), and for optical pumping (20). Lasing was observed at three wavelengths, 5035, 4966 and 4891 Å.

Hurwitz (21) observed lasing at 4900 Å in cadmium rich samples, and obtained a power output of 350 watts. The overall efficiency was 26.5% at 110^OK which was equivalent to an internal efficiency of 35%. He also obtained lasing action up to a temperature of 350^OK. This high efficiency was thought to be due to very good crystal uniformity, and to the high efficiency of the radiative transition through the recombination centres introduced by the cadmium rich growth conditions.

References for Chapter Two.

1. Gross E.F. & Yakobson M.A., 1955, Zhur, Tekh. Fiz.

    U.S.S.R. $\underline{25}$, 364.

2. Gross E.F. & Yakobson M.A., 1955, Doklady Akad.

    Nauk. S.S.S.R., $\underline{102}$, 485

3. Smith R.W., 1957, Phys. Rev., $\underline{105}$, 900

4. Hohler G., 1949, Ann. Physik, $\underline{4}$, 371

5. Piper W.W., Marple D.F.T. & Johnson, 1958, Phys.

    Rev. $\underline{110}$, 323

6. Smith R.W., 1951, R.C.A. Review, $\underline{12}$, 350

7. Bube R.H., 1956, J.A.P., $\underline{27}$, 1237

8. Moore A.R., Smith R.W.., 1965, Phys. Rev., $\underline{188}$, 1250

9. Zook J.D. & Dexter R.N., 1963, Phys. Rev., $\underline{129}$, 1980

10. Hopfield J.J. & Thomas D.G., 1961, Phys. Rev., $\underline{122}$, 35

11. Piper W.W. and Marple D.F.T.., 1961, J.A.P.., $\underline{32}$, 2292

12. Hutson A.R., 1960, Phys. Rev. Letters, $\underline{4}$, 505

13. Smith R.W., 1962, Phys. Rev. Letters, $\underline{9}$, 87

14. Hutson, A.R.; McFee J.H. & White D.L., 1961, Phys.

    Rev. Letters, $\underline{7}$, 237

15. Foster N.F., 1965, Proc. I.E.E.E.., $\underline{10}$, 1400

16. Hill E.R. & Keramidas B.G., 1966, Rev. Phys.Appl., $\underline{1}$, 189

17. Shirland F.A., 1966, Adv. Energy Conversion, $\underline{6}$, 201

18. De Graaff H.C. & Koelmans H., 1966, Philips

    Tech. Rev., $\underline{27}$, 200

19. Basov N.G., Bogdankevich O.V. & Devyatkov A.G.,

    1965, Sov. Phys. J.E.T.P., $\underline{20}$, 4.

20. Basov N.G., Grasuik A.Z., Efimkov V.F. & Zubarev I.G.,

    1966, J. Phys. Soc. Jap., $\underline{21}$, 277

21. Hurwitz C.E., 1966, Appl. Phys. Letters, $\underline{9}$, 420

CHAPTER THREE

THERMALLY STIMULATED CURRENTS

1. Introduction

An important method of detecting and studying trapping centres in a semi-insulator, is to study its conductivity or luminescence as filled traps are emptied thermally be raising the temperature of the sample. Strong illumination at liquid nitrogen temperatures raises the electron Fermi level so that electrons excited into the conduction band from the valence band can fall into trapping centres and remain trapped. If, after equilibrium has been reached, the exciting radiation is removed, then most of the electrons in the conduction band return to the valence band through recombination centres. When the sample is heated up, the electrons in the shallowest filled traps will first acquire enough thermal energy to be released from the traps to the conduction band. As these electrons can now contribute to conduction, they can be detected by monitoring the current through the crystal under a fixed potential difference. They can also be detected by the luminescence that may be emitted as the electrons return

to the valence band through recombination centres. As
the temperature is increased further, the deeper traps
will be emptied; and for each set of discrete traps
there will be a corresponding peak in the conductivity.
A plot of conductivity against temperature under these
conditions is called a thermally stimulated current
curve. If the luminescence is measured as the temperature
is raised, it is known as the method of thermal glow.

Determination of depth, capture cross-section and
density of traps from thermally stimulated current curves
is not a straightforward process for several reasons. One
difficulty is that the shape of the T.S.C. curve depends
on the extent to which electrons are retrapped after
excitation, and an equation to describe the curve can
only be derived for three special cases. Another difficulty
is that further simplifications need to be made before
expressions for the trap parameters can be obtained from
these equations. Many different methods have been proposed
for obtaining the appropriate values, but as these depend
upon different approximations, it is not surprising that
quite large discrepancies can be found between them.

2. Kinetics of Trap Emptying

An electron excited thermally from a trap to the conduction band can either return to the valence band through a recombination centre, or else it can be retrapped one or more times before recombining. To obtain equations to describe the T.S.C. curves, three cases are considered. The electrons released from traps:-

1) spend time τ in the conduction band before recombination takes place. This is the case of monomolecular kinetics.

2) have an equal probability of being retrapped or recombining. This case is described by bimolecular kinetics

3) are retrapped several times before returning to the valence band. This also leads to bimolecular kinetics, but will be called the case of fast retrapping to avoid confusion.

Before considering these possibilities, we shall define some of the parameters common to all three. We shall consider a sample cooled to $T^{o}K$, having N_t traps per cm^3 at depth E eV below the conduction band, of which

n_{to} are initially filled. The probability of an electron at depth E being thermally excited from the trap is given by:-

$$f = \nu\, e^{-E/kT} \qquad \qquad \text{Eq. 3.1}$$

where ν is the attempt to escape frequency, and $\nu = N_c v S_T$ for a semiconductor with simple energy band surfaces. N_c is the density of states in the conduction band, v is the thermal velocity of the electrons, and S_T is the capture cross-section of the traps. If at any time there are n_t filled traps, then the rate of excitation of electrons to the conduction band is:-

$$\frac{dn}{dt} = -\frac{dn}{dt}t = n_t\, \nu\, e^{-E/kT} \qquad \qquad \text{Eq. 3.2}$$

For a constant heating rate β, the temperature increases linearly with time, and:-

$$dT = \beta\, dT$$

2.a. Monomolecular Kinetics

If the recombination process of the electrons can be described in terms of a free life time, then the rate of change of electron concentration, n_c in the conduction band at any time t, is described by:-

$$\frac{dn}{dt}c = -n_c/\tau \quad - dn_t/dt \qquad \qquad \text{Eq. 3.3}$$

If τ is very small, then $dn_c/dt \ll n_c/\tau$, and

$$n_c = -\tau \frac{dn}{dt} t \qquad \text{Eq. 3.4}$$

From eq. 3.4, Randall and Wilkins (1) derived an expression for thermal glow curves. The equivalent of this for T.S.C. data is given by:-

$$\sigma = n_c e\mu = n_{to}\,\tau\, e\mu\, \nu\, \exp(-E/kT)\exp\left[-\int_{T_o}^{T} \frac{\nu}{\beta}\exp(-E/kT)dT\right] \qquad \text{Eq. 3.5}$$

where σ is the change in conductivity, and μ and e are the mobility, and charge of the free electrons.

2.b. Bimolecular Kinetics

Garlick and Gibson (2) first considered this case, and obtained the expression for the T.S.C. curve:-

$$\sigma = \frac{e\mu n^2_{to}\,\tau\,\exp(-E/kT)}{N_t\left[1 + \frac{n_{to}}{\overline{N}_t}\int_{T_o}^{T}\frac{N_c v S_T}{\beta}\exp(-E/kT)dT\right]^2} \qquad \text{eq. 3.6}$$

An important difference between this and eq. 5, is that in the bimolecular case, the shape of the T.S.C. curve depends upon the extent to which the traps are initially filled.

2.c.   Fast Retrapping

Haering and Adams (3) obtained an expression to
describe the T.S.C. curve for the fast retrapping case:-

$$\sigma = \frac{N_c e \mu}{N_t} n_{to} \exp(-E/kT) - \frac{e}{N_t \beta \tau} \int_{T_o}^{T} N_c \exp(-E/kT) dT \qquad \text{Eq. 3.7}$$

This equation does not contain ν, and so a value
of S_T cannot be obtained for fast retrapping. However,
Boer, Oberlander and Voigt (4) have shown that S_R, the
capture cross-section of the recombination centres can
be obtained, and is given by:-

$$S_R \nu = \frac{E}{kT^*} \frac{\beta}{n_c^* T^*}$$

where the asterisk denotes values at the maximum
of the T.S.C. curve.

3.   Methods of Analysis

3.a.   Monomolecular Kinetics

(a) Randall and Wilkins Method

The approximation:-

$E = 25kT^*$ was proposed by Randall and Wilkins
(1) to obtain trap depths from thermal glow measurements.
This is obviously an oversimplification which would mean
that T^* is independent of heating rate.

(b) Grossweiner's Method

Grossweiner (5) simplified the Randall and Wilkins equation for monomolecular trap emptying and obtained the expression:-

$$E = \frac{1.51 \, kT^* T'}{(T^* - T')} \qquad \text{Eq. 3.8}$$

where T' is the temperature at the half height on the low temperature side of the peak. This expression is stated as being valid provided that E/kT^* is greater than 20, and $N_c v S_T/\beta$ is greater than 10^7.

Grossweiner also obtained an expression for the capture cross-section, S_T, by differentiating $\ln[\sigma(T)]$ with respect to T in equation 3.5, and equating the result to zero to find the conditions for maximum conductivity. This gives:-

$$\exp(E/kT^*) = \frac{N_c v S_T kT^{*2}}{\beta E} \qquad \text{Eq. 3.9}$$

From equations 3.8 and 3.9, Grossweiner obtained:-

$$S_T = \frac{3T' \exp(E/kT^*)}{2N_c v T^*(T^*-T')} \qquad \text{eq. 3.10}$$

(c) Keating's Method

Randall and Wilkins in their derivation of eq. 3.5, assumed that $N_c v S_T$ is independent of temperature. This is equivalent to assuming $S_T \propto T^{-2}$, since $N_c \propto T^{3/2}$, and

$v \propto T^{\frac{1}{2}}$. Keating (6) followed a similar procedure to this except that he put $S_T \propto T^{-a}$, and obtained the expression:-

$$\ln(\sigma/\sigma_0) = b \ln T - E/kT - \frac{B}{\beta} \int_{T_0}^{T} b \exp(-E/kT) \, dT$$

Eq. 3.11

where b and B are identified by $N_c v S_T = BT^b$.

Using an asymptotic expansion Keating obtained the result:-

$$kT*/E = \frac{T''-T'}{T*}(1.2\gamma - 0.54) + 5.5 \times 10^{-3} - \frac{(\gamma - 0.75)^2}{2}$$

Eq. 3.12

where $\gamma = (T'' - T*)/(T* - T')$, and T'' is the temperature at the half height on the high temperature side of the curve. He showed that the approximations he used are valid as long as $10 \langle E/kT* \langle 35$, and $0.75 \langle \gamma \langle 0.9$

(d) <u>Variation of Heating Rate</u>

From equation 3.9 it can readily be seen that the use of two different heating rates will yield a value of trap depth which is given by the expression:-

$$E = \frac{kT_1^* T_2^*}{(T_1^* - T_2^*)} \ln\left[\frac{\beta_1 T_2^{*2}}{\beta_2 T_1^{*2}}\right]$$

Eq. 3.13

This method was first proposed independently by Booth (7) and Bohun (8). Hoogenstraten (9) later suggested the use of several heating rates, for which a plot of $\ln(T*^2/\beta)$ against $1/T*$ should yield a straight line from the slope of which value of E can be determined. A value of S_T for this monomolecular case can be determined by substituting the value of E in equation 3.9.

3.b. Methods applicable to all Recombination Kinetics

(a) Haering and Adams

Haering and Adams (3) used the technique of differentiating the expression for the T.S.C. curve to find the conditions for the maximum. They applied this to the limiting cases of no retrapping and fast retrapping, and obtained similar expressions for the conductivity at the maximum:-

$$\sigma(T*) = \sigma_0 \exp(-E/kT - 1) \qquad \text{eq. 3.14}$$

where for the case of no retrapping

$$\sigma_0 = N_c S_T v \mu \tau n_{to}$$

and for the case of fast retrapping

$$\sigma_0 = N_c \mu n_{to} e / N_t$$

For either case, a plot of $\ln \sigma(T^*)$ against $1/T^*$ for several different heating rates will yield a value of E. This is also the technique proposed by Boer, Oberlander and Voigt (10), although their calculations were based on a fast retrapping model only.

(b) <u>Garlick and Gibson</u>

As a set of traps begins to empty when the temperature is raised, the integrals in equations 3.5, 3.6 and 3.7 are all small, and the equations reduce to the form:-

$$\sigma = \text{const.} \times \exp(-E/kT) \qquad \text{eq. 3.15}$$

This technique was suggested by Garlick and Gibson (2), and allows a value of E to be determined from a plot of $\ln \sigma$ against $1/T$ for the initial part of the curve.

(c) <u>Halperin and Braner</u>

Halperin and Braner (11) made the geometrical approximation that the T.S.C. curve can be represented by a triangle, and derived the following equations for the value of E:-

$$E = (0.72/T^* - T') \, kT^{*2}(1 - 2.58 \Delta) \qquad \text{Eq. 3.16}$$

- 46 -

for molecular kinetics, and:-

$$E = (2/T^* - T') \, kT^{*2}(1 - 3\Delta) \qquad \text{Eq. 3.17}$$

for bimolecular kinetics. In both equations

$\Delta = 2kT^*/E$. To distinguish between the two possible

recombination processes, they proposed the following

rules:-

if $\Delta \leqslant e^{-1}(1 + \gamma)$, the centre behaves mono-

molecularly, and if $\Delta \geqslant e^{-1}(1 + \gamma)$, the centre is

bimolecular.

(d) Schoen's Method

The work of Schoen (12) was concerned only with

thermoluminescence, and for several different cases

he came . to the conclusion that:-

$$E = \frac{kT_1^* T_2^*}{(T_1^* - T_2^*)} \, \ln \left[\frac{\beta_1 T_2^{*7/2}}{\beta_2 T_1^{*7/2}} \right] \qquad \text{Eq. 3.18}$$

This is the same as equation 3.13, except that $T^{7/2}$

replaces T^2 in the final bracket.

3.c. Fast Retrapping Theories

(a) Bube's Theory

For the extreme case of fast retrapping, the

conduction electrons can be considered as being in thermal

equilibrium with the electrons still in traps. This means

that:-

$$E = kT \ln \frac{N_c \eta}{n_c(1-\eta)} \qquad \text{Eq. 3.19}$$

where n_c is the density of free electrons, and η is the fraction of traps occupied at temperature T.

Bube (13) assumed that at the T.S.C. maximum the quasi Fermi level coincides with the depth of the trapping levels. This would mean that $\eta = \frac{1}{2}$, and all that needs to be done is to calculate the position of the Fermi level at the peak. Equation 3.19 then becomes:-

$$E = kT^* \ln \frac{N_c}{n_c^*} \qquad \text{Eq. 3.20}$$

This equation obviously cannot be used for the case of monomolecular kinetics.

(b) Luschik

Luschik (14) used a geometrical approximation, and proposed the following expression for trap depth:-

$$E = \frac{kT^{*2}}{(T'' - T^*)} \qquad \text{Eq. 3.21}$$

This is similar to that of Grossweiner, except that it requires measurement of the half height temperature on the high temperature side of the peak.

- 48 -

4. Discussion of the Different Methods

Two published papers, Nicholas and Woods (15) and Dittfeld and Voigt (16), have surveyed the various methods of T.S.C. curve analysis, but have, unfortunately, arrived at opposite conclusions.

Nicholas and Woods analysed the peaks in twenty samples by nine different methods, and demonstrated the different conditions under which the various methods may be correctly applied. They observed a total of six sets of traps at 0.05, 0.14, 0.25, 0.41, 0.63, and 0.83 eV below the conduction band, and showed that these fitted well with previously published results, if allowance was made for incorrectly applied analysis methods. Most of the methods were found to give results in agreement with these trap depths, as long as the methods of analysis were applied only to peaks for which they could be correctly used. Bube's method was found to give consistently high results for the monomolecular traps, and results that were too low for the bimolecular traps. It gave a correct value for the traps at 0.41 eV - perhaps fortuitously. Support for these results was given by Bueget and Wright (17) who obtained trap depths from more than a hundred samples that were grouped around 0.16, 0.24

0.45, 0.63 and 0.82 eV below the conduction band.
Their results were based on measurements of Hall effect,
conductivity and space-charge-limited current.

Dittfeld and Voigt analysed three peaks occurring
in three samples, and found that Bube's method gave the
most reliable analysis. They found peaks at 0.22, 0.34,
and 0.42 eV. The 0.42 eV peak gave consistent results
using the other methods, as was found by Nicholas and
Woods. The peaks at 0.22 and 0.34 eV gave values of
0.16 and 0.22, respectively if analysed by Grossweiner''s
method. Dittfeld and Voigt calculated the trap
distribution from the experimental curves for different
heating rates, using both mono- and bimolecular kinetics.
From the extent to which these distributions for
different heating rates agreed, they decided whether the
trap emptying was mono- or bimolecular. Having decided
that two of their samples emptied monomolecularly, they
still used Bube's calculation to work out trap depths.
They prefer Bube's method because it gives more consistent
results, which of necessity, it must do, because the
measured parameters fall inside a logarithm when used
to calculate E. Most other methods require measurement
of small temperature differences, which can lead to much

larger inaccuracies. The other main reason for their choice of Bube's method was the agreement between their trap depths and those of Niekisch (18) obtained from a method based on modulated light intensity measurements. The results of Niekisch, however, were also based on the assumption of equilibrium between free and trapped electrons.

Bube (19) compares the method of Fermi level analysis with that of Garlick and Gibson, and shows very good agreement between the two methods for one peak in one sample of CdS. However, the author admits that this may be fortuitous, for in some CdS-CdSe samples also considered in that paper, Garlick and Gibson's method was found to give results that were more consistent with position of the maximum temperature, and with the associated shift in band gap from CdS to CdSe.

In a more recent paper Bube (20) measured the trap distribution in $CdS_{0.73}-CdSe_{0.27}$ crystals by using (a) the Fermi level method of analysis, and (b) various photoconductive decay experiments. He found a quasi-continuous trap distribution and obtained good agreement between the two methods. Again the photoconductivity results depended upon the same assumption of equilibrium between free and trapped electrons. If there is a

continuous trap distribution, this equilibrium is more likely to exist, and the conditions for correct application of this method are most likely to be met.

In a later paper Bube et al. (21) repeat the assertion that the Fermi level method of analysis can be used to determine trap depth in CdS-CdSe crystals in which a quasi-continuous distribution is found. However, a discrete trap at 0.73 eV was also found, which had an apparent capture cross-section of 10^{-14} cm^2. A trap with such a large capture cross-section should be associated with fast retrapping but according to Bube et al., the trap obeys monomolecular kinetics, and the Fermi level method gives an erroneous value of trap depth. (For possible explanations, see Chap. 5).

5.   Conclusions

Most of the methods mentioned will give values of trap depth that are correct to within the experimental errors, provided that the limitations of each method are recognised. If this is done, the differences in theory between the methods are not large, but some of them are found to have experimental advantages over others. Peaks that overlap to a large extent with other peaks,

can have their leading edges cleaned by the process
of thermal decay, in which shallower traps are first
emptied thermally before recording a particular peak.
The high temperature side of the curve cannot be so
easily cleaned, and therefore methods that require
knowledge of T" are somewhat limited in their use. The
most generally applicable method seems to be the initial
rise method of Garlick and Gibson, because measurements
can be made using repeated thermal cleaning processes.
The only limitation to the use of this method are, (a)
with grossly overlapping peaks, for which none of the
methods can be used (although different heating rates
can be used to help separate the peaks), and (b) low
temperature peaks just above the illumination temperature.
In the latter case the difficulties are the experimental
one of obtaining a constant heating rate, and the
theoretical one of observing only acceleration of trap
emptying already begun at the low temperature, and not
true trap emptying.

The conclusion drawn is that the work of Nicholas
and Woods is a far more reliable guide to the use of
T.S.C. curve methods of analysis, because of the very
wide scope of their work, and because of the support

from the results of Bueget and Wright who obtained the same trap depths in CdS on a large number of crystals by completely independent methods.

References for Chapter Three

1. Randall J.T. & Wilkins M.H.F.., 1945, Proc. Roy.
    Soc. A, 184, 347, 365, 390

2. Garlick G.J.F. & Gibson A.F., 1948, Proc. Phys.
    Soc., 60, 574

3. Haering R.R. & Adams E.N., 1960, Phys. Rev.,
    117, 451

4. Boer K.W., Oberlander S. & Voigt J., 1958, Ann.
    Phys. Lpz., 2, 136.

5. Grossweiner L.I., 1953, J. Appl. Phys. 24, 1306.

6. Keating P.N., 1961, Proc. Phys. Soc., 78, 1408

7. Booth, A.H., 1954, Canad. J. Chem., 32, 214

8. Bohun A., 1954, Czech. J. Phys., 4, 91.

9. Hoogenstraaten W., 1958, Philips Res.Rep., 13, 515

10. Boer, K.W., Oberland S. & Voigt J., 1958, Ann.Phys.
    (German), 2, 130.

11. Halperin A. & Braner A.A., 1960, Phys. Rev. 117, 408

12. Schön M., 1958, Techn. Wiss. Abh, Osram Ges. 7, 175

13. Bube R.H., 1955, J. Chem. Phys., 23, 18

14. Luschik C.B., 1955, Dok. Akad. Nauk. S.S.S.R.., 101, 641

15. Nicholas K.H. & Woods J., 1964, Brit. J. Appl. Phys.,
    15, 783

16. Dittfeld H.J. & Voigt J., 1963, Phys. Stat. Sol., 3, 1941

17. Bueget U. & Wright G.T., 1965, Brit. J. Appl. Phys.,
16, 1457

18. Niekisch E.A., 1961 Z. Phys. Chem., 217, 110

19. Bube R.H., 1964, J. Apply. Phys. 35, 586

20. Bube R.H., 1964, J. Appl. Phys., 35, 3067

21. Bube R.H. Dussel G.A., Chiang-Tao Ho, & Miller L.D.,
1966, J. Appl. Phys., 37, 21

CHAPTER FOUR

PHOTOLUMINESCENCE IN CADMIUM SULPHIDE

1. Introduction

Photoluminescence is the luminous emission produced
by the absorption of light, usually visible or ultra-
violet. The two possibilities that exist for this are
fluorescence and phosphorescence. In fig. 4.1, fluorescence
occurs when an electron in the ground state of an activator
centre absorbs energy a_1, and then emits energy e_1 ($< a_1$),
when returning to the ground state. The emission is
delayed in the case of phosphorescence by the intermediate
trapping of the electron in a metastable state m, from
where it must return to the excited state before emission
can take place. The phosphorescence e_2 can have the same
wavelength as the fluorescence, but the relative
intensities may be difference.

In the case of CdS type phosphors, the lowest state
is the valence band, and the highest excited state the
conduction band. Between the two bands exist the traps,
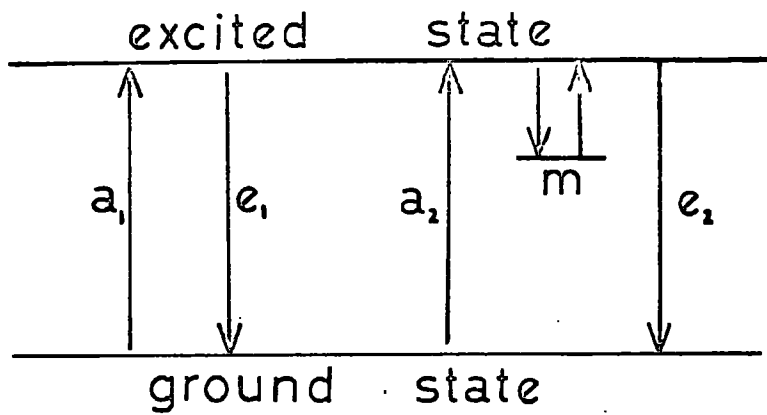donors and recombination centres that must be taken into
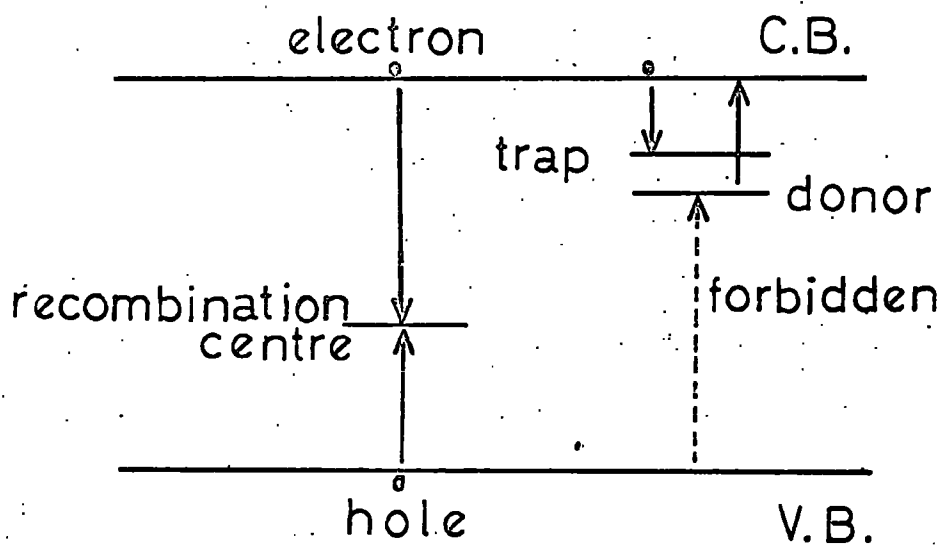

- 57 -

FIG. 4.1.

FIG. 4.2.

account to explain the luminescence. Fig. 4.2 shows

the type of energy level diagram that can explain most

of the luminescence phenomena in CdS phosphors. σ_e

and σ_h are the capture cross-sections of the

recombination centres for the electrons and holes

respectively. For these centres σ_e and σ_h are of the

same order of magnitude. For the traps and donors

$\sigma_e \gg \sigma_h$, in fact the value of σ_h is so small that

the probability of capture of a hole can be neglected.

If a centre close to the conduction band is normally

empty it is called a trap, if normally full it is

called a donor. The centre can, of course, be made to

change its function under different conditions, e.g.

changes of temperature or illumination. Hole traps and

acceptors are defined by the opposite relationship,

$\sigma_h \gg \sigma_e$.

2. Conservation of Momentum

   If electron-hole pairs are produced by the absorption

of light, then the electrons will accumulate at the bottom

of the conduction band, and holes at the top of the

valence band. This is caused by the interactions of the

electrons and holes with the crystal lattice. Since the

- 58 -

mean free path of the electrons is $\sim 10^{-7}$ cms, and the
mean velocity is $\sim 10^{7}$ cms/sec, it is a very fast process,
and equilibrium can be reached in 10^{-12} to 10^{-10} secs.
It is this that allows us to use the concept of a
quasi-Fermi level. The quantum mechanical selection
rule for radiative transitions states that the difference
between initial and final values of the wave vector
(k and k' respectively) of the electron must equal the
wave vector of the radiation. In general the photon
wavelength is large compared with that of the electron
(λ = 1.22 x 10^{-7} cms for a 1 eV electron). This means
that k = k', and transitions involving only an electron
and a photon must be vertical in the E against k
diagram. Since excited electrons and holes rapidly
migrate to the points of lowest energy in the conduction
and valence bands, an electron transition downwards
will only be possible in materials that have simple
energy surfaces with conduction band minima and valence
band maxima at k = 0. Germanium, for example (1) has
a conduction band minimum at k = 0, but also has eight
equivalent minima at the band extremities that are lower
by approximately 0.16 eV. The valence band maximum is
at k = 0, but it is complex, (fig. 4.3). At low
temperatures, only the lowest minima contain electrons,
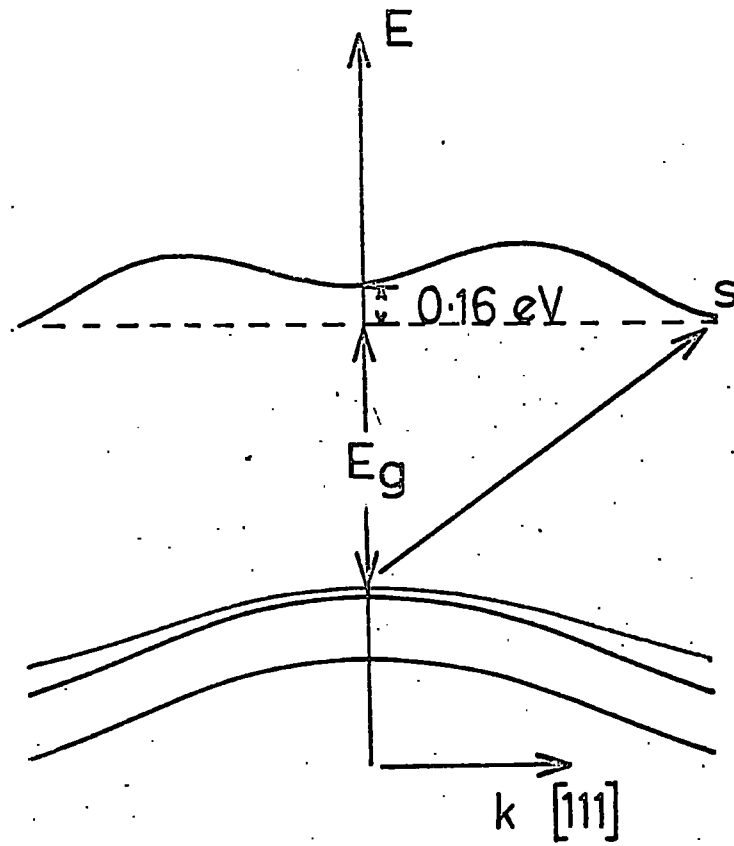
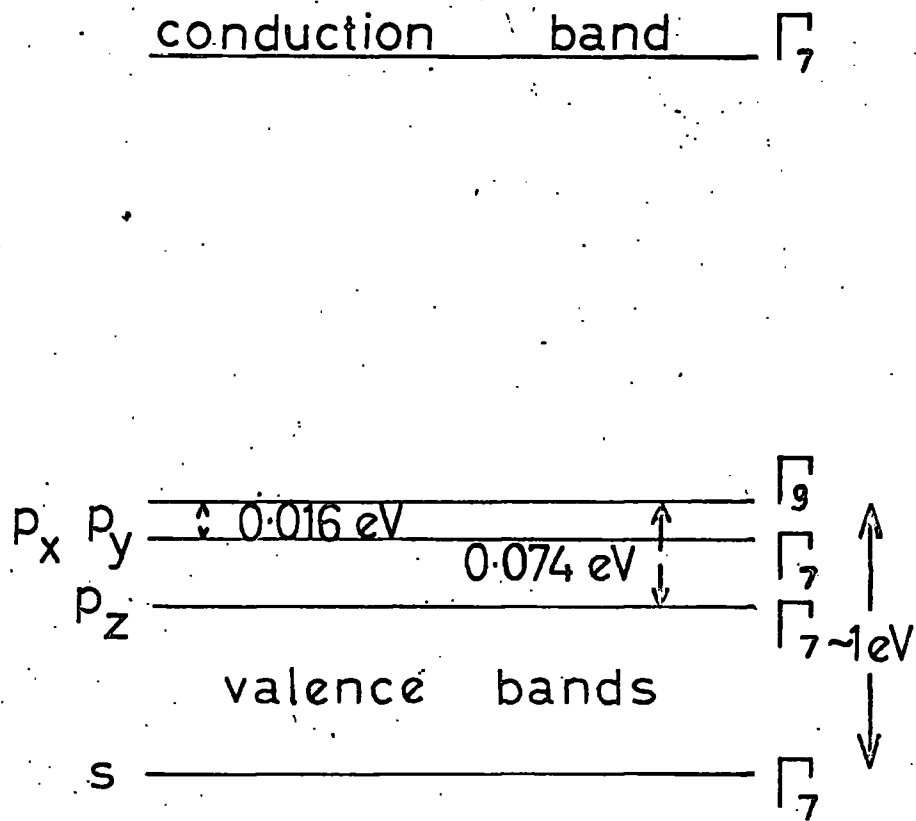Band Structure of Germanium

FIG. 4.3.

and so electron transitions to the valence band cannot take place. At higher temperatures, $kT \approx E_G$, transitions can take place because the $k = 0$ minimum has appreciable probability, P, of containing an electron. The probability of this transition is given by $P \approx exp(-E_G/kT)$. The transition s, can only take place with the simultaneous emission or absorption of a phonon that is necessary to absorb the excess momentum. However, the energy absorbed by the phonon is small.

3. The Band Structure of Cadmium Sulphide

The structure of the valence band of CdS, as proposed by Balkanski and Cloiseaux (2), is shown in fig.4.4. The band is divided into four parts, of which the lowest is due to the s-orbitals of the sulphur atoms, and the other three arise from the p-states. The p_z-orbitals along the hexagonal axis are more strongly bound that the p_x- and p_y- orbitals. This is due to the fact that the c/a ratio in the CdS lattice is not the same as the value of $(8/3)^{\frac{1}{2}}$ in an ideal hexagonal structure. The p_x- and p_y-orbitals also lose their degeneracy due to spin-orbit coupling. The higher energy state is that for which spin is parallel to orbital momentum (Γ_9 symmetry), and the lower is that for which spin is antiparallel (Γ_7 symmetry).

conduction   band Γ_7

$P_x \; P_y$ $\updownarrow$ 0·016 eV $\uparrow$ Γ_9
                              0·074 eV $\downarrow$ Γ_7
P_z Γ_7 ~1eV

valence   bands

s Γ_7

band structure of CdS

FIG. 4.4.

4. Edge Emission

A typical edge emission spectrum of CdS is shown in fig. 4.5, which, although it is so-called because of its proximity to the optical absorption edge, is not due to band to band transitions. The large equidistant bands with a line spacing of approximately 300 cm^{-1}, occur at 0.15 eV to the long wavelength side of the fundamental absorption edge. These bands are thought to be due to either recombination of a free hole with an electron trapped 0.15 eV below the conduction band, (model I), or a free electron with a hole trapped 0.15 eV above the valence band, (model II) with the simultaneous emission of 0, 1, 2, 3 . . . longitudinal optical phonons to explain the multiplicity of the bands. Model I, first proposed by Schoen (4), found support in the work of Lambe et al. (3), who compared the green luminescence decay with the photoconductive decay produced by infra-red quenching at 4° K. Model II was proposed by Klasens (5), and supported by the work of Broser et al. (6) who observed a decay of luminescence in step with the photo-current, and interpreted this in favour of model II. Recently Spear and Bradbury (7)
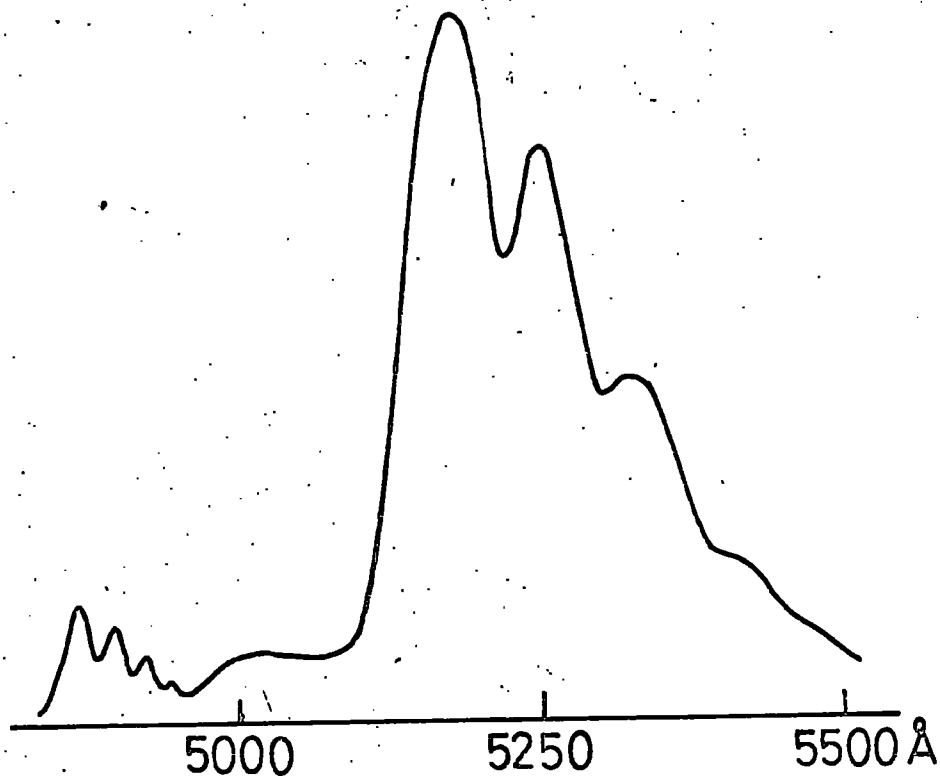
Visible Luminescence of CdS

at 4°K

FIG. 4.5.

have compared experimental results with those computed from a three centre model, and have shown that model II gives results which are more consistent with those of their experiments than does model I. However, the problem is still unresolved.

The series of the fine structure is due to the simultaneous emission of 0,1,2,3, etc. phonons, and the frequency difference corresponds to that of the longitudinal optical phonons (8). A substructure is sometimes seen at $4.2^\circ K$, which consists of a weak set of similar lines with the same separation, but shifted by 150 wave numbers to the short wavelength end of the spectrum. These could be due to recombination through the second level at the top of the valence band. However, recent work (9), (10) has suggested that the weak lines are those normally observed at higher temperatures, and the strong lines at $4.2^\circ K$ are due to a bound electron-bound hole recombination.

The emission closer to the absorption edge in fig. 4.5, consists of two parts. One of these is attributed to recombination through surface states and has been observed by many workers (3). It shows multiphonon series similar to that of edge emission. The other part,

at even shorter wavelengths is ascribed to free and
bound exciton recombination and has been studied
extensively by Beil and Broser (11), and Thomas and
Hopfield (12),(13),(14). The emission takes the form
of a hydrogen-like series, due to the recombination
of electrons in the various states of the exciton, with
holes in the valence band. Emission lines can arise
from excitons bound to various defect centres. The
main exciton peaks are seen at 4930$\AA$ (I_1), 4885$\AA$(I_2)
and 4869$\AA$(I_5), at 4.2^{O}K. The I_5 line is thought to be
due to an exciton bound to a cadmium vacancy (15). I_1
is due to a neutral acceptor centre, possibly associated
with an interstitial sulphur atom. The I_2 line is
thought to originate in an exciton bound to a sulphur
vacancy, or to its complex.

5. <u>Luminescent Centres</u>

Most of the work on luminescent centres in II-VI
compounds has been done on zinc sulphide, but since the
value of the band gap for mixtures of zinc and cadmium
sulphides varies almost linearly between the two extreme
compositions, with no discontinuities, results from the
two materials are directly comparable (16).

The main luminescent bands in zinc sulphide are a

blue band at 4,450 Å (2.79 eV), and a green band at

5,230 Å (2.37 eV), and these are equivalent to bands at

0..82 microns (1.51 eV) and 1.02 microns (1.22 eV) in

cadmium sulphide. The energy level schemes for the

two materials are shown in fig. 4.6. As can be seen

from this diagram, the separation of the luminescent

centres from the valence band does not change very much

from ZnS to CdS. Experiment associates these luminescent

bands with the presence of copper impurities that act

as activation centres. From measurements of magnetic

susceptibility as a function of temperature, it can be

shown that the copper exists in the lattice as a Cu^+

ion (17). This ion replaces a Zn^{++} or Cd^{++} ion, and

reduces the bond strengths of the surrounding sulphur

ions. Electrons on these ions are less tightly bound

and therefore have a larger electrostatic energy. This

gives rise to allowed electron levels somewhat above

the valence band, and explains why the levels should

be a fixed distance from the valence band for both zinc

and cadmium sulphides.

Williams (18) first showed that the green luminescence

band in ZnS is enhanced by the substitution of a halogen

as an impurity for sulphur. This process of co-activation

does not produce any shift in the position of the
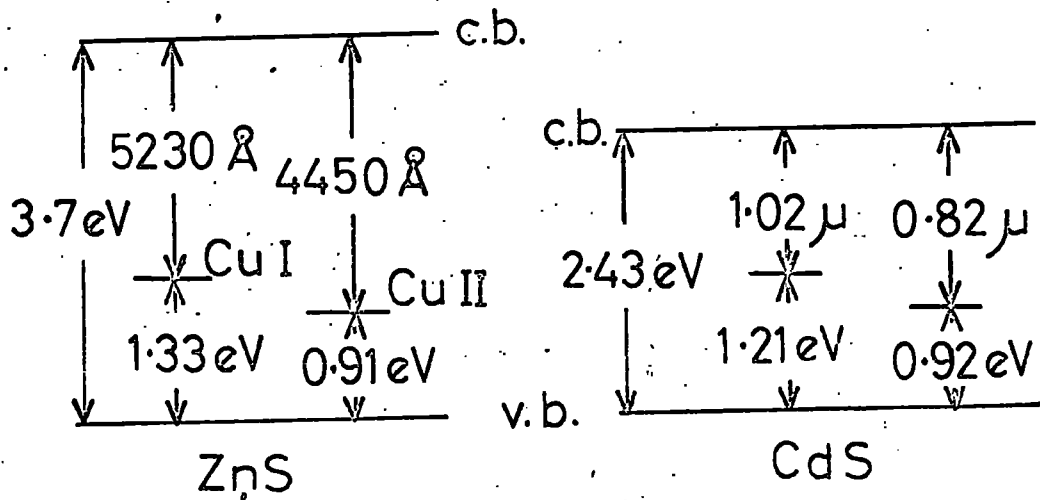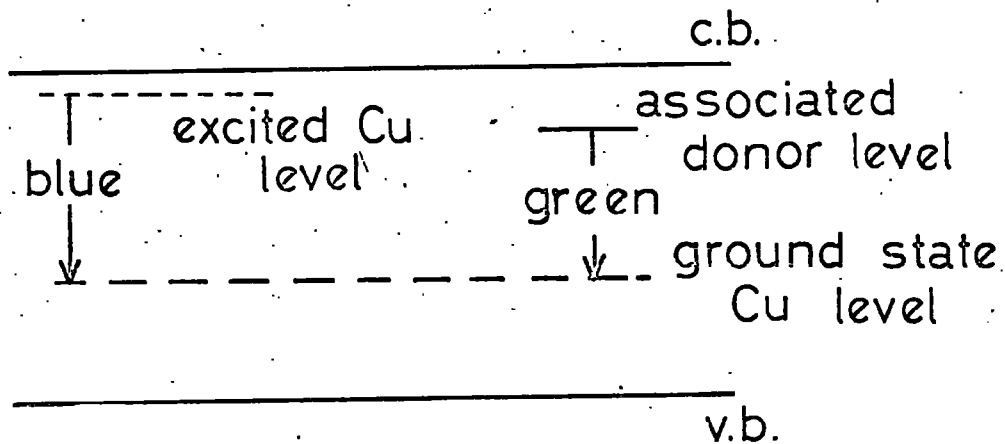
FIG. 4.6.

Luminescent Bands in ZnS after

Curie and Curie

FIG. 4.7.

luminescent peaks, whatever the halogen used. This
suggests that the effect is due to the substitutional
charge -e of the activator in the lattice. The
trivalent elements Al, Ga and In may also be used as
co-activators, and oxygen is believed to have a similar
effect. Many models have been proposed to explain these
luminescent bands (19), (20), (21). Fig. 4.7 shows the
model due to Curie and Curie (22). They suggest that
the blue luminescence is due to the return of an electron,
either from the conduction band, or from an excited state
of the copper level just below the conduction band, to
the ground state of the copper level. The green
luminescence arises from the return of an electron to the
same ground state, but this time from the co-activator
donor levels. One reason for the belief that the ground
state is the same for both the green and blue luminescence
is that the infra-red quenching band is the same for both
bands.

Further luminescent bands are frequently observed
in ZnS and CdS. Garlick and Dumbleton (23) first
observed some of these in ZnS at 1.5 and 1.7 microns.
Browne (19) studied these infra-red bands further in the
CdS-ZnS system, and found that the peaks shifted very
little during the transition from zinc to cadmium sulphide.

(Peaks were seen at 1.6 and 1.85 microns in CdS.) He
also found a peak at the long wavelength end of the
spectrum at 1.85 for zinc and 2.05 microns for cadmium
sulphide. The fact that the emission bands do not
shift very much, suggests that they are associated
with perturbed levels of the valence band. Browne
found more support for this in the fact that the
excitation bands coincide with the spectra for infra-
red quenching of visible emission and photoconduction,
and also that the dependence of emission intensity
upon crystal preparation pointed to cation vacancies
as the cause of the emission. Garlick (21) proposed
the energy band model shown in fig. 4.8 to account
for the luminescent and infra-red quenching spectra
of cadmium sulphide. Transitions a and c are the
0.78 and 1.02 micron emissions that are equivalent
to the blue and green bands in zinc sulphide, where A
is the excited state of level B. The transitions b and
d are those that cause infra-red quenching, and e, f, g
are the infra-red emission levels at 1.6, 1.85 and 2.05
microns. The level B is the same as B', only the energy
for absorption must be greater than that of the emission.
Meijer (24) measured the infra-red emission, infra-red
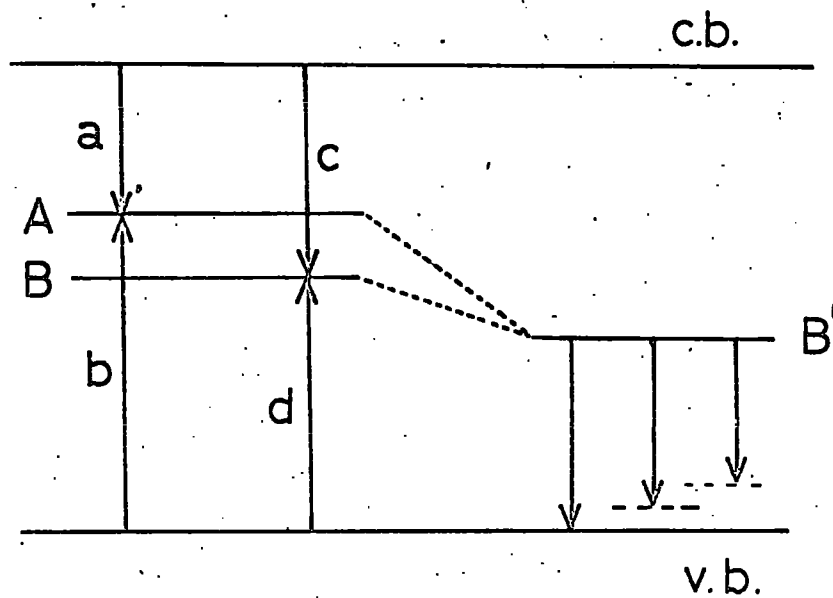
Luminescent and Infra-red
Quenching Bands in
CdS.

(Garlick)

F I G. 4.8.

quenching and the infra-red stimulation of the visible
luminescence in copper activated ZnS, and concluded
that the emission peaks at 1.57 and 1.72 microns are
due to the return of an electron to the valence band
from the ground and excited states of a level caused
by the substitution of a copper ion for a zinc.
However, Garlick et al. (25) in measuring the effect
of Co-60 gamma radiation upon the luminescent intensity
of samples containing varying amounts of copper, could
find no evidence for the belief that copper is the
cause of the luminescence. They considered that the
gamma radiation was insufficient to produce new point
defects, and could only cause readjustment of existing
complexes. Since the radiation caused changes in the
infra-red luminescence and not in the "green" and "blue"
bands, they concluded that the latter are due to point
defects, and the 1.6, 1.85 micron bands are associated
with centres that require much smaller energies of
formation.

Bryant and Cox (26) proposed a model for zinc
sulphide in which it was not necessary for the defect
centre to have more than one level in the forbidden
gap. From the fact that the complete luminescent

spectrum could be excited by the bands at both 0.89 and 1.49 microns, they deduced that the infra-red quenching bands must be due to excitations from the p and s-states of the valence band, and not due to excitations from a p-state to two levels in the forbidden gap. It is in this respect only that their model differs from that of Garlick previously mentioned (fig. 4.8). They also considered that the single level in the forbidden gap is the same as that proposed by Curie and Curie (fig. 4.7) to explain the 0.8 and 1.02 micron bands in CdS. In Curie's model this would require a trap at 0.49 eV below the conduction band (see fig. 4.7). In a further paper Bryant and Cox (27) studied the polarisation of the infra-red luminescence, and in addition to the splitting of the valence band considered the splitting of the recombination centre level due to spin-orbit and crystal field coupling. This proposition overcomes the outstanding difficulty of their earlier model, which was the difference in energy between the splitting of the infra-red peaks and the splitting of the valence band.

Bryant and Cox (28) studied further luminescence in the region 2.0 to 2.8 microns, and found a similar

structure to that of the 1.6 to 1.8 micron bands. With the appearance of this long wavelength band they found an associated shift of the 1.02 micron emission to shorter wavelengths. To explain this they suggested that the emission is due to a centre similar to that previously proposed, except that it is shifted 0.2 eV towards the valence band. This gives the 2.0 to 2.8 micron structure similar to the normal 1.6, 1.8 micron bands, and also gives rise to emission at 0.9 microns, which appears as a shift in the origin of this new centre.

6. Conclusions

The model of Bryant and Cox for the infra-red luminescence spectrum in CdS gives the most complete picture of all the various phenoma observed. It does not, however, give any clue to the process of co-activation. There is also no existing evidence for their positioning of the s-levels of the valence band, but equally there is no evidence to refute it.

References for Chapter Four

1. Herman F., 1955, Proc. I.R.E., $\underline{43}$, 1703

2. Balkanski M. & Des Cloiseaux J., 1960, J. Phys.
   Rad., $\underline{21}$, 825 & $\underline{22}$, 41

3. Lambe S.J., Klick C.C. & Dexter D., 1956, Phys.
   Rev., $\underline{103}$, 1715.

4. Schön M., 1942, Z. Phys., $\underline{119}$, 463

5. Klasens H.A., 1940, Nature, $\underline{158}$, 306

6. Broser I., Broser-Warminski R., Klipping G.,
   Ross R., & Schulz H.J., 1961, J. Phys. Chem.
   Solids, $\underline{22}$, 213

7. Spear W.E. & Bradbury G.W., 1965, phys. stat. sol.
   $\underline{8}$, 649

8. Kroger F.A. & Meyer H.G.J., 1965, Physica, $\underline{20}$, 1149

9. Van Doorn C.Z., 1966, Philips Res. Repts., $\underline{21}$, 163

10. Pedrotti L.S. & Reynolds D.C., 1960, Phys. Rev.
    $\underline{120}$, 1964

11. Beil C.E. & Broser I., 1964, J. Phys. Chem. Solids,
    $\underline{25}$, 11.

12. Thomas D.G. & Hopfield S.J., 1959, Phys. Rev.,
    $\underline{116}$, 573

13. Thomas D.G. & Hopfield S.J., 1961, Phys. Rev.,
    $\underline{122}$, 35

14. Thomas D.G. & Hopfield S.J., 1962, Phys. Rev.,
    128, 2135

15. Ibuki S. & Ohso A., 1966, J. Phys. Chem. Solids,
    27, 1753

16. Gross G.E., 1959, Phys. Rev., 116, 1478

17. Bowers R. & Melamed N.T., 1955, Phys. Rev., 99, 1781

18. Williams F.E., 1953, Adv. in Electr., 5, 148.

19. Browne P.F., 1956, J. Electronics, 2, 1, 95

20. Bube R.H., 1953, Phys. Rev., 90, 70

21. Garlick G.F.J., 1959, J. Phys. Chem. Solids, 8, 449

22. Curie G. & Curie B., 1960, J. Phys. Rad., 21, 127

23. Garlick G.F.J. & Dumbleton M.J., 1959, Proc. Phys.
    Soc., 67B, 442

24. Meijer G., 1958, J. Phys. Chem. Solids, 7, 153

25. Garlick G.F.J., Bryant F.J. & Cox A.F.J., 1964,
    Proc. Phys. Soc., 83, 967

26. Bryant F.J. & Cox A.F.J., 1965, B.J.A.P., 16, 463.

27. Bryant F.J. & Cox A.F.J., 1966, Proc. Phys. Soc.
    87, 55.

28. Bryant F.J. & Cox A.F.J., 1966, phys. stat. sol.
    14, 427.

CHAPTER FIVE

DEFECT CENTRES IN CADMIUM SULPHIDE

1. Introduction

The defect centres that give rise to thermally stimulated current peaks and infra-red luminescence have been treated in earlier chapters. Another important property of a crystal which the defect centres can influence is the phenomenon of photo-conductivity. Electron and hole traps, and recombination centres determine to a great extent the variation of photocurrent with temperature, with excitation intensity, and with exciting wavelength. They also control the response time of the photo-conductivity and the luminescence. Measurement of all these parameters can thus yield information about the most important centres in the material, provided that the results can be made to fit some sort of pattern. This has been adequately done by Bube whose results are given in the next section.

A further problem arises with cadmium sulphide because the important defects seem to be caused by

sulphur or cadmium vacancies, or complexes of these
two. Difficulties arise because these centres are
very mobile, and can be easily redistributed.
Redistribution requires only small energies and so
can be brought about by heat treatment at quite low
temperatures or by the action of visible light. The
regrouping of these centres causes changes in the
properties of the material, and this means that care
must always be taken to ensure that the taking of a
measurement does not alter the properties being
investigated. A survey of the work done on the effects
of low temperature heat treatment and on photochemical
effects is given in the later sections of this chapter.

2. Photoconductivity

2a. Bube's Model

Models to describe the behavious of photoconductivity
is CdS using two different types of centre in the
forbidden gap, have been proposed by many authors, among
whom are Schön (1) and Klasens (2). The model given here
is that due to Bube (3) who generalised the other models
by dividing the traps into two sets, deep and shallow
traps. The deep traps can also be considered as

recombination centres.   Bube started with the hypothetical model shown in fig. 5.1.   The symbols used are as follows:-

N_i = density of states i

n_i = density of filled states i

S_{ni} = capture cross-section of states i for electrons

S_{pi} = capture cross-section of states i for holes

n = density of free electrons

p = density of free holes

$S_n^{''}$ = cross-section for recombination between free carriers

F = density of electron-hole pairs created by excitation

v_n = thermal velocity of an electron

v_p = thermal velocity of a hole

P_1 = probability of ejection of hole from centres 1

P_2 = probability of ejection of electron from centres 3

From the equation for charge neutrality, and from five equations expressing the rates of change of densities of the various states, Bube obtained equations that give F in terms of n.   These are:-

$$p = n - N_1 - N_2 + N_1\left[1 + v_p S_{p1}p/(S_{n1}nv_p + P_1)\right]^{-1}$$

$$+ N_2(1 + S_{p2}v_p p)/(S_{n2}v_n n_2 n)^{-1} + N_3\left[1 + (S_{p3}v_p p + P_3)/S_{n3}v_m n\right]^{-1}$$

Eq. 5.1

- 74 -
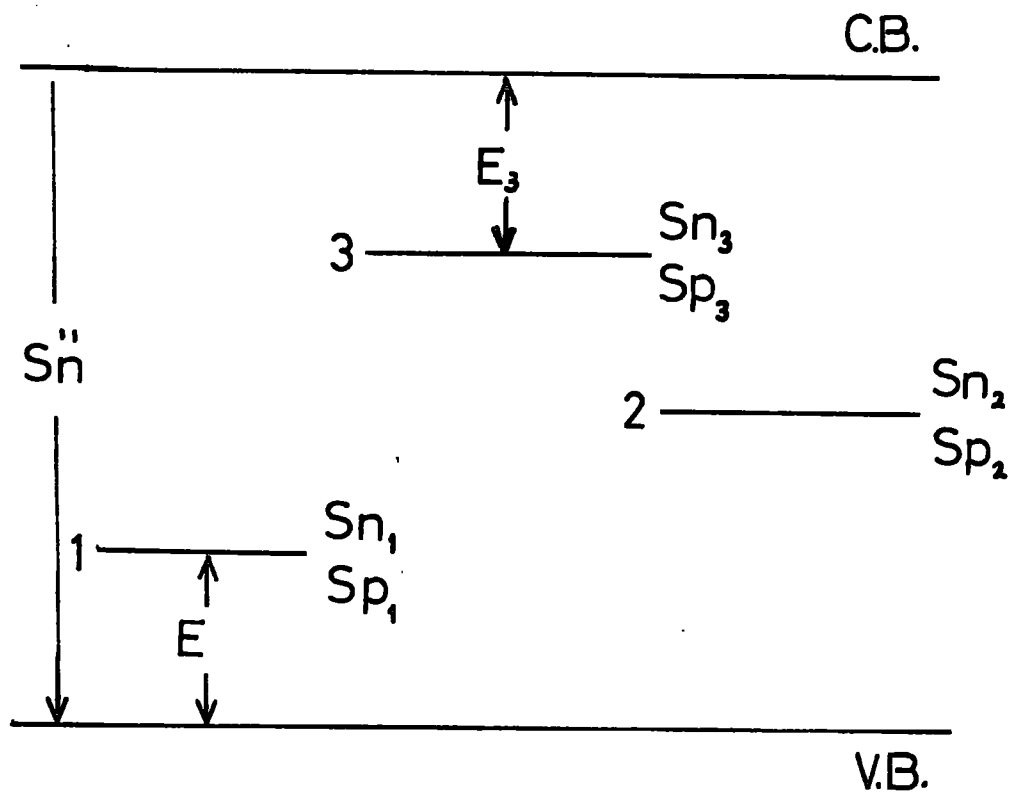
F I G. 5.1.

$$F = p\left[S_{p1}v_pN_1\left\{1 + (S_{p1}v_pp + P_1)/S_{ni}v_nn\right\}^{-1} + \right.$$

$$+ S_{p2}v_pN_2(1 + S_{p2}v_pp/S_{n2}v_n)^{-1} +$$

$$\left. + S_{p3}v_pN_3\left\{1 + (S_{p3}v_pp + P_3)/S_{n3}v_n\right\}^{-1} + S_n''vn\right]$$

<div align="right">Eq. 5.2</div>

2b. <u>Variation of Photosensitivity with Excitation Intensity</u>

In order to make arithmetical calculations on the basis of these equations Bube made certain assumptions and inserted reasonable values for some of the parameters in them. He assumed that centres 2 and 3 are of the same type with equal capture cross-sections for holes and electrons. (These could be replaced by a single set of levels that are only partially filled in the dark, to give the two centre model of Schön.) Centres 1 were assumed to have the same capture cross-sections for holes as 2 and 3, but much smaller cross-section for electrons. The values inserted were:-

$$N_1 = N_2 = 10^{15}/cm^3$$

$$S = S_{p1} = S_{p2} = S_{p3} = S_{n2} = S_{n3} = 10^{-15}cm^2$$

$$S' = S_{n1} = 10^{-19}cm^2$$

$$S_n^{''} = 10^{-20} cm^2$$

$$P_1 = 10^{-1} sec^{-1} \text{ at } 300^\circ K \text{ (i.e. } E_1 = 0.7 \text{ eV)}$$

$$P_3 = 10^{-4} sec^{-1} \text{ at } 300^\circ K \text{ (i.e. } E_3 = 0.9 \text{ eV)}$$

Bube then calculated the variation of n with F for various densities of the recombination centres 3. The results for $N_3 = 10^{15} cm^{-3}$ are shown in fig. 5.2. F is proportional to the excitation intensity, and n is proportional to the photocurrent. For low light intensities the quasi Fermi level for electrons lies below centres 3, and the density of free electrons varies as the square root of the intensity since many carriers are trapped in centres 3. When Svn exceeds P_3 the electron Fermi level passes through the centres 3, and the density of free electrons is proportional to the intensity, because all the centres 3 are now full, and do not cause any further trapping. At higher light intensities the hole Fermi level passes through the energy level of centres 1, which causes them to capture holes. Since they have small capture cross-section for electrons they are not very efficient recombination centres, and so they effectively remove holes that otherwise could take part in recombination

FIG. 5.2.
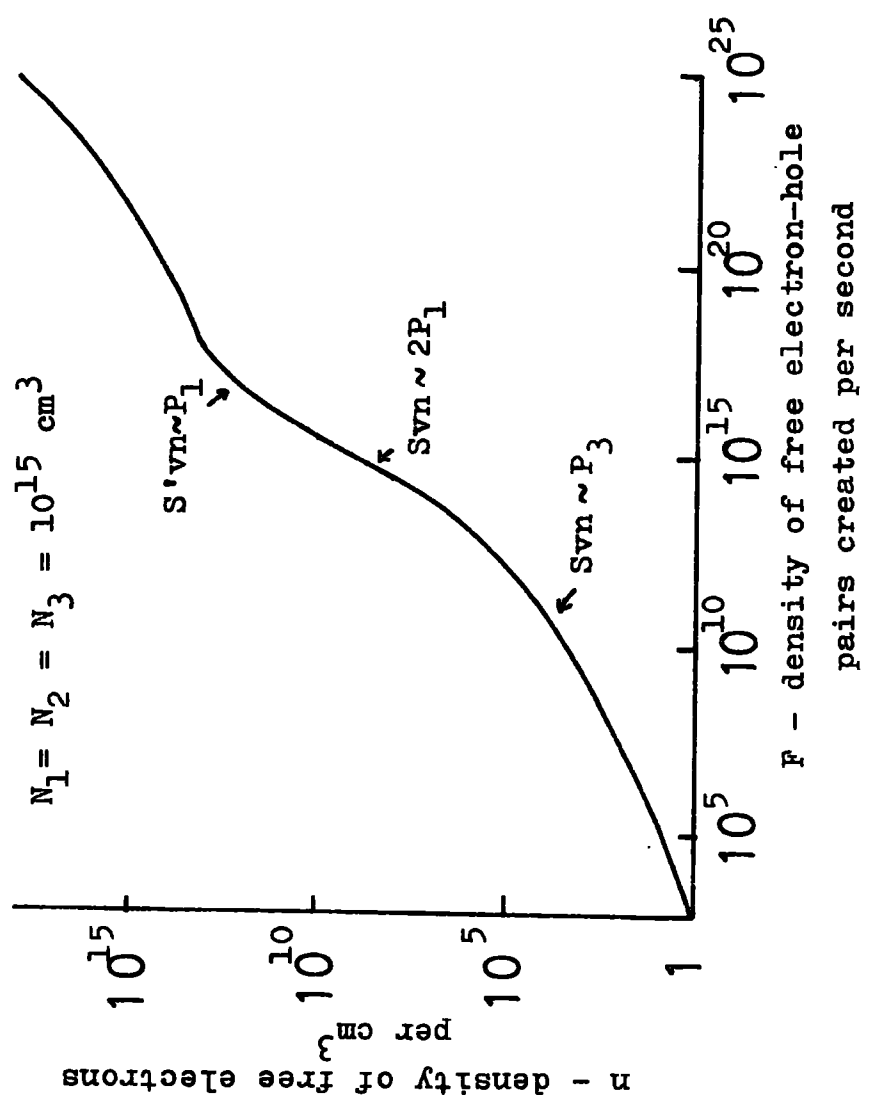
through centres 2 and keep the photosensitivity down.
In this region the density of free electrons varies
superlinearly with light intensity. At higher
intensities, when the hole demarcation level for
centres 1 lies well below levels 1, all the centres
contain trapped holes, and the free electron density
again varies linearly or sublinearly with excitation
intensity.

These calculations describe qualitatively the
variation of photosensitivity with light intensity
for many samples of CdS and also CdSe. Bube's
calculations with other values of N_3 showed similar
results, except that for values of $N_3 \gg N_1$ and N_2,
superlinearity is not found.

2c.   <u>Variation of Photosensitivity with Temperature</u>
The photoresponse against temperature can be
divided into three regions:-

a) at low temperatures $Sv_n n$, $Sv_p p \gg P_3$, and $\gg P_1$
and the crystal is sensitive since the hole demarcation
level for centres 1 lies below 1, and the electron
demarcation level for centres 3 lies above 3.

b) at intermediate temperatures $Sv_n n$, $Sv_p p \gg P_3$,
but $Sv_n n$, $Sv_p p \ll P_1$, and the crystal passes through

- 77 -

a thermal quenching temperature and has less sensitivity, because the hole demarcation level now lies above the centres 1. These latter now act as hole traps and not as recombination centres, and so the efficient recombination centres 2 can cause faster recombination.

c) at higher temperatures $Sv_v n$, $Sv_p p \langle P_3$, and $\langle\langle P_1$. The electron demarcation level lies below centres 3, and these centres cease to contribute to recombination. The photosensitivity begins to rise again because the number of recombination centres is reduced. The calculated curve for $N_1 = N_2 = N_3 = 10^{15} cm^{-3}$, and for $F = 10^{16} sec^{-1}$, is shown in fig. 5.3 for the regions a) and b) above.

Again these calculations describe the behaviour or photoconductivity with temperature in a qualitative way for cadmium sulphide and selenide. The opposing effects of light intensity and temperature can be seen, since increased light intensity causes the electron and hole demarcation levels to move away from each other, and increased temperature causes them to converge towards the centre of the forbidden gap. In practice the whole range of intensity variations cannot be observed at a single temperature, because of the experimental difficulties of obtaining a sufficiently large range of excitation intensities. Suitable use of different temperatures,
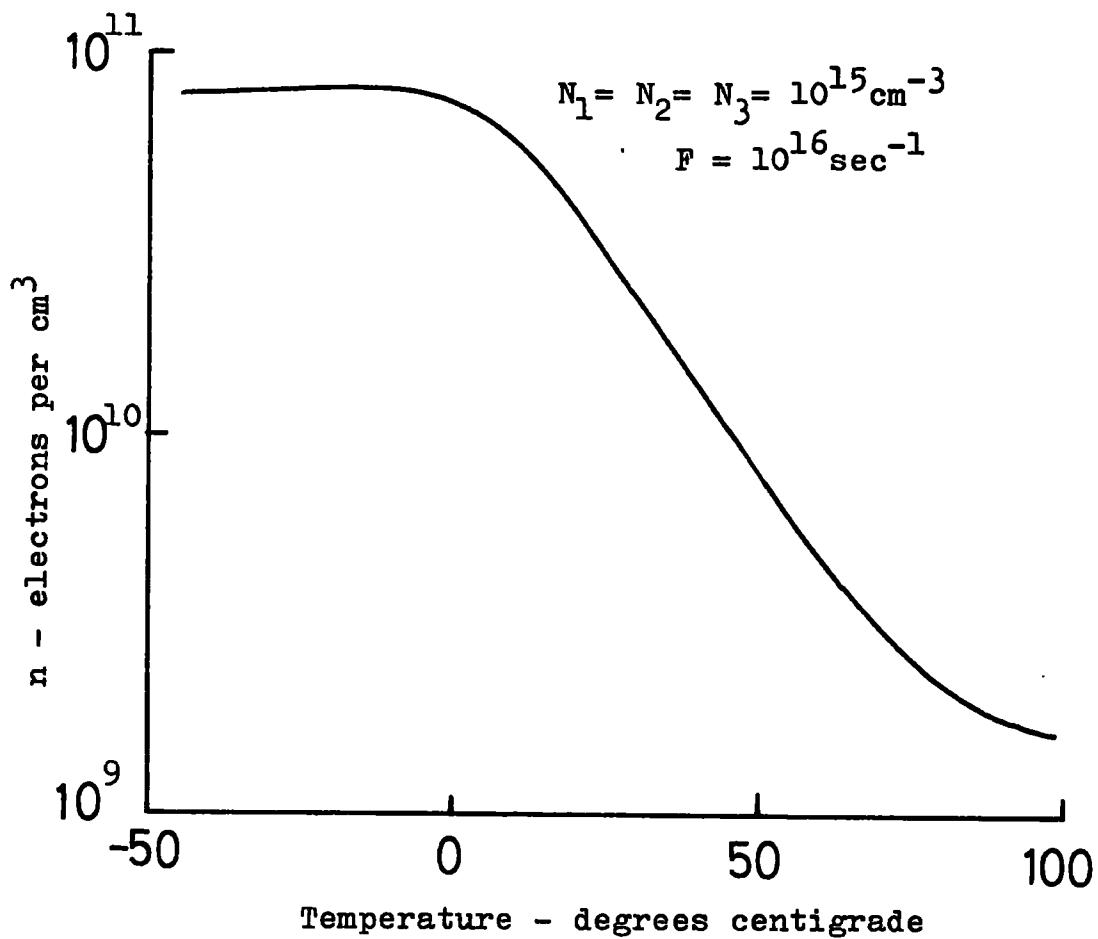
FIG. 5.3.

however, allows the different parts of the curve to be observed.

From the consideration of the onset and cessation of superlinearity in CdSe, Bube obtained a value of 8×10^5 for the ratio of the cross-section for hole capture to that for electron capture for centres 1. He also found that these centres lie 0.64 eV above the valence band. Using the same ratio for hole to electron capture cross-section, Bube determined that the sensitising centres lie 1.0 eV above the valence band for cadmium sulphide.

3. Photochemical and Heat Treatment Effects

3a. Methods of Measurement

The effects of light and low temperature heat treatment upon the properties of cadmium sulphide have been studied by many workers who have used a variety of techniques to study the changes that arise. The techniques include measurement of dark resistance, photoresistance, photocurrent against exciting wavelength, quenching spectra, thermally stimulated currents and measurement of photoluminescence both in the visible and infra-red ranges.

3b. Photochemical Changes in Recombination Centres

Boer (4) observed changes in photoconductivity that could not be explained by ordinary excitation or trapping of electrons. He found that only at temperatures below 50°C did the cessation of illumination cause the monotonic fall to the stationary value of the photocurrent which is expected. Above this temperature the photocurrent undershot the steady state value by as much as two orders of magnitude. Similarly following the onset of illumination overshoot was observed which could be five orders of magnitude greater than the final steady state value. Bube (5) has maintained that the phenomena of undershoot and overshoot can be explained by the relatively slow changes in occupation of two different types of recombination centre. However, Boer found that illumination at temperatures above 50°C and subsequent cooling to room temperature, caused the photoconductivity to be much less than it had been previously at that temperature. The original state could be regained by heating in the dark to above 50°C, and again recooling. This phenomenon could not be explained in terms of Bube's theory, and it was found necessary to introduce the idea of photochemical changes. To explain the observed effects,

Boer suggested that the effect of the light at high temperatures is to create recombination centres, that can be destroyed by baking in the dark at these temperatures. He gave no suggestions as to the chemical origin of these centres.

In special samples of copper doped CdSe, and iodine doped, sulphur compensated CdS, Bube (6) observed changes in photoconductivity which are similar to those described by Boer. Crystals that had been photochemically treated by illumination at high temperatures (PCT samples) were found to have greatly reduced sensitivity over the whole range of temperatures from -200 to +100°C. Calculations from measurements of photocurrent against light intensity, yielded the normal value of 1 eV for the distance of the recombination centres from the valence band, for samples in the untreated state. However, for the PCT samples a distribution of recombination centres, spread from 0.15 to 1.0 eV above the valence band was found. (A possible alternative explanation is that a centre exists in this region with a strongly temperature dependent cross-section.) Bube considered that these photochemically created centres took over the function of the normal sensitising centres which lie 1.0 eV from the valence band. He proposed that

the new centres were an agglomeration of cation

vacancies or Cu^+ ions, and that the effect of the

light was to remove the repulsive barriers between

the components, and thus facilitate agglomeration.

Bube found that the photochemical effects could be

produced by illumination at room temperatures, and

that the heating to above $150^{\circ}C$ was necessary to

restore the original condition of the samples. He

stressed that these were specially prepared samples,

and that no photochemical changes were found in the

centres with levels 1 eV above the valence band.

Borchardt (7) studied the changes produced in

the spectra of infra-red quenching of photoconductivity

by the occurrence of photochemical effects. The two

generally recognised quenching bands at about 1.45 and

0.92 microns, were seen, for both the normal and PCT

samples, but the latter type of crystal showed much

stronger quenching at both wavelengths. He found that

temperatures of about $300^{\circ}C$ were necessary for the

effects to occur, and that heating to temperatures of

the same order in the dark was required to destroy

these effects. In a later paper Borchardt (8) studied

the overshoot effect previously reported by Boer, and

found that the critical temperature, above which the

photochemical effects took place, varied a great deal from sample to sample, and could be as low as -35°C for pure CdS crystals. This was raised to $+130^{\circ}$C for the same samples after tempering in sulphur vapour. For this reason, it was considered that sulphur vacancies were the chief components of the centre affected. Measurement of photocurrent against exciting intensity for two states showed a linear response for the normal samples, and a superlinear response for the PCT samples. From this he concluded that the extra centres being created photochemically are the sensitising centres 1, of the photoconductivity model. (at 1 eV above the valence band.) These are also the centres involved in infra-red quenching. Borchardt considered that these centres are due to the sulphur vacancies becoming associated with cadmium vacancies under the influence of illumination above a certain critical temperature. The complexes formed, disassociate in the dark above this temperature.

Albers (9) measured the red luminescence of cadmium sulphide (0.73 microns) over a range of temperatures, and found that the luminescent intensity dropped as the temperature was raised. However, if the temperature was

then lowered again, it was found that the high temperature value of intensity was "frozen in". The higher value could be regained by heat treatment in the dark at between 150 and 200°C. This cycle was found to be repeatable indefinitely. He also found analogous behaviour of the green luminescence. In order to measure the true luminescent intensity variation with temperature, without causing photochemical effects, Albers (10) used light pulses of 4×10^{-2} seconds duration, and a ballistic method of measurement. The temperature variation of luminescence on the basis of the Schön-Klasens model, is of the form:-

$$\frac{I'}{I} - 1 = C \exp(E_{th}/kT) \qquad \text{Eq. 5.3}$$

I' is the maximum intensity of the luminescence, I is the intensity at temperature T, and C is a constant. E_{th} is the thermal energy separation of the centre from the valence band. A plot of $\ln\left[(I' - I)/I\right]$ against $1/T$ yields a value of E_{th} from the slope of the straight line obtained. The presence of photochemical effects obviously makes this calculation meaningless, and in practice, straight lines cannot usually be obtained. Albers' use of light pulses overcame this difficulty and yielded a value for E_{th} of 0.49 eV for the red luminescence.

The optical energy position for this band E_{op} is

0.87 eV above the valence band, when allowance is

made for the shift in band gap with temperature and

so the ratio E_{op}/E_{th} is 1.77. Albers also measured

the decrease of luminescence with time at a constant

temperature, and found that the exponential decay

obtained could be described by an equation of the

form:-

$$I(t) = (I_0 - I_\infty) \exp(-\gamma t) + I_\infty \qquad \text{Eq. 5.4}$$

I_0 is the initial, maximum intensity; I_∞ is

the value to which it decays for large t; and γ is a

constant.

Values of γ can be obtained from the experimental

results at different temperatures, and these are

related to temperature by the equation:-

$$\gamma(T) = \gamma_0 \exp(-E\gamma/kT) \qquad \text{Eq. 5.5}$$

where $E\gamma$ is the energy of creation for the photo-

chemical effect involved. Albers obtained a value for

$E\gamma$ of 0.74 eV. Kulp and Kelley (11) had shown that

the energy required to remove a sulphur atom from its

site in the lattice, is 8.7 eV. This value was obtained

by using a technique of electron bombardment. Albers'

value of energy of formation was obviously insufficient

to achieve displacement of a native atom from the lattice, and so he concluded that the effect of the light is to cause association of existing vacancies to form a complex. The effect of the light at elevated temperatures, is to create new recombination centres that thus reduce the number of electron hole pairs recombining through the luminescent centres. This is the same explanation proposed by Bube and Borchardt, although no information is obtained as to whether the new recombination centres are at 1 eV above the valence band, as suggested by Borchardt, or are at shallower depths as proposed by Bube.


3c. Photochemical Changes in Electron Traps

Woods and Wright (12) noted that the effect of strong illumination at temperatures above -40°C on their samples of cadmium sulphide, was to cause the disappearance of a sharp T.S.C. peak with a maximum at 0°C, and greatly to enhance a second peak at $+60^{\circ}$C. The photocurrent against temperature curves showed a similar behaviour to that reported by Bube (6). The 0°C peak could be regained by heating in the dark at 100°C. The trap causing this peak was assigned a depth of 0.50 eV below the conduction band, using

Bube's method of T.S.C. analysis. Because this
behaviour was found only in cadmium rich samples,
it was assumed that the trap was due to sulphur
vacancies. They proposed that the effect of the
light was to produce cadmium vacancies by a process
of photochemical deposition of cadmium from the
lattice at dislocations. The sulphur vacancies then
associate with the cadmium vacancies, and give rise
to the peak at 60°C. As this happens, the trap
emptying at 0°C is destroyed. Heating at 100°C
causes dissociation of the cadmium and sulphur
vacancies complex. In a later paper Woods (13)
obtained further evidence for the above hypothesis,
when he noted that the original state cannot be
completely regained from the PCT samples by heat
treatment in the dark. The effect of the heat
treatment is to cause some loss of cadmium, and so
repetition of the cycle of treatment causes a gradual
increase in the concentration of cadmium vacancies.
This is seen as a gradual decrease in the height of
the 0°C peak, and also as an increase in the height
of a peak with a maximum at -100°C. In the first
paper, Woods and Wright had associated this peak with
cadmium vacancies.

Woods and Nicholas (14) divided their samples into two categories, i.e. cadmium rich and sulphur rich. They found photochemical effects in both kinds of crystal, although of very different natures. From measurement of T.S.C. curves they found that in cadmium rich samples a set of traps at 0.25 eV below the conduction band could be changed by photochemical treatment into two new traps at 0.41 and 0.83 eV below the conduction band. The process was reversible, and the 0.25 trap could be regained by heat treatment at $100^{\circ}C$ in the dark. The 0.25 eV trap was not found in sulphur rich samples, and heat treated crystals showed no T.S.C. peaks. The 0.41 and 0.83 eV traps could be produced by illumination at around $0^{\circ}C$, and a further set of traps was observed at 0.63 eV after illumination at above $+80^{\circ}C$. The trap at 0.83 eV below the conduction band was found to have a capture cross-section of $10^{-14} cm^2$, which meant that it should have been a fast retrapping centre. However, photoconductive decay measurements showed that it emptied monomolecularly. Essentially the same theory is used to explain the behaviour of these traps as had been used in the earlier papers. (The trap at 0.5 eV in the previous paper could be the same as the 0.83 eV trap proposed here, because of the different methods of analysis used.) The reason

for the anomalous behaviour of the 0.83 eV trap is
that although it has a large capture cross-section,
it cannot take part in retrapping since it dissociates
as soon as it loses an electron.

Trofimenko et al. (15) found very similar
behaviour for sulphur doped crystals to that found by
Woods et al. Two T.S.C. peaks at around $0^{o}C$ could be
removed by illumination between +15 and -75° C whilst
cooling from $100^{o}C$, and they could be replaced by a
third peak at $65^{o}C$. To explain these phenomena, they
proposed the energy scheme shown in fig. 5.4. Three
traps closely associated in the lattice are surrounded
by a potential barrier of height E when empty, which
becomes even higher when any of the traps are filled.
The traps have capture cross-sections for electrons S_1,
S_2 and S_3 which vary with temperature, so that at above
$+15^{o}C$, $S_1 \rangle S_2$, S_3; and below $-75^{o}C$, $S_1 \langle S_2, S_3$. At low
temperatures E_2 and E_3 fill preferentially, and raise
the height of the barrier, so that E_1 cannot be filled.
At high temperatures E_1 fills, and does not allow E_2
and E_3 to be filled. They obtained values for E_1, E_2
and E_3 of 0.65, 0.45 and 0.4 eV. One difficulty with
their model is that they obtained a value of E between
0.7 and 1.0 eV, and it is difficult to see how E_1, E_2
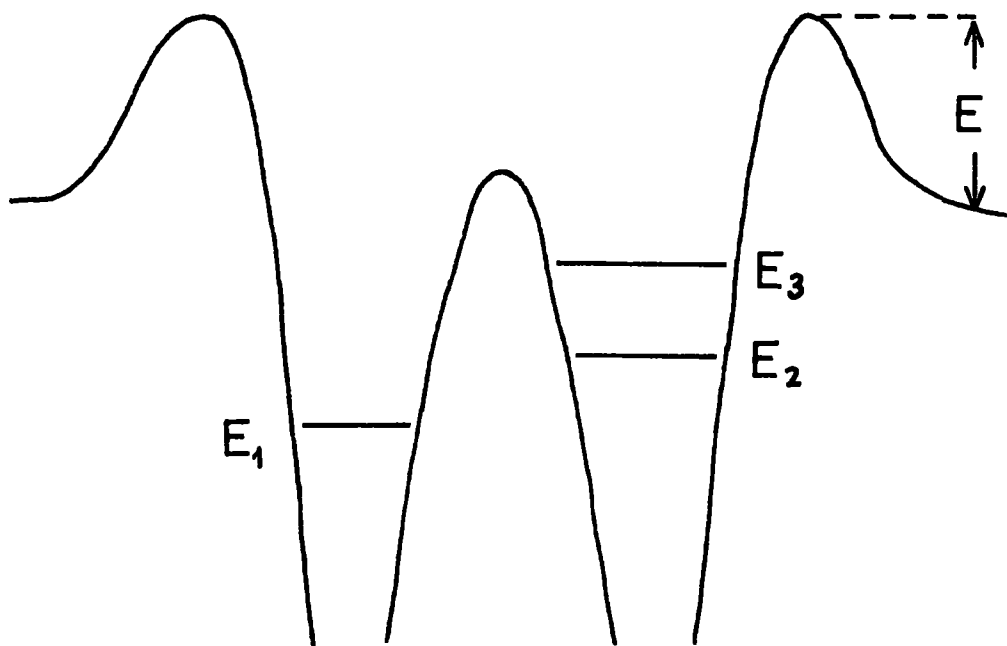
Trapping Centre Surrounded by a
Potential Barrier

FIG. 5.4.

E_3 can be less than E. Bube et al. (16), obtained similar results on CdS-CdSe crystals, and proposed a similar explanation to that just described. They found a trap at 0.73 eV below the conduction band which could be created by photochemical treatment. This trap also had a large capture cross-section, but emptied monomolecularly, as had been found for the 0.83 eV trap studied by Woods and Nicholas. Bube obtained a barrier height of 0.28 eV.

Korsunskaya et al. (17) found one low temperature peak in T.S.C. measurements on samples of pure CdS, after cooling in the dark, and a further four maxima for samples cooled in the light. Two of these new sets of traps occurred at low temperatures, and two at around 0°C. Because the two low temperature traps could be refilled at the lowest temperature after thermal emptying, as long as the high temperature traps were not emptied, they discounted the possibility of a potential barrier, and again proposed the existence of photochemical effects. Once more the cause is attributed to the association of sulphur and cadmium vacancies, and it is proposed that all four traps are connected with one original complex. They also studied

the photochemical creation of recombination centres by
measurement of photoconductive decay and spectral
response of photocurrent, and found that new
recombination centres are formed at the same time as
the new traps. These were considered also to be part
of the same complex. The energies of creation for all
the types of centre were between 0.15 and 0.3 eV,
although the reason for different parts of the same
complex having different energies of creation is
difficult to understand.

Bryant and Cox (18) correlated the photochemical
changes observed in the infra-red luminescence of CdS,
with the changes seen in the T.S.C. curves. They used
a temperature of $220^{\circ}C$ for light treatment, and found
that this caused the 1.02 micron emission band to grow
larger, and the 0.73 micron band to decrease with a
reaction enthalpy of 1.32 eV. The opposite effect was
produced by heat treatment in the dark at this temperature,
but this time with an associated energy constant of 0.42
eV. The intensity of emission bands at 1.5 to 2.2
microns was found to be enhanced by heat treatment under
illumination at high temperatures. For this process a
range of activation energies of 0.19 to 0.30 eV was

found. A maximum in the T.S.C. measurements at 100°C
was found to appear as the luminescence grew, and
Bryant and Cox proposed that both are due to the same
centre. The trap depth was calculated to be 0.86 eV,
and as the optical energy of the luminescence would
be 1.68 eV at 100°C, this gives a ratio of 1.95 for
the optical to the thermal depth of the centre.

3d. <u>The Effect of the Ambient Atmosphere</u>

The effects of oxygen and other gases upon
different types of measurement on CdS have been reported
by many workers. The purpose of this section is not to
summarise these, but just to mention the work of Mark
(19) (20) in this connection. He has studied the
phenomenon of overshoot of photoconductivity in CdS, and
has attributed it to the presence of oxygen on the
surfaces of the samples. In his work this may well
have been the cause, but the other results on this
subject, previously mentioned, have been taken from
measurements in a variety of atmospheres and degrees of
high vacuum. For this reason it is assumed that these
are genuine photochemical effects, and cannot be due to
the presence of oxygen. Mark obtained a value of 0.90
eV for the activation energy of the adsorption process,

which agrees well with the values obtained for the photochemical process reported by other workers.

4. Conclusion

From table I, it can be seen that the values of activation energy for the photochemical creation fall neatly into two groups. The low energy group ranges from 0.15 to 0.3 eV and the values at high energy from 0.7 to 1.0 eV. The only exceptions to this are the values obtained by Bryant and Cox for the creation and destruction of the 1.02 micron emission band in CdS. (1.32 and 0.42 eV) The low energy value of the activation energy is associated with the creation of one or two T.S.C. peaks at around 0°C, (one of depth 0.83 eV, according to Woods and Nicholas) and is seen in pure or cadmium doped crystals. The higher value of activation energy is seen in sulphur doped or high resistance samples, and is associated with the creation of both a T.S.C. maximum at 60 to 65°C, and recombination centres in the bottom half of the forbidden energy gap. Estimates of the exact location of the new recombination centres vary from 0.15 to 1.0 eV above the valence band.

The idea of a potential barrier having an effect upon trap filling may be correct, although this sort of effect cannot explain the changes in luminescence observed. Photochemical effects do occur in CdS, and since the energies of creation obtained from overshoot and luminescence fit with those obtained from T.S.C. curves, it seems probable that the changes in T.S.C. trap spectra are also due to a photochemical effect.

The explanation of the results of Bryant and Cox may be that they were studying a different kind of photochemical effect from that seen by the other workers, or it may be that in their samples they had other recombination centres changing photochemically at the same time as the ones under study. This could have caused some distortion of their results.

It would seem that at least two types of photochemical effect take place in cadmium sulphide; perhaps one involving principally sulphur vacancies with an activation energy of ~ 0.2 eV, and the other with an activation energy of ~ 0.8 eV involving mainly cadmium vacancies.

References for Chapter Five

1. Schön M., 1954, Physica, 20, 930.

2. Klasens H.A., 1958, J. Phys. Chem. Solids, 7, 175

3. Bube R.H., 1957, J.Phys.Chem.Solids, 1, 234.

4. Boer K.W., 1954, Physica, 20, 1103.

5. Bube R.H., 196 , Photoconductivity of Solids,
   John Wiley and Sons, New York.

6. Bube R.H., 1959, J.Chem.Phys., 30, 266.

7. Borchardt W., 1961, phys.stat.sol., 1, K52.

8. Borchardt W., 1962,   "   "   "   2, 1575.

9. Albers K., 1961,   "   "   "   1, K58.

10. Albers K., 1962,   "   "   "   2, 1268.

11. Kulp B.A., and Kelley R.H., 1960, J.Appl.Phys.,31,1057

12. Woods J. and Wright D.A., 1958, Proc.Internat.Conf.,
    Brussels, 880.

13. Woods J., 1958, J.Elec. and Control, 5, 417.

14. Woods J. and Nicholas K.H., 1964, Brit.J.Appl.Phys.,
    15, 1361.

15. Trofimenko A.P., Fedorus G.A. and Sheinkman M.K., 1964,
    Sov. Phys.-Sol.State, 5, 1316

16. Bube, R.H., Dussel G.A., Ho C-T., Miller L.D., 1966,
    J. Appl.Phys., 37, 21.

17. Korsunskaya N.E., Markevich I.V., and Sheinkman M.K.,

        1966, phys.stat.sol., $\underline{13}$, 25.

18. Bryant F.J. and Cox A.F.J., 1965, Brit.J.Appl.Phys.,

        $\underline{16}$, 1065.

19. Mark P., 1964, J.Phys.Chem.Sol., $\underline{25}$, 911

20. Mark P., 1965, "   "   "   " $\underline{26}$, 959

CHAPTER SIX

EXPERIMENTAL APPARATUS

1. Introduction

The measurements made can be divided into two types – electrical and optical. Although these two were often made simultaneously, the description of the apparatus involved is divided into two parts. First, however, the cryostat and the method of temperature measurement will be described, since these are necessary for both kinds of experiment.

2. The Cryostat

The cryostat is shown in fig. 6.1. Its main chamber was milled out of a copper block. It contained a window (window 1) in one of its sides. The double walled neck consisted of german silver tubes soldered to each other through a brass ring. The solid copper block on which the sample was mounted was soldered to the inner of the two tubes. It was bored out in the middle to allow the heater to lodge in it. One octagonal face of the cryostat was open to allow access. The face could be closed by a copper plate containing another window (window 2). Both
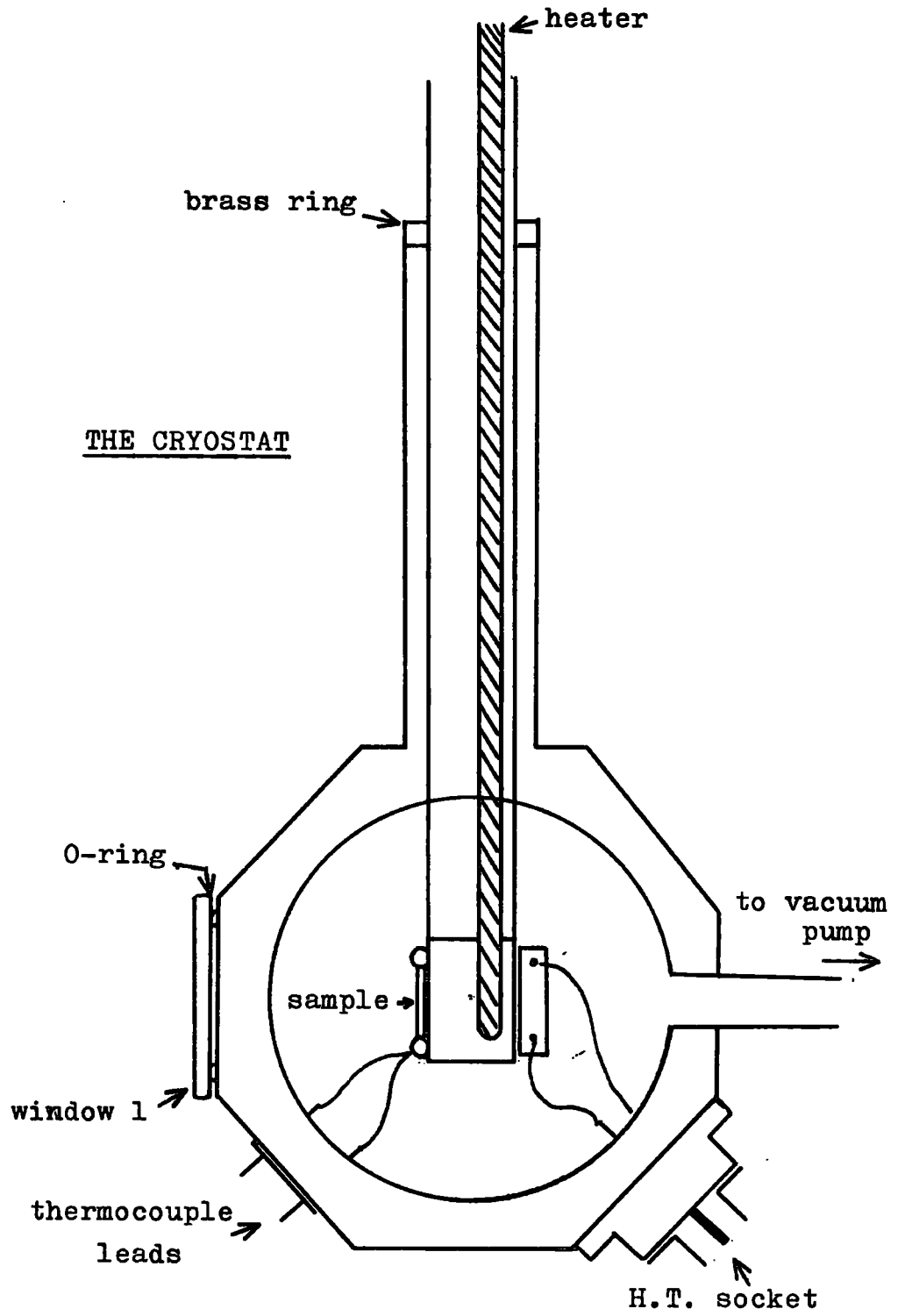
THE CRYOSTAT

FIG. 6.1.

windows were quartz glass, and could be made light proof
by special covers. The thermocouple and H.T. leads were
led out of the cryostat through glass-to-metal seals.
The H.T. leads were further connected to a coaxial socket.
A silica microscope cover slip was fixed to the copper
block with araldite, and the sample mounted on top of
this. The sample was held down by the indium contacts
that were melted on. The thermocouple junction was
immersed in one of these contacts. The thermocouple
consisted of copper-constantan, and the reference junction
was kept in a mixture of water and ice. The thermocouple
voltage was read by means of a potentiometer, and was
recorded by marking the thermocouple readings on the
current trace from the pen recorder. The cryostat was
evacuated to a pressure of 10^{-5} torr by a mercury diffusion
pump and a rotary backing pump. It was cooled by pouring
liquid nitrogen into the inner tube, and was warmed up by
the heater, which could be set for different heating rates.

3. <u>The Circuit for Thermally Stimulated Current Measurement</u>

The circuit used for the measurement of thermally
stimulated currents is shown in fig. 6.2. The voltage was
supplied by a battery power pack, and the voltage across
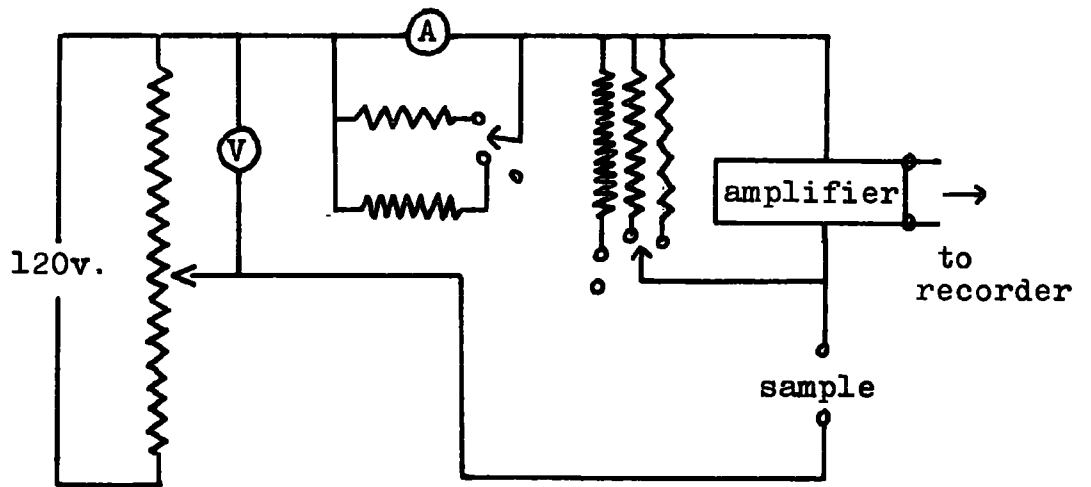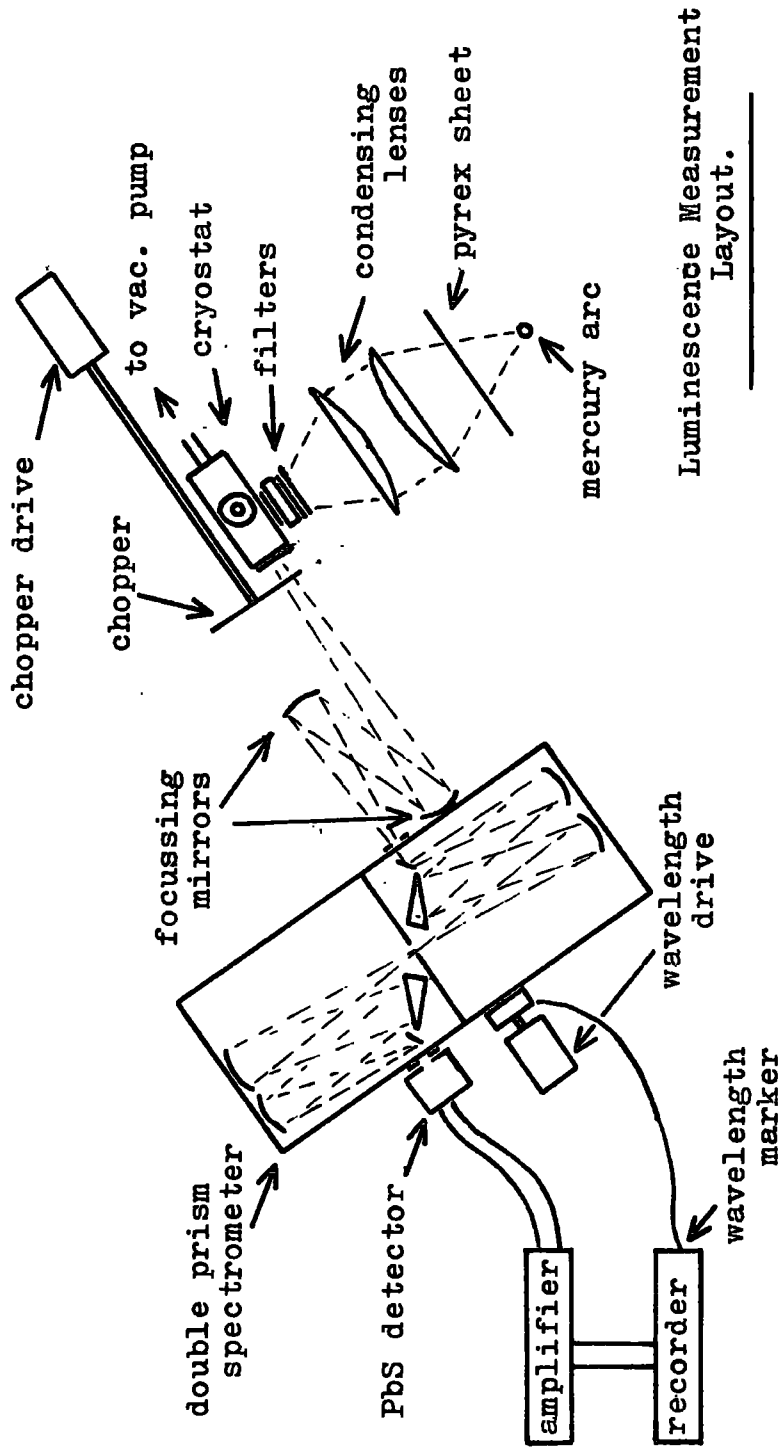
T.S.C. Measurement Circuit

FIG. 6.2.

the sample was variable from 0 to 100 volts. The ammeter
A, was a microammeter used for photoconductivity
measurements. Parallel resistances could be switched
in to allow for full-scale deflection readings of 10μa,
100μa and 1 ma. The D.C. amplifier had an input
resistance of 50 ohms, and allowed detection of currents
down to 10^{-11} amps. The amplifier had four sensitivity
ranges, 10^{-11} amps, and 10dB, 20dB and 30dB down on this.
Further resistances could also be switched in parallel
with the amplifier to bring the sensitivity down, by a
maximum of 80dB.

4. Infra-red Luminescence Measurements

The arrangement for the luminescence measurements is
shown in fig. 6.3. The exciting radiation was provided
by a mercury point source arc. This was focussed on to
the sample by two six inch diameter, ten inch focal length,
condenser lenses. Between the source and the lenses was an
eighth inch pyrex plate, to remove enough of the infra-red
radiation to avoid cracking the lenses. The remaining
infra-red was removed by two .Chance filters, ON 10 and one
centimetre of 10% copper sulphate solution. The visible
radiation was not removed from the incident light, because
its removal was found to decrease the infra-red emission

chopper drive

to vac. pump

cryostat

filters

condensing
lenses

pyrex sheet

chopper

mercury arc

focussing
mirrors

double prism
spectrometer

PbS detector

wavelength
drive

wavelength
marker

amplifier

recorder

Luminescence Measurement
Layout.

FIG. 6.3.

by two orders of magnitude. The emitted radiation was collected and focussed on the slit of the spectrometer by two focussing mirrors. The spectrometer was a Barr and Stroud double prism spectrometer type VL2, containing quartz prisms. The input signal was mechanically chopped at 800 c.p.s., and was detected at the output slit by a lead sulphide detector. The signal was amplified by an amplifier tuned to 800 c.p.s., and the output from this drove a pen recorder. The wavelength drive on the spectrometer could be driven by a six speed gear box, and had facilities for marking the wavelength on the recorder paper. The response of the lead sulphide detector was calculated by using a thermopile as a detector, and a tungsten lamp source. Because of the slow response of the thermopile, the input signal could only be chopped at 10 c.p.s., and the amplifier had also to have its filters changed to this frequency.

CHAPTER SEVEN

CRYSTALS GROWN IN SEALED TUBES

1. Introduction

In order to study the photochemical effects that occur in CdS, it is not sufficient to use measurements of one isolated property only. The heights of T.S.C. maxima depend upon the number and kind of recombination centres present, as well as the density of trapping centres causing the maxima, so that photochemical changes in the T.S.C. spectra can be due to changes in the trapping centres themselves, or to changes in the recombination centres. In order to study both kinds of centre at the same time, the following procedure was used:- The sample was heating to $390^{\circ}K$ in order to have it in some known state before each set of measurements. It was then cooled to liquid nitrogen temperature. During cooling the illumination was allowed to fall on the sample over different termperature ranges in order to produce the photochemical effects to be studied. In most cases the illumination was started at a variable temperature, T_r, and continued down to liquid nitrogen temperature. The source of the illumination was

- 101 -

described in chapter six. Its intensity was 5,000 foot
candles. At liquid nitrogen temperature, the infra-red
luminescence was measured first, after which the
illumination was removed. The sample was then reheated
to 390^OK, at a constant heating rate, and a thermally
stimulated current was obtained. The measurement of
the infra-red luminescence gave information about the
state of the recombination centres immediately prior
to the measurement of the trapping spectra.

The results described in this chapter were obtained
from measurements on a crystal of CdS, which had been
part of a large single crystal, grown by a pulling
technique at a temperature of $1,100^O$C. The sample had
a dark resistivity of 10^{11} ohm cm. at room temperature.
The results described below are typical of the high
resistance samples grown by the pulling method.

2. <u>Trapping Spectra</u>

The thermally stimulated current spectra following
the different irradiation treatments, all showed four
peaks, as can be seen in fig. 7.1. Values of trap
depth of 0.2, 0.16, 0.25 and 0.33 eV, were obtained for
peaks 1, 2, 3 and 4 respectively, using a variety of
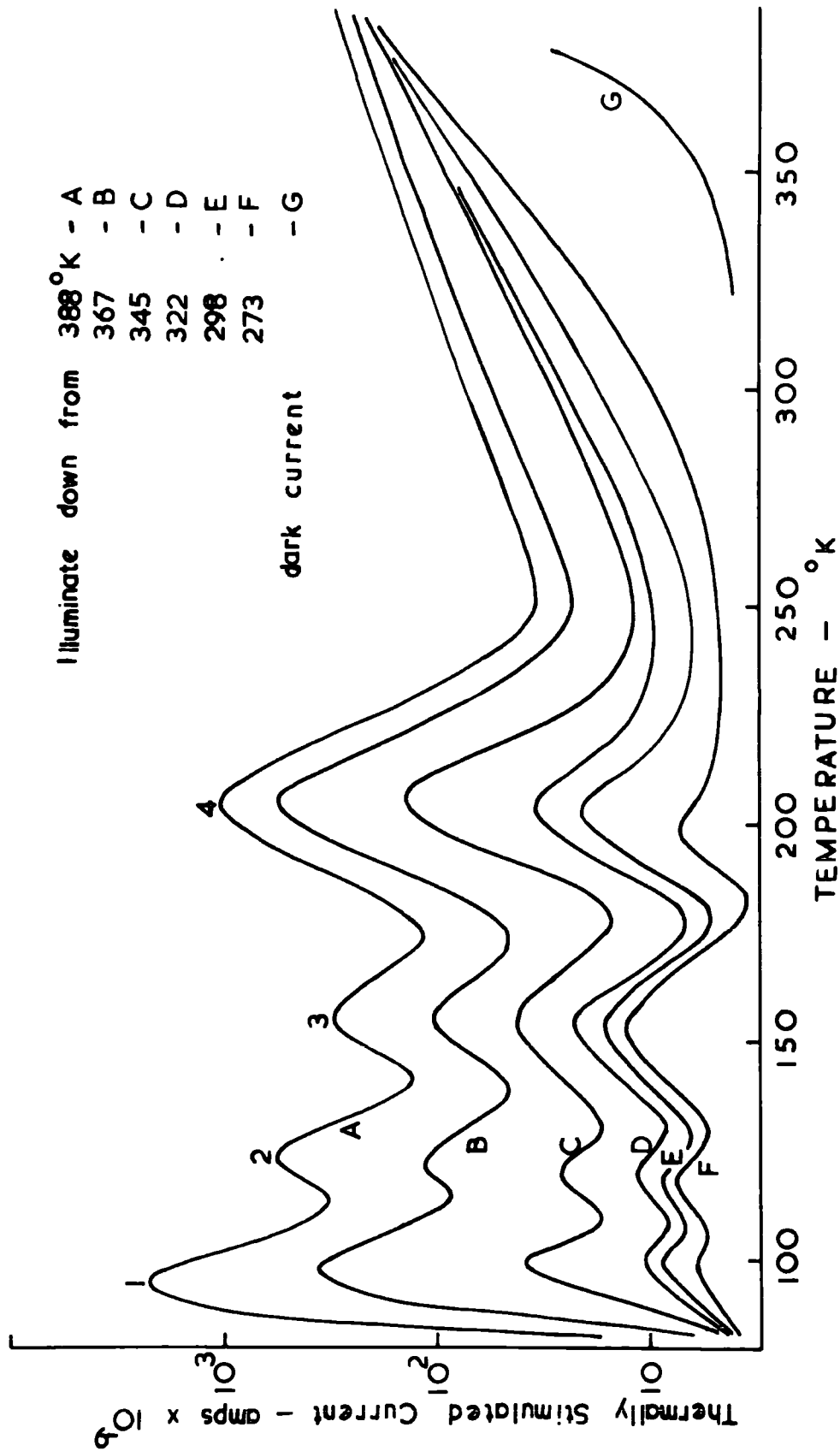
- 102 -

FIG. 7.1.

the analytical methods described in chapter three, and the results from several runs. The high temperature part of the curves yielded a value of 0.67 eV, using Garlick and Gibson's method in conjunction with thermal cleaning.

2.a. Peak at 98°K.

The lowest temperature peak yielded a wide spread of values for trap depth which varied around a mean value of 0.2 eV. It was assumed that this spread was due to two causes:- 1) liquid nitrogen temperature is not sufficiently low for the whole of the peak to be observed, and 2) it is experimentally difficult to obtain linear heating rates at temperatures just above the initial temperature. To obtain information about these two factors, an attempt was made to plot the theoretical curve for this peak.

The equation for the T.S.C. curve obtained from the thermal emptying of a monomolecular centre is given by eq. 3.5 :-

$$\sigma = n_{to} \, \tau e \mu \nu \, \exp\left[-E/kT - \int_{T_0}^{T} \frac{\nu}{\beta} \, \exp(-E/kT) dT \right]$$

If one assumes that ν is temperature independent, which is equivalent to saying $S_T \propto T^{-2}$, this can be

rewritten:-

$$\sigma = A \exp\left[(-t) + B \int_{t_0}^{t} \exp(-t).t^{-2}dt.\right] \qquad \text{Eq. 7.1}$$

where $t = E/kT$; A and B are constants; and $B = \dfrac{\mathcal{V}\,E.}{\beta\,k}$
The mobility is proportional to $T^{-3/2}$, and $\mathcal{V}$ may also
be temperature dependent, but for the present purposes
they can be assumed to be essentially constant over the
temperature range of a single peak.

Integrating by parts, gives:-

$$\sigma = A \exp\left[-t + B\left\{-\frac{e^{-t}}{t} - \int_{t_0}^{t} e^{-t}.t^{-1}dt\right\}\right] \qquad \text{Eq. 7.2}$$

The integral in the above equation is a standard
integral for which values have been tabulated. However,
for large values of t, it can be approximated to:-

$$\int_{t_0}^{t} e^{-t}/t\ dt = \left[(e^{-t}/t) - (e^{-t}/t^2 + \ldots \right]\Big|_{t_0}^{t} \qquad \text{Eq. 7.2.a}$$

Resubstitution of this in eq. 7.2, causes two of the
terms to cancel out, and the equation becomes:-

$$= A \exp\left[-t - B(e^{-t}.t^{-2})\ \Big|_{t_0}^{t}\right] \qquad \text{Eq. 7.3}$$

If the initial temperature is well below the
temperature span of the T.S.C. curve, then $e^{-t}/t^2 \gg e^{-t_0}/t_0^2$,
and the limits can be ignored.

Differentiation of σ with respect to t, gives the
equation:-

$$\frac{d\sigma}{dt} = A \exp \left[\; \right] \; x \; \left[-1 + B.e^{-t}.t^{-3}(t + 2) \right]$$

Equating this to zero to find the conditions at the maximum, yields the expression:-

$$B = e^{t*}.t^{*3}/(t* + 2) \qquad \text{Eq. 7.4}$$

Since the value of B cannot be determined accurately, the experimental value of t* can be inserted in Eq. 7.4, to give a value of B, for which the theoretical curve will have a maximum at the correct temperature. This value of B can then be used to plot the theoretical curve using Eq. 7.3 and thus to decide whether the experimental value of trap depth fits the theory.

A value of $B = 2.9 \times 10^{12}$ was obtained for peak 1, using eq. 7.4, and a value of $E = 0.2$ eV. In fig. 7.2, the experimental curve is shown as points, and the values obtained from the theoretical eq. 7.3, are shown as a full curve. It can be seen that although the high temperature side of the curve fits quite well with theory, the leading edge does not. The disparity at low temperatures shows that the initial temperature was not sufficiently low for the theoretical curve to be obtained, because the assumptions made in deriving the equation for the curve, require T_0 to be appreciably lower than the
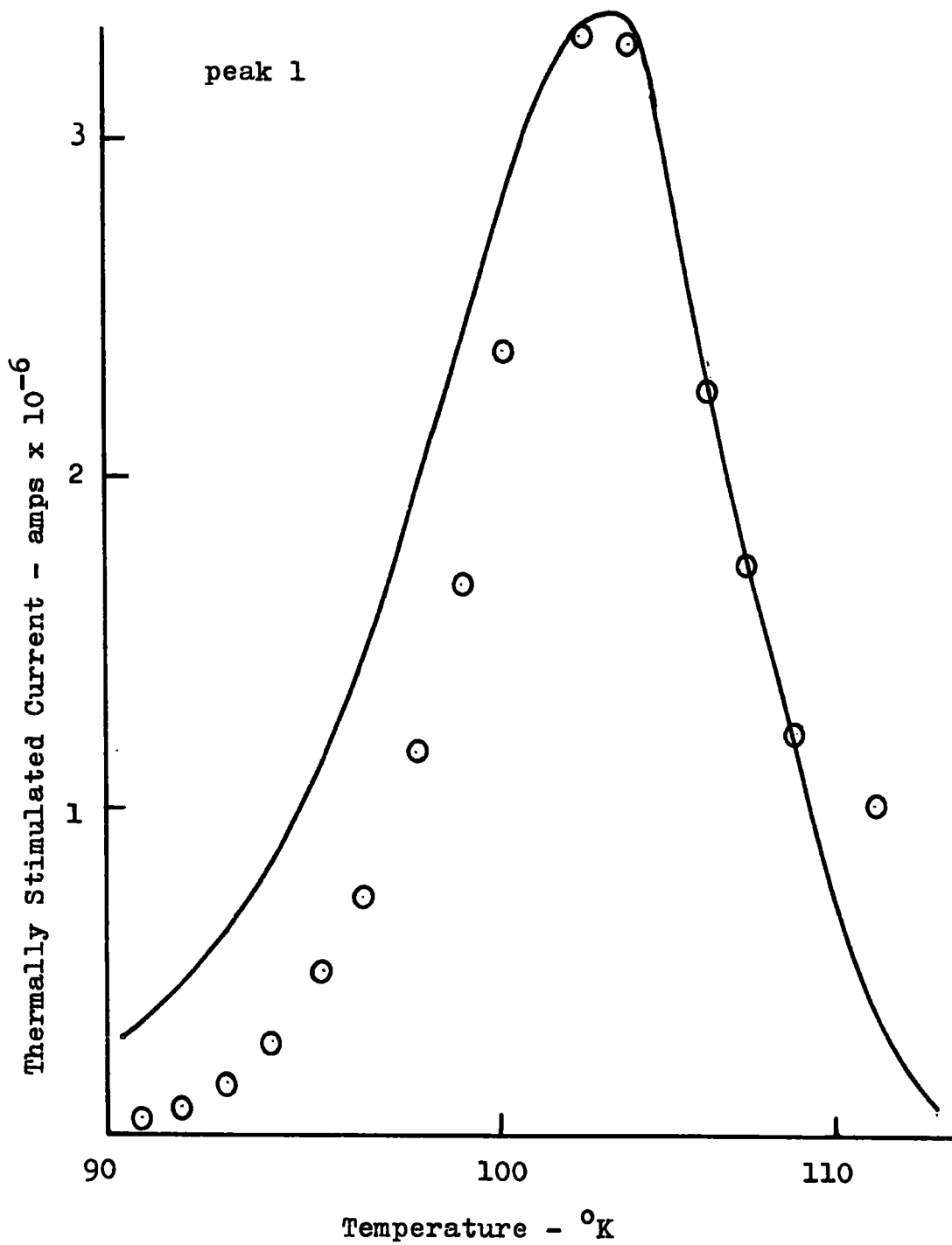
FIG. 7.2.

temperature of the maximum. In deriving eq. 7.3, it was assumed that $e^{-t}/t^2 \gg e^{-t_0}/t_0^2$. For e^{-t_0}/t_0^2 to be one per cent of e^{-t}/t^2, t_0 must be lower than t^* by approximately 4. For this curve, with a maximum at about $100^{\circ}K$, it would mean that a value of $T_0 = 70^{\circ}K$ would be needed. In practice T_0 was $85^{\circ}K$, which is obviously too high. However, if the curve is plotted taking into account the value of T_0, it is found to be the same shape as before, and the only difference is that a higher constant is needed to normalise the curve to the experimental one. The insufficiently low starting temperature will thus only lead to miscalculation of trap densities, and not of trap depth. The reason for the distortion of the T.S.C. peak must then be insufficiently linear heating rates at these low temperatures, and it is this that causes the uncertainty in the values of trap depth.

Because of this distortion of the T.S.C. curve, the values of trap depth evaluated by most of the methods described in chapter three are too high, so that no very exact value of trap depth can be quoted for this centre.

Since $B = E\mathcal{V}/\beta k$, and $\mathcal{V} = N_c v S_T$, a value of S_T, the electron capture cross-section for the trap, can be

obtained once B is known. A value of $6.7 \times 10^{-18} \, cm^2$ is obtained for this centre, which suggests that it is due to a defect that has zero electrical charge.

Use of Grossweiner's equation (eq. 3.10) for the capture cross-section, yields a value of $S_T = 5.8 \times 10^{-18}$ cm^2, which is in good agreement with the value obtained from the previous method.

From eq. 7.1, it can be seen that:-

$$A = n_{to} \, \tau \, e \mu \vartheta, \text{ and since } \vartheta = N_c v S_T,$$

$$A = n_{to} \, \tau \, e \mu N_c v S_T$$

A is the adjustable factor required to make the theoretical curve fit the experimental one. From a knowledge of A, values of n_{to} can be obtained, provided that one knows the value of τ. For this peak, a value of $\tau = 1.25 \times 10^{-5}$ seconds was obtained from measurement of the photoconductive gain. This yields a trap density of $n_{to} = 1.3 \times 10^{18}$ per cm^3. Because of the high intensity of the exciting radiation, and the appreciable length of time for which the excitation was maintained, it was assumed that n_{to}, the number of traps initially filled, was the same as the number of traps existing in the lattice.

Because of the distortion of the T.S.C. curve for
these traps, and the consequent possible error in the
value obtained for trap depth, further errors will
have been introduced to the calculations of trap density
and capture cross-section. The true value of capture
cross-section will tend to be less than that obtained
experimentally; similarly, the value of trap density
provides an upper limit.

2..b. <u>Peaks at 120 and 150°K</u>

Application of the standard techniques of analysis
to the results from several runs, yielded values of trap
depth of 0..16 and 0.25 eV for these two peaks. The
large spread of values obtained for the peak at 120°K,
suggests that this peak is also distorted because the
heating rate is not linear just above the starting
temperature. The values of trap depth agree with those
of Nicholas and Woods, who found traps at 0..14 and 0.25
eV below the conduction band. Fig. 7.3 shows the
experimental curves plotted as continuous lines, and the
theoretical shapes as shown as points. It can be seen
that in neither case do the points fit the curves, and
it was necessary to assume values of trap depth of 0.18
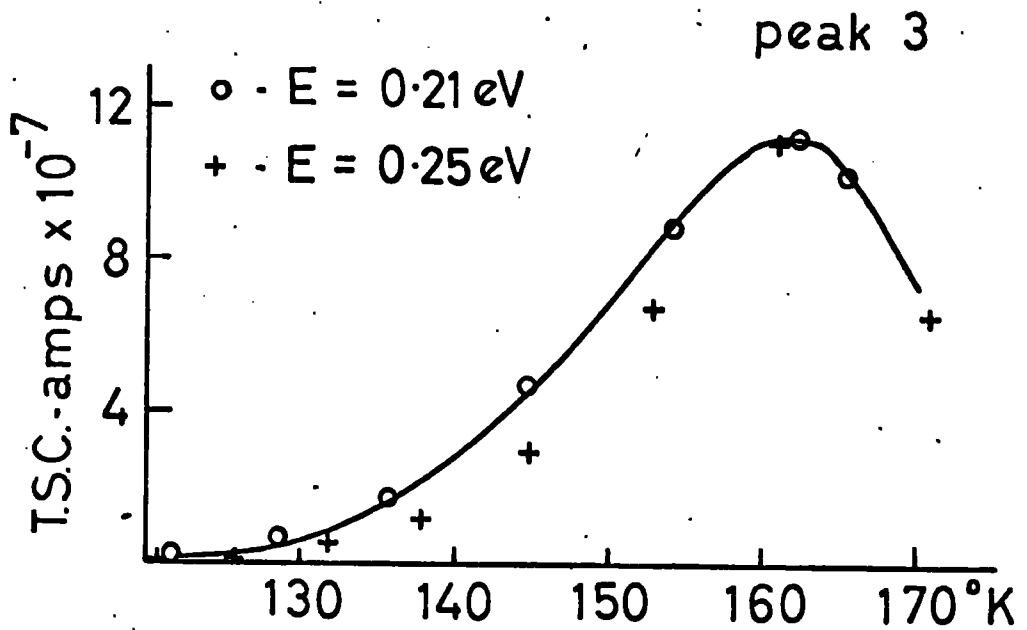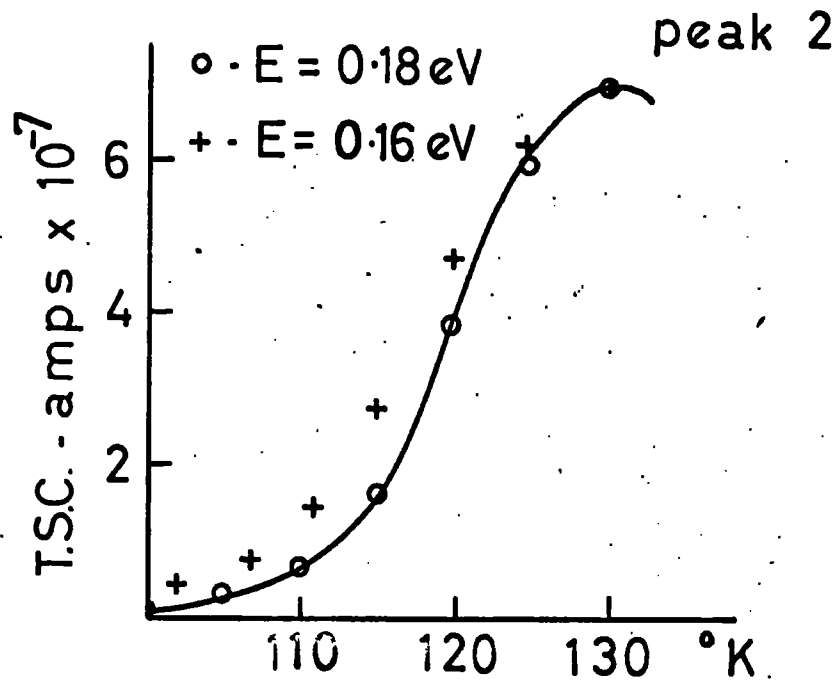and 0.21 eV respectively, in order to obtain a good fit.

FIG. 7.3.

Values of capture cross-section of 4.6×10^{-20} and $3 \times 10^{-21} cm^2$, and trap densities of 2×10^{14} and 1.3×10^{15} per cm^3, were obtained for the traps at 0.18 and 0.21 eV below the conduction band respectively.

2.c. Peak at $230^{o}K$.

Because of the fact that Nicholas and Woods, unlike several other authors, had found no traps at 0.3 eV below the conduction band, these centres were studied more thoroughly to try and determine the exact value of trap depth. The reason for this was that the various methods of chapter three, when applied to this peak, had led to a value of 0.33 eV. Using the method of analysis described in section 2.a., a value of B = 5.6 x 10^8 was obtained. Points from the theoretical curve for this trap were plotted and compared with the experimental curve, fig. 7.4.a. It can be seen that the points do not lie on the curve. Using a value of 0.30 eV, the points can be made to fit better on the leading edge, but again the high temperature side of the peak does not fit. This suggests that the trapping centre is, in fact, double. To elucidate this situation, a slower heating rate was used (0.1 instead of $0.5^{o}C$ per second), and the resultant curve shown in fig. 7.4.b confirms that this
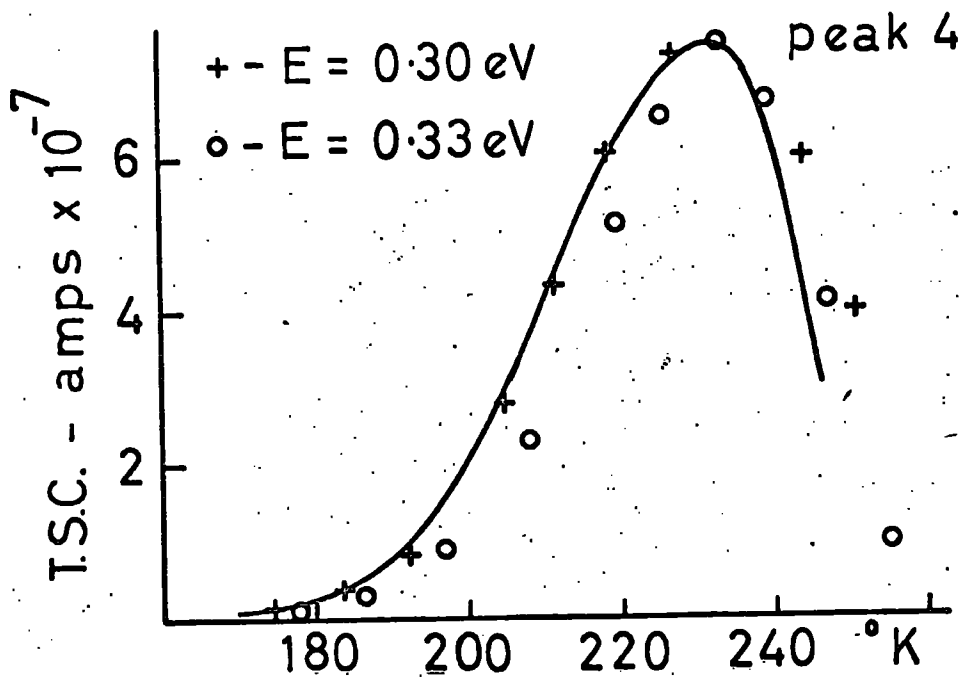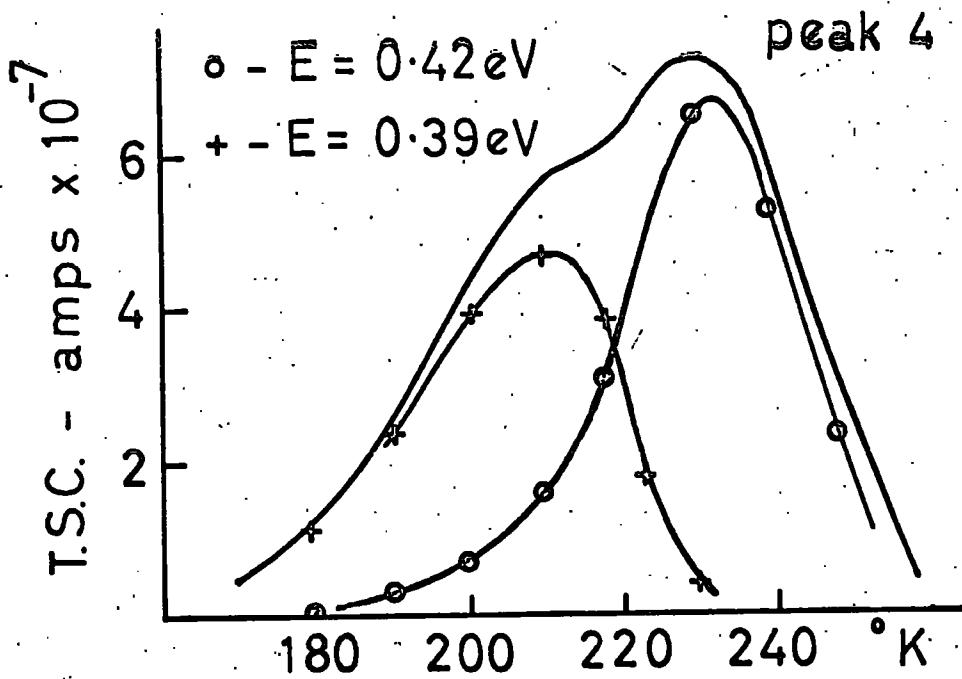
fig. 7.4.a.

fig. 7.4.b.

is a case of severe overlapping. Another factor that
had suggested this possibility was that a value of
$B = 5.6 \times 10^8$, leads to a value of S_T of $10^{-23} cm^2$,
which is extremely small. Using values of trap depth
of 0.42 and 0.39eV, it is possible to plot the double
theoretical peak to give a good fit with the
experimental results.

It is assumed that the major part of the T.S.C.
peak is attributable to a trap at a depth of 0.42 eV
below the conduction band, and that the peak was
distorted by the presence of another trap at a slightly
shallower depth. The capture cross section for the
more populous centre was calculated to be $2.6 \times 10^{-18} cm^2$;
the trap density was 2×10^{17} per cm^3.

2.d. Photochemical Effects

It can be seen in fig. 7.1, that the effect of
irradiating a crystal with light at high temperatures
is to increase the heights of the T.S.C. peaks. Below
$273^\circ K$, illumination had no effect, and the same curve
f, was obtained for all irradiation treatments tried
below this temperature. Because of this, and because
all the peaks changed proportionately together, it is
assumed that the concentrations of the centres

responsible for the peaks are not changing themselves, but that the differences in height are due to changes in the number of recombination centres. It is supposed that new sensitising recombination centres are produced photochemically, and as these have large hole capture cross-section, but small electron capture cross-section, their effect is to increase the electron free life time by removing holes that would otherwise recombine rapidly. The life time τ, is proportional to the conductivity at a peak, and a consideration of the kinetics of recombination of a simple model containing a discrete set of traps and two types of recombination centre, shows that:-

$$1/\tau = \beta_1(N_1 - n_1) + \beta_2(N_2 - n_2) + \beta_3(N_3 - n_3)$$

where N_i is the number of centres i, n_i is the number of these centres filled with electrons, and β_i is the product of S_i and v, the capture cross-section of centres i for electrons, and the thermal velocity of electrons. The subscripts 1, 2 and 3 have the meaning given to them in chapter four.

Assuming no retrapping, then:-

$$\beta_3(N_3 - n_3) = 0$$

and:-

$$1/\tau = \beta_1(N_1 - n_1) + \beta_2(N_2 - n_2)$$

Now if p holes are created, and levels 1 and 2
have equal probability of capturing holes, the ratio
of holes in centres 1 and 2 equals the ratio of the
concentration of these centres, i.e.:-

$$\frac{N_2 - n_2}{N_1 - n_1} = \frac{N_2}{N_1} \qquad \text{Eq. 7.5}$$

therefore:-

$$1/\tau = \beta_2(N_2 - n_2) + 1\frac{N_1}{N_2} \qquad \text{Eq. 7.6}$$

The total number of holes created, p, have been
assumed to be captured at centres 1 and 2. Therefore:-

$$(N_1 - n_1) + (N_2 - n_2) = p$$

Substituting from eq. 7.5 gives:-

$$(N_2 - n_2)(1 + N_2/N_2) = p$$

Substituting in eq. 7.6 :-

$$1/\tau = \frac{p}{(1 + N_1/N_2)}\left[\beta_2 + \beta_1\frac{N_1}{N_2}\right]$$

Now τ approaches a limiting value, τ_m, when
$N_2 \gg N_1$. Then, $1/\tau_m = p\beta_2$, since all the holes are
concentrated in centres 1. Therefore:-

$$N_2 = \frac{N_1\left(\frac{\beta_1}{\beta_2} \frac{\tau}{\tau_m} - 1\right)}{1 - \tau/\tau_m} \qquad \text{eq. 7.7}$$

It can be seen from the curves in fig. 7.1 that the value of τ does not approach a limiting value, so that N_2 cannot be much greater than N_1 for any of the different states of the crystal. For this reason an alternative theory must be used.

Since N_2 is seen to be small compared to N_1 in this sample:-

$$1/\tau = \beta_1(N_1 - n_1)$$

If p holes are created, they are all trapped at type I centres, so that $\left(N_1 - n_1\right) = p$, and:-

$$\frac{1}{\tau_o} = \beta_1 p$$

If now N_2 type II centres are created:-

$$\frac{N_1 - n_1}{N_2 - n_2} = \frac{N_1}{N_2}$$

and once again:-

$$N_1 - n_1 + N_2 - n_2 = p$$

From these three equations it follows that:-

$$N_2 = N_1\left(\frac{\tau}{\tau_o} - 1\right) \qquad \text{eq. 7.8}$$

If N_2 varies with an activation energy E_n, according to the equation:-

- 113 -

peak 1 – ●
peak 2 – ⊙
peak 3 – ○

$1/T_r \quad {}^\circ K \times 10^{-3}$
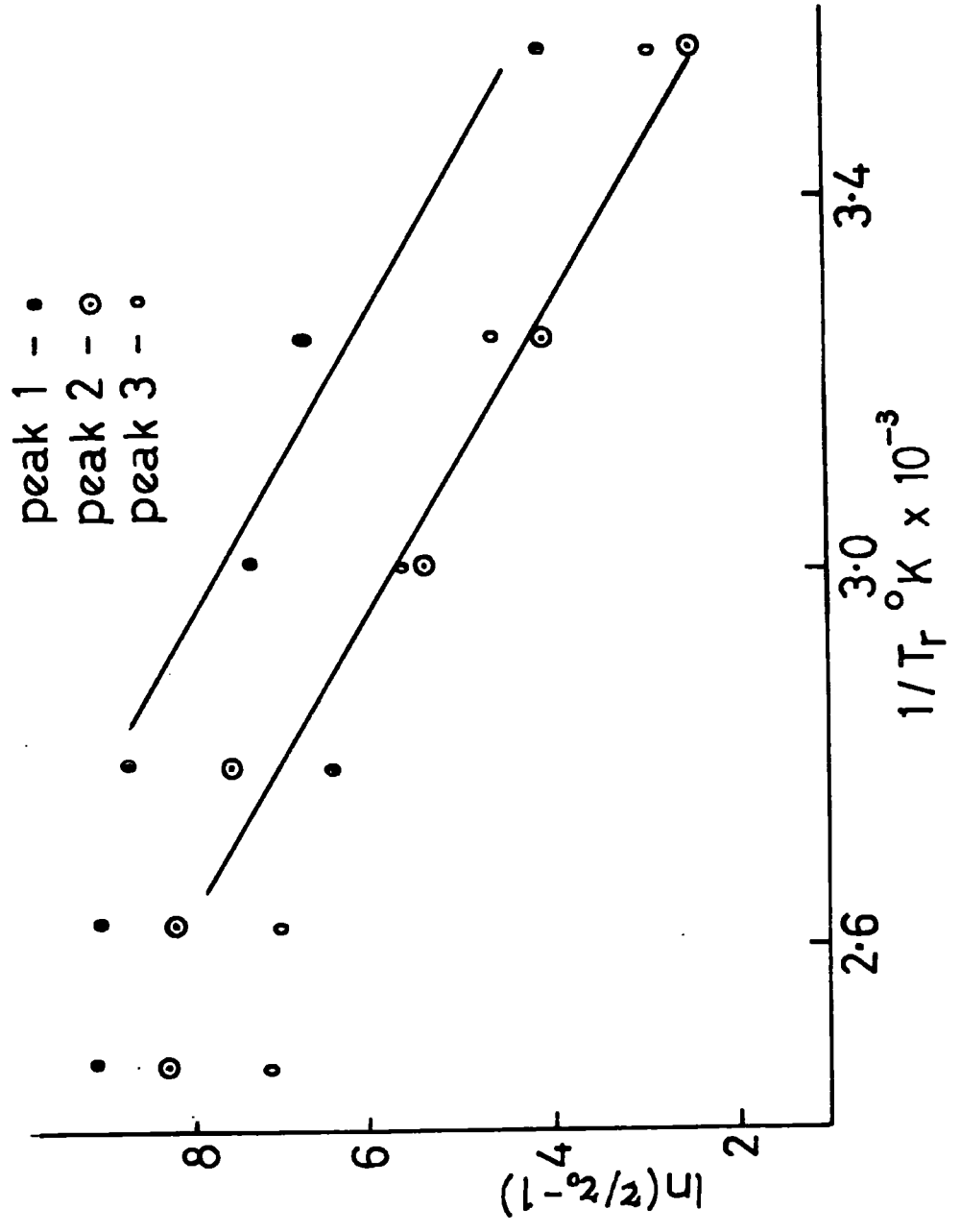
$\ln(z/z_o - 1)$

FIG. 7.5.

$$N_2 \propto \exp(-E_n/kT_r)$$

then a plot of $\ln(\eta/\eta_0 - 1)$ against $1/T_r$ yields a value of E_n. T_r is the temperature at which the illumination is started, as the sample is being cooled. Fig. 7.5 shows this curve plotted for peaks 1, 2 and 3. A value of E_n of 0.2 eV was obtained from the slopes of these curves.

3. Infra-red Luminescence.

The only infra-red luminescence emitted by this sample was the double band with maxima at 1.6 and 1.8 microns. None was detectable at 1.02 microns for any of the different treatments. The effect of prior illumination at high temperatures was to increase the intensity of the radiation emitted, as can be seen in fig. 7.6. Assuming that the intensity of the emission is proportional to the number of luminescent centres in the lattice, then:-

$$I = I_0 \exp(-E_1/kT_r)$$

where I_0 is the lowest value of the luminescent intensity, and E_1 is the energy of creation for the centres causing the luminescence. In fig. 7.7, $\ln I$ is plotted against $1/T_r$. A value of 0.29 eV was obtained from the slope of the curve.
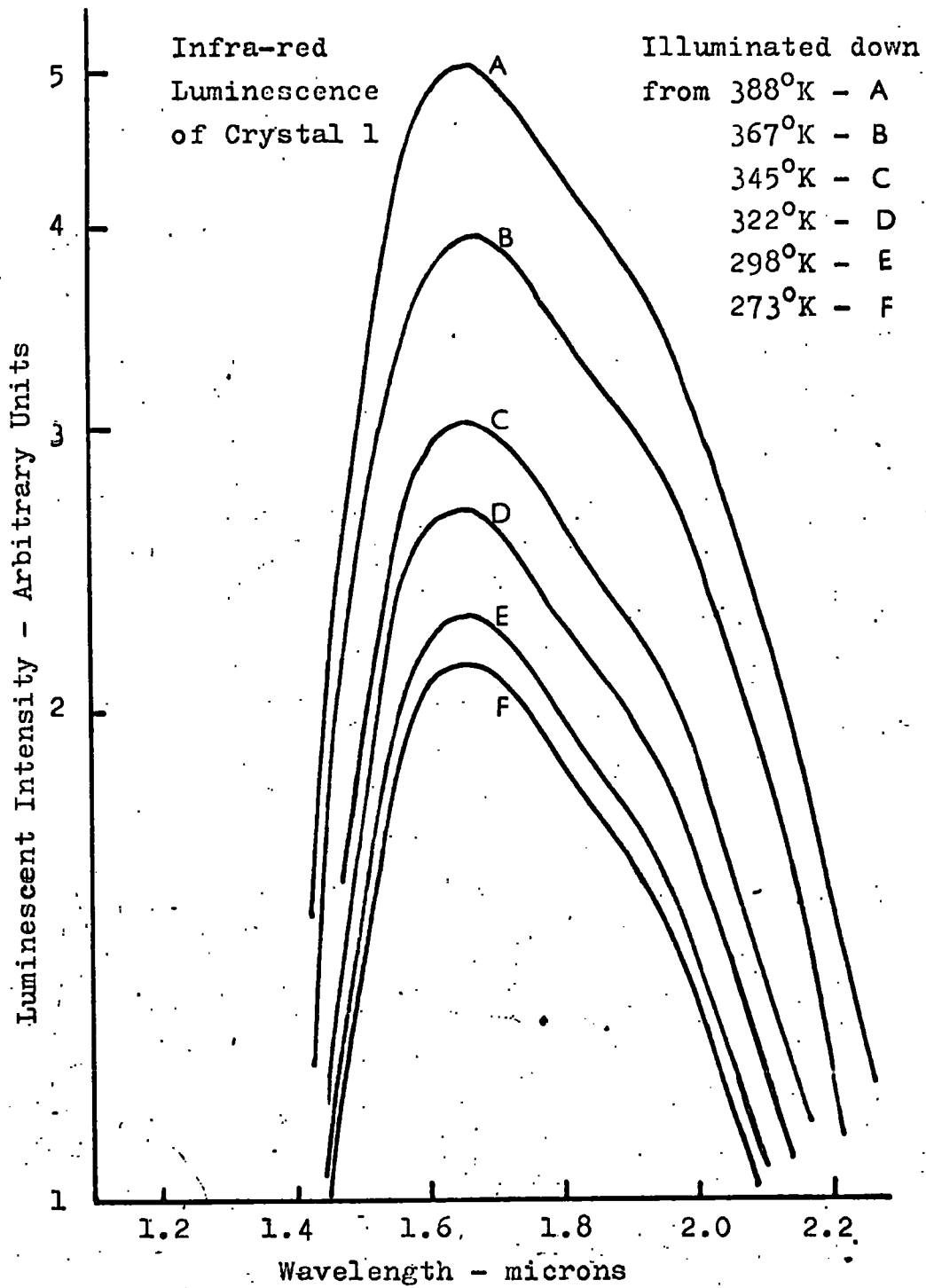
Infra-red
Luminescence
of Crystal 1

Illuminated down
from 388°K – A
367°K – B
345°K – C
322°K – D
298°K – E
273°K – F

FIG. 7.6.

Plot of ln(I) against I/T$_r$ for Crystal 1.
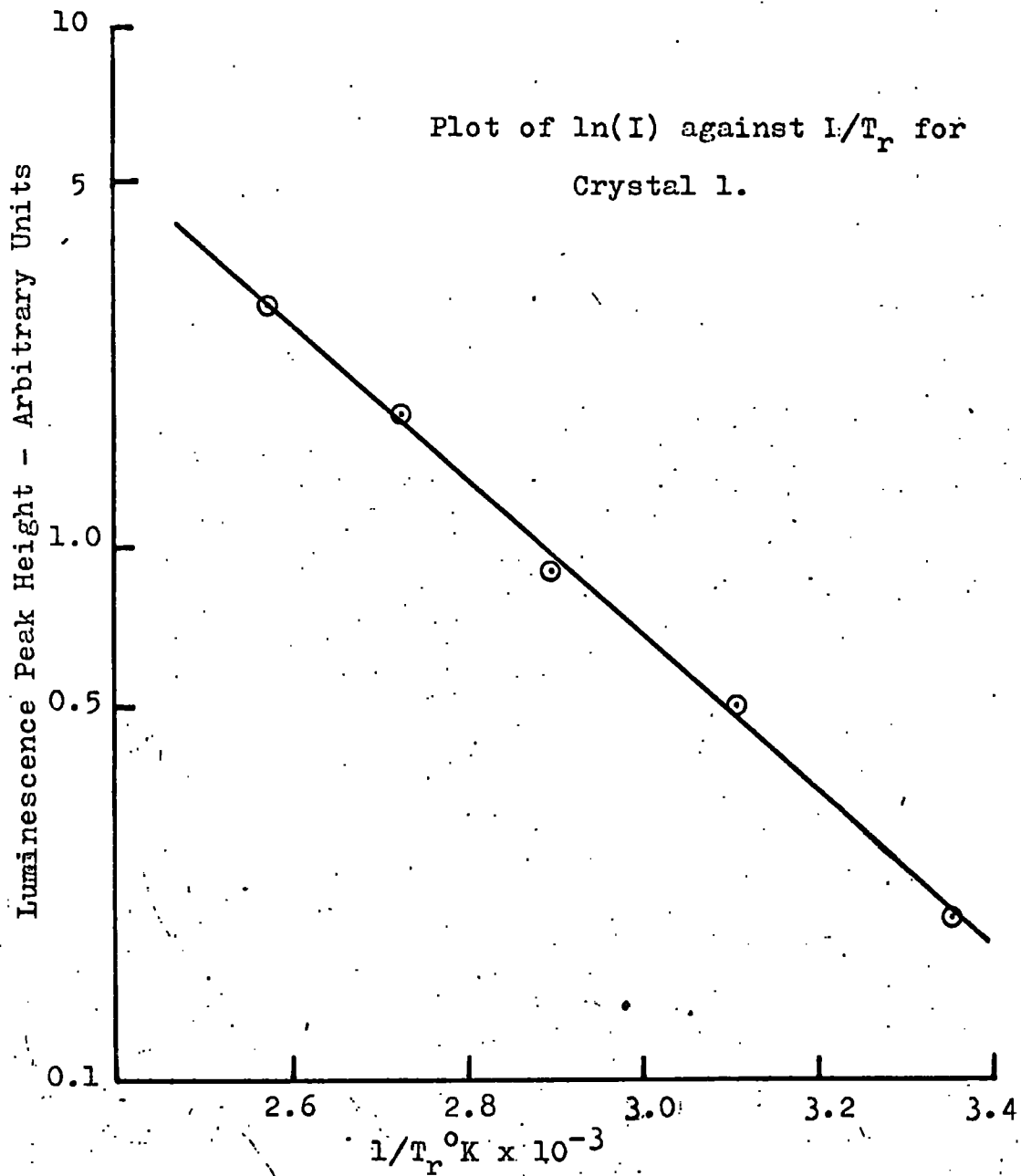
FIG. 7.7.

4. Conclusions

At least four discrete electron traps exist in this sample. The first, which empties thermally at very low temperatures can only have a depth of <0.2 eV assigned to it. The two emptying at 120 and 150°K yield values of trap depth of 0.18 and 0.21 eV, if the theoretical curves are to fit the theory. The fourth maximum in the T.S.C. curve seems to be due to two traps of similar depth. Values of 0.39 and 0.42 eV give a good theoretical fit to the experimental curve.

Photochemical effects occur that cause variations in the number of sensitising centres, and also cause changes in the number of centres involved in the infra-red luminescence at 1.6/1.8 microns. If the crudities of the theory governing the sensitising effect are allowed for, it can be considered that the activation energy is the same for the two processes, and in fact, the two centres involved are the same.

CHAPTER EIGHT

CRYSTALS GROWN BY THE FLOW METHOD

1. Introduction

The results given in this chapter are those obtained from measurements made on a sample of pure CdS in the form of a rod. The crystal was grown from the powder by the flow method, at a temperature of 900°C. It had a dark resistivity of 10^{11} ohm cm. at room temperature. The behaviour of this crystal, which is described in detail below, is typical of high resistance pure samples as grown.

With this crystal the dark current increased with time if the sample was held at a steady temperature above 100°C. With other samples, a difficulty had been to determine the state of the sample before any photo-chemical treatment was carried out, but the property of this crystal just mentioned, gave some indication of the state of the sample at high temperatures.

2. Trapping Spectra

The same procedure was adopted as in the previous chapter, except that at the beginning of each run, the sample was kept at the high temperature (390°K) until

the dark current had reached the value of 10^{-6} amps.
The resulting T.S.C. curves are shown in fig. 8.1.
The peaks in the curve overlap so strongly that it is
difficult to determine a value of trap depth for any
of the traps involved. The number of peaks between
100 and 250°K cannot be determined since the overlap
is so strong, but two definite peaks can be seen at
290 and 330°K.

2.a. Low Temperature Peaks

Although no information can be obtained about trap
depths from the low temperature positions of the T.S.C.
curves, the curves are interesting because they show a
similar behaviour to that observed at low temperatures
in the crystal grown by the pulling technique. An
important difference, however, is that in this case
the life time can be seen to approach a limit, so
that the original theory of chapter seven, section 2.d.,
can be used to determine the activation energy of
creation of recombination centres of type 1. The
appropriate equation is eq. 7.7 which, since $\beta_2 \gg \beta_1$
can be simplified to:-

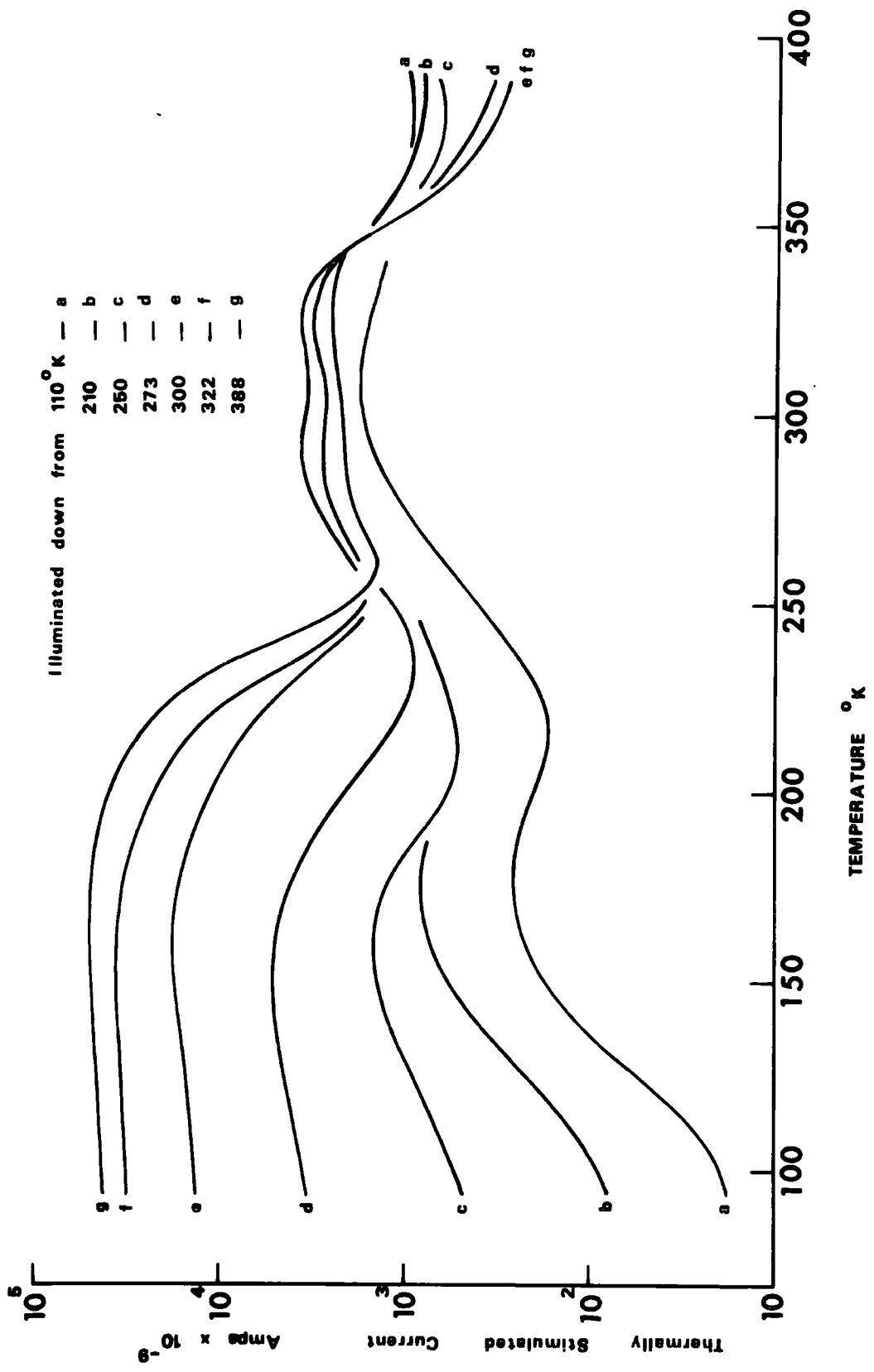$$N = N \frac{\beta_1}{\beta_2} \frac{\tau}{\tau_m} (1 - \tau/\tau_m)^{-1}$$

F I G. 8.1.

If the number of sensitising centres, N_2, is governed by the expression:-

$$N_2 \propto \exp(-E_n/kT_r)$$

then a plot of $\ln(\frac{\tau}{\tau m} (1 - {}^\tau/\tau m)^{-1})$ against $1/T_r$ will have a slope of E_n/k, and the value of E_n can be determined. The appropriate plot is shown in fig. 8.2. A good straight line is obtained with a slope giving a value of E_n of 0.33 eV. This value is comparable to the value obtained in chapter seven of 0.2 eV, which provides some justification for using two different theories for the two samples. The effect of irradiation during cooling is to produce the sensitising centres, with an energy of creation of 0.33 eV.

2.b. Peaks at 290 and 330°K.

A value of trap depth of 0.51 eV was obtained for the peak at 290°K, using the methods of Grossweiner, Luschik and Garlick and Gibson, on the results from a number of different runs. It was difficult to thermally clean the peak at 330°K, with the result that the values of trap depth obtained were very scattered. These values, however, were spread around a mean of 0.62 eV. In neither case could the peaks be sufficiently cleaned for any attempt at curve fitting to be made.
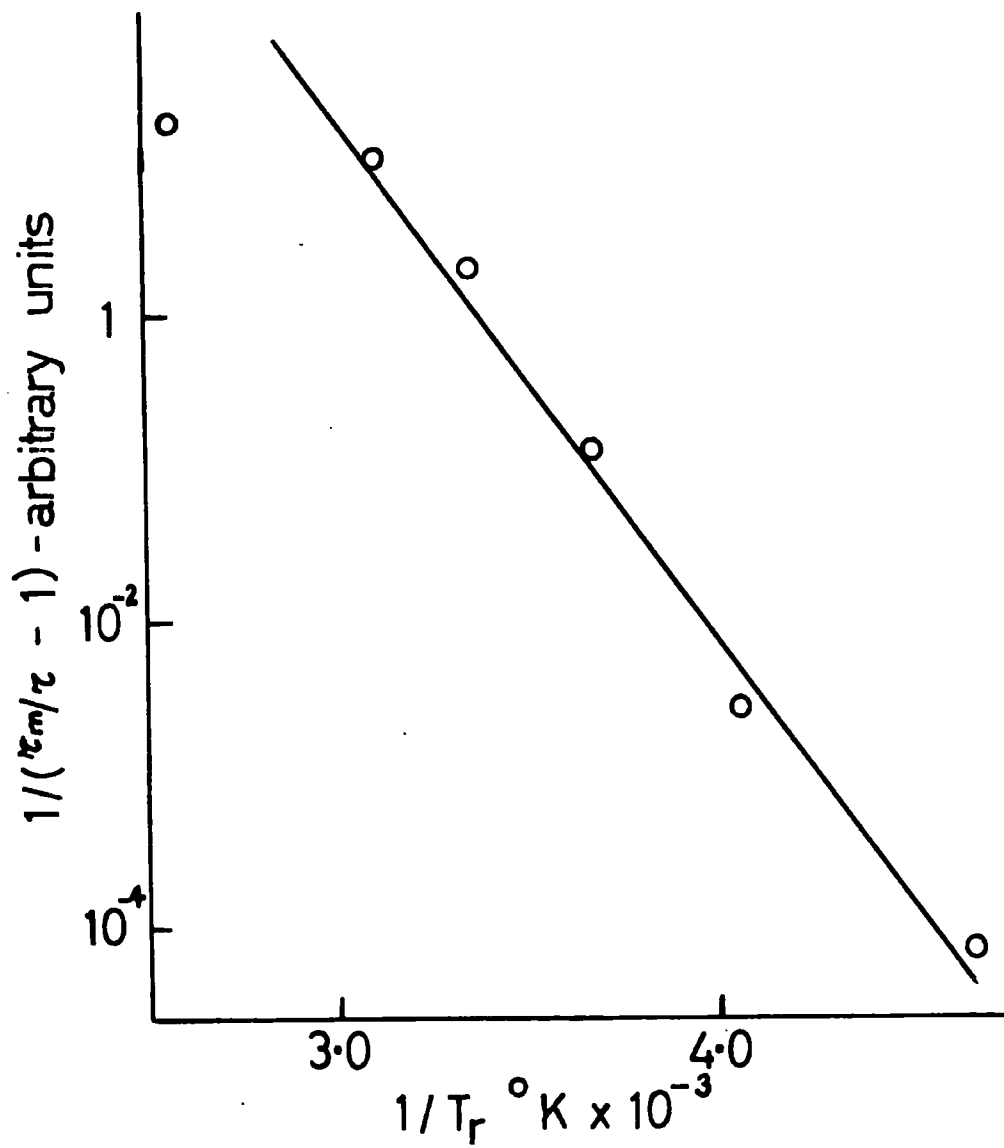
FIG. 8.2.

3. Infra-red Luminescence

This sample showed large luminescent peaks at both 1.02 and 1.6/1.8 microns, but because the intensities seemed to display an almost random behaviour, it was impossible to obtain any quantitative results from the experimental curves. It will be shown later that other centres change photochemically as well as the centres involved in luminescence, and it is probably this fact that caused the seemingly random behaviour of the luminescent bands with irradiation treatment.

It was found that the dark current at 390° could be slowly increased by baking at this temperature in the dark. To study this further, thermally stimulated current curves were obtained by starting from different dark current values at $390^{\circ}K$, before measurements were taken. Fig. 8.3 shows the T.S.C. curves obtained. It can be seen that in each case the current through the sample returned to the value at which it started before the T.S.C. curve was measured. The 1.02 micron luminescent band was absent for all the runs in which the sample was cooled in the dark. The absence of this band allows some calculations on the activation energy
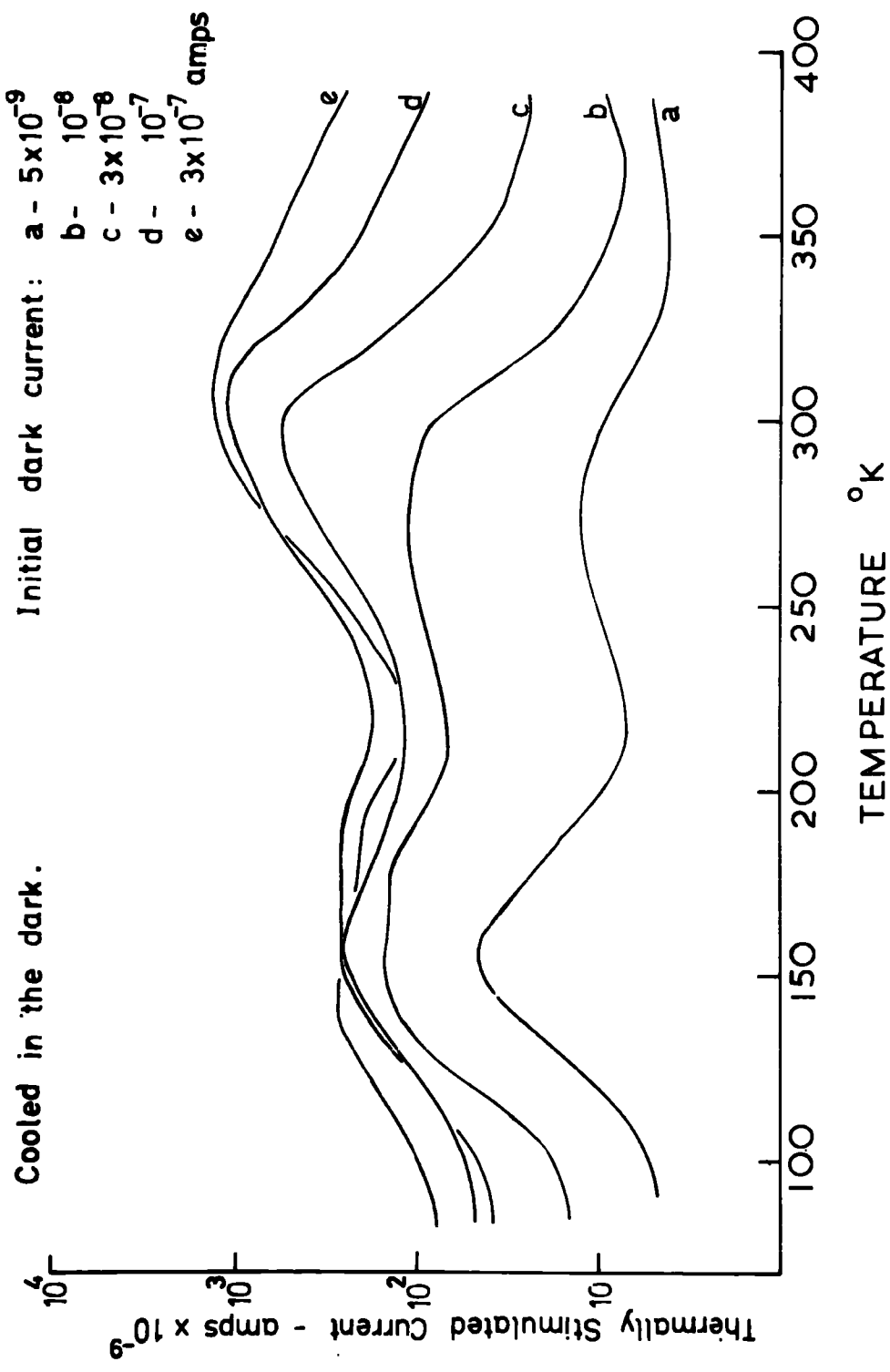
Cooled in the dark.   Initial dark current :   a – 5×10^{-9}
                                                      b– 10^{-8}
                                                      c – 3×10^{-8}
                                                      d – 10^{-7}
                                                      e – 3×10^{-7} amps

Thermally Stimulated Current – amps $\times 10^{-9}$

TEMPERATURE $^{\circ}$K

FIG. 8.3.

of the 1.6/1.8 micron band to be made. From fig. 8.1 it can be seen that illumination during cooling reduces the final dark current at $100^{\circ}C$. From this it is possible to determine the values of T_r that are required to reduce an initial dark current of 10^{-6} amps to final dark currents of different values. The final dark current values were measured after each of the runs shown in fig. 8.1, and the values of T_r obtained from these. The values of T_r were then used to obtain a value of activation energy E_1, for the creation or destruction of the centres involved. Fig. 8.4 shows the different luminescent spectra obtained for the various initial dark current values, if the sample was cooled in the dark. Fig. 8.5 is a plot of $ln(I)$ against $1/T_r$, where T_r was obtained as described above. This crude method of calculation led to a value of E_1 of 0.1 eV. It is proposed that the centres involved in the changing dark current at high temperatures are the sensitising centres observed in this and the previous sample. There are two reasons for this statement: (i) the similarity in the behaviour of the infra-red emission from the two samples; (ii) the order of magnitude agreement between the activation energies of creation. It is realised that there exists some

Initial dark current
a- 5×10^{-9}
b- 10^{-8}
c- 3×10^{-8}
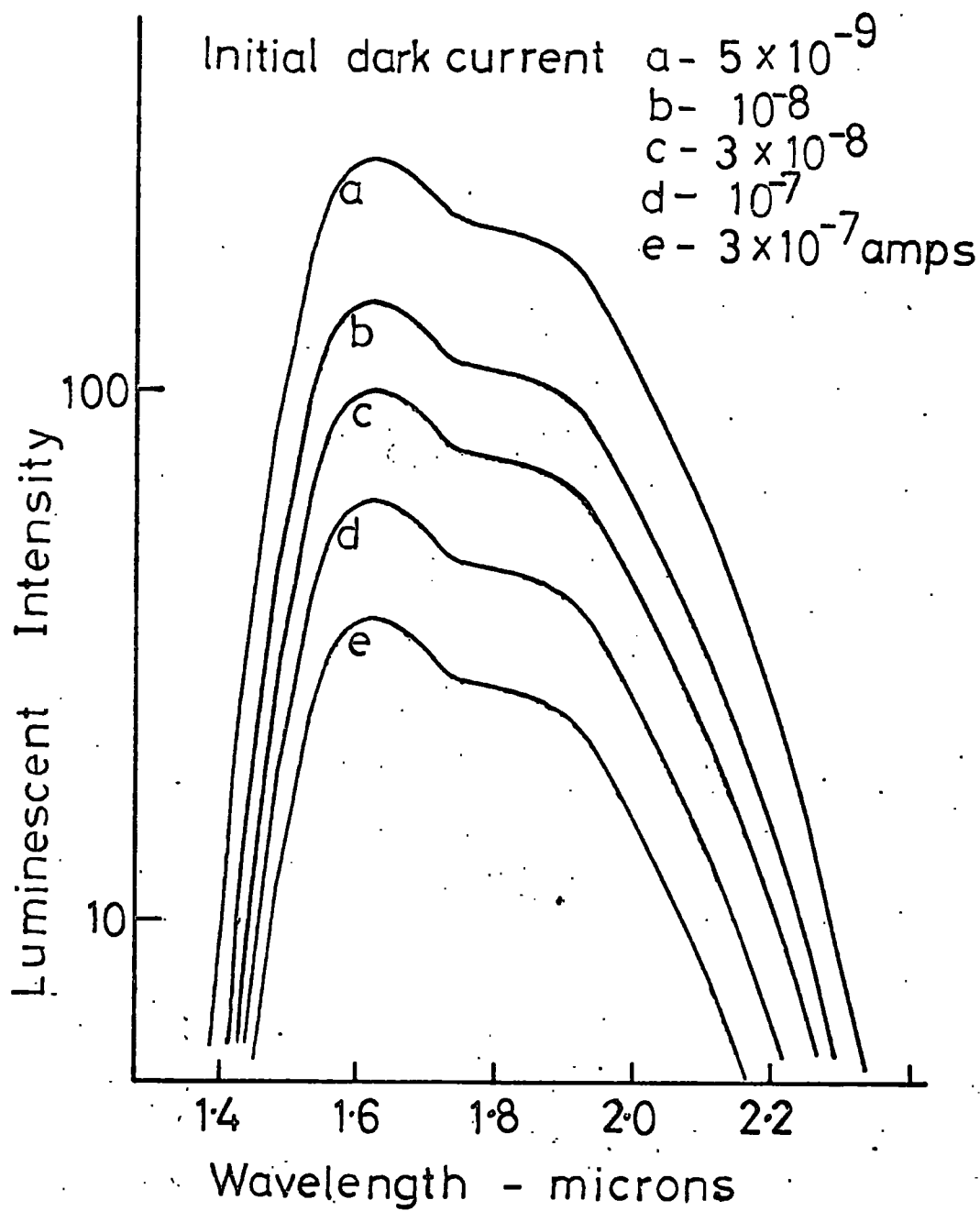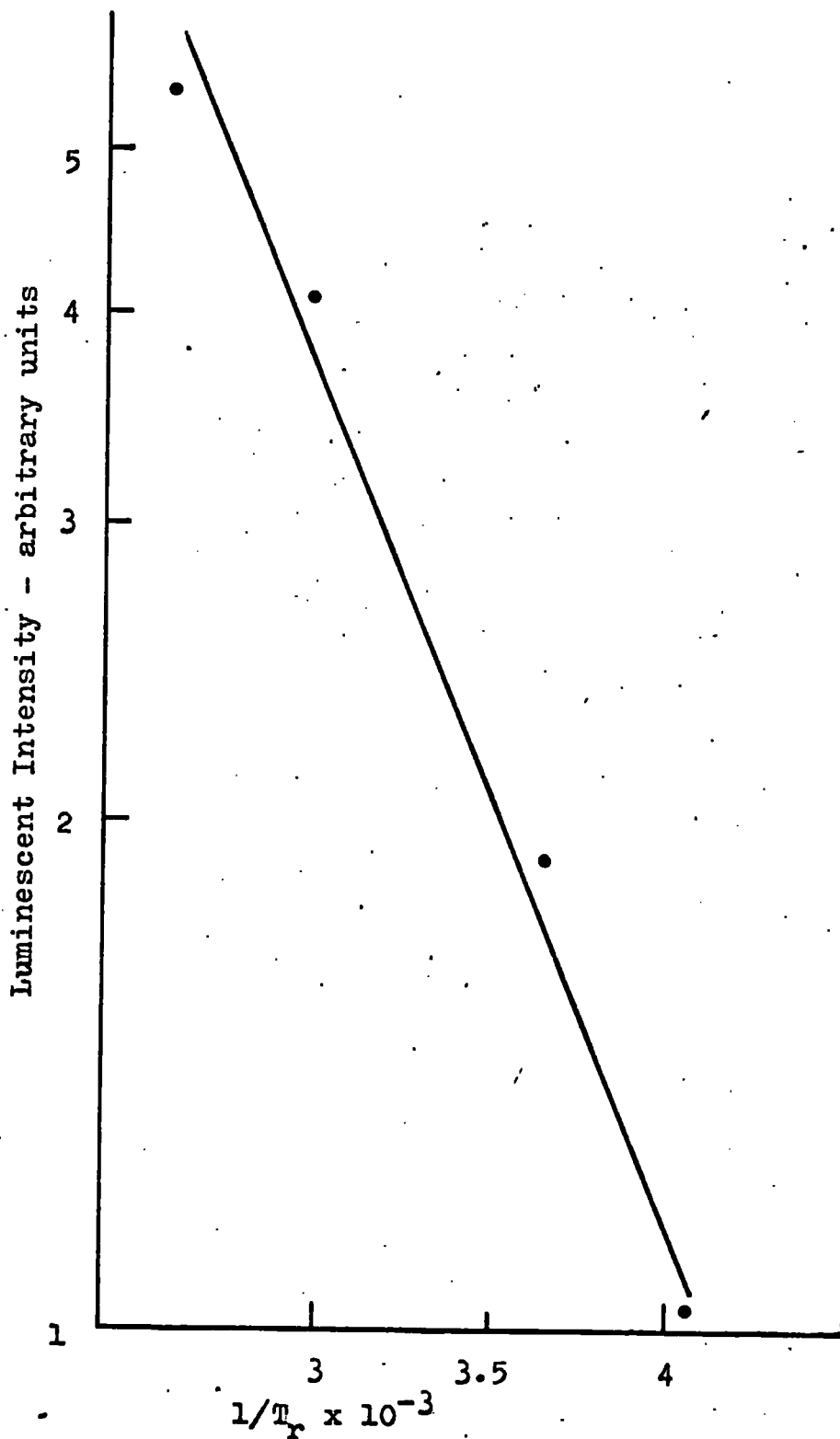d- 10^{-7}
e- 3×10^{-7} amps

FIG. 8.4.

FIG. 8.5.

discrepancy between the activation energy values, but
allowance must be made for the crudity of the
calculations. It is believed that the sensitising
centres are created by the action of the light, and
destroyed by baking at elevated temperatures. At
these temperatures the centres will be behaving as
acceptors rather than sensitising recombination centres.

4. <u>Variation of Dark Current at 390°K.</u>

Figs. 8.6 and 8.7 show thermally stimulated current
curves for the same initial dark current values as those
used for fig. 8.3, except that the sample was cooled in
the light from 273° and 390°K, respectively. It can be
seen in figs. 8.3, 8.6 and 8.7 that the height of the
peak at 330°K is changing in relation to the other peaks.
In all cases, for higher values of initial dark current,
the height of the 330°K peak is larger. It seems possible,
therefore, that it is the centres responsible for this
peak, traps at 0.62 eV, that are being created from the
sensitising recombination centres by baking in the dark
at high temperatures. Because of the strong overlapping
of the peaks in this part of the T.S.C. spectrum, it is
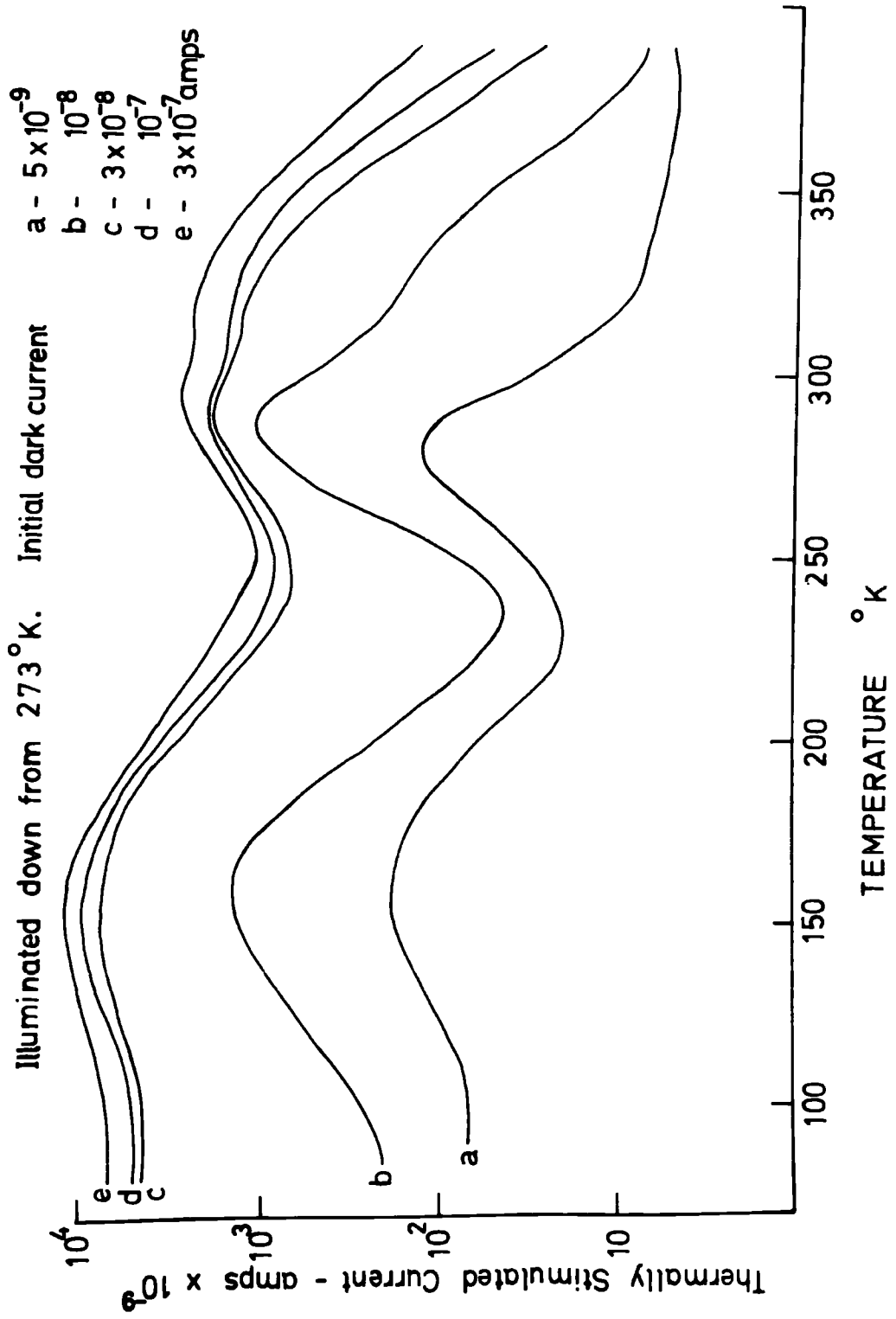not possible to obtain any energy of creation value for
this process.

FIG. 8.6.

Initial dark current

a – 5x10⁻⁹
b – 10⁻⁸
c – 3x10⁻⁸
d – 10⁻⁷
e – 3x10⁻⁷

Illuminated down from 390°K

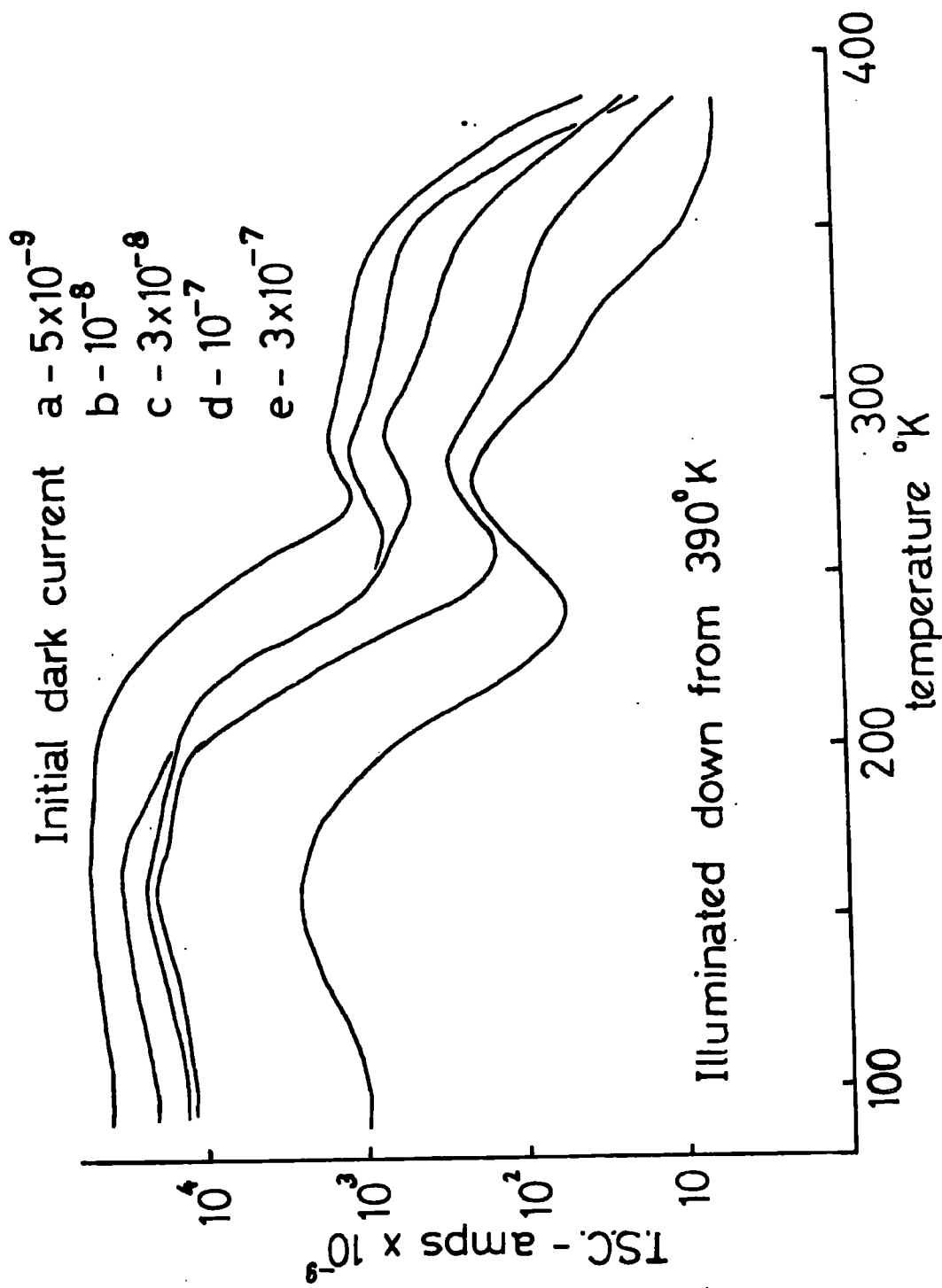temperature °K

TSC.- amps x 10⁻⁹

FIG. 8.7.

5. Conclusion

The fact that the luminescent bands showed different patterns of behaviour with photochemical treatment, does not mean that the possibility that they are associated with transitions to or from the same centre, is not true. The 1.02 micron band involves the transition of an electron from a trap to this centre, whilst the 1.6/1.8 micron band involves transition from this centre to the valence band. The behaviour of the intensity of the 1.02 micron band will depend upon the magnitude of the capture-cross section of the trap involved, relative to those of the other traps in the forbidden gap. Since the number of these other traps is changing, it cannot be expected that the two luminescent bands will show parallel behaviour.

The creation of the 0.62 eV trap, by the baking of the sample at high temperatures, leads to a decrease in the intensity of the luminescence (fig.8.4). It could be that the photochemical process destroys the trap at 0.62 eV, by causing the centre involved to associate with some other defect, to form the luminescent centre, which is presumed identical with a sensitising centre. Baking in the dark at high temperatures has

the opposite effect, and destroys the association that forms the luminescent centre to restore the trap at 0.62 eV.

Further evidence for the relationship between the final dark current and the luminescence is shown in fig. 8.8, where the height of the luminescent peaks at 1.6/1.8 microns is plotted against the final value of dark current at $390^{\circ}K$, after the respective runs. It can be seen that for high dark current values the luminescent intensity is small, which again suggests that the centres causing the low dark currents are the same as the luminescent centres.

In fig. 8.9, the intensity of the 1.02 micron band is plotted against the low temperature peak heights, (i.e. against τ). In this case, as the luminescent intensity increases, the value of τ, increases, which is some evidence for the possibility that the luminescent centres are the same as the sensitising centres. For this to be true, it would be necessary for a trap at 0.49 eV to exist in the forbidden gap, in order to provide an excited state for an electron in the correct energy position to give luminescence of 1.02 microns. A large peak was found in the T.S.C. spectra of this
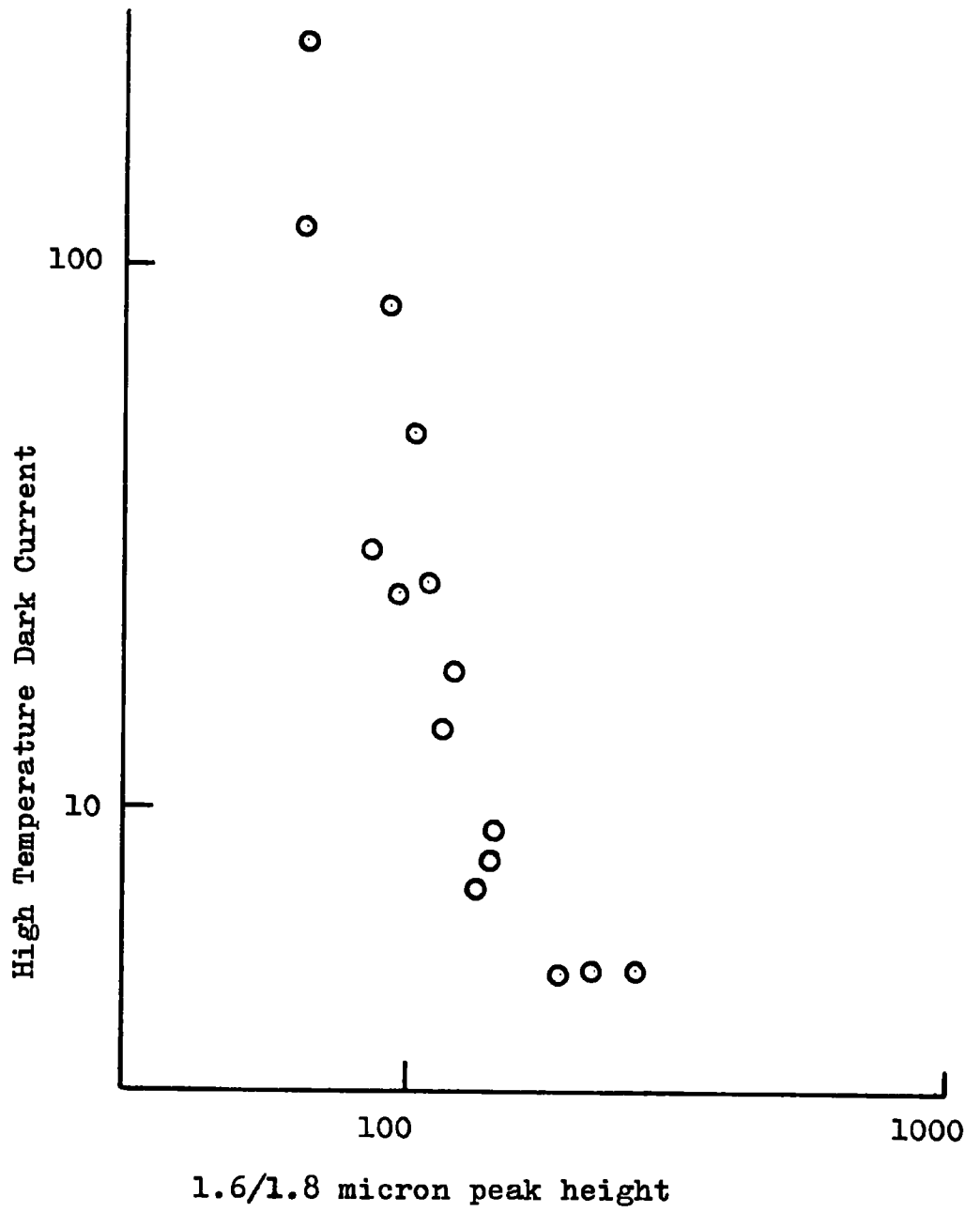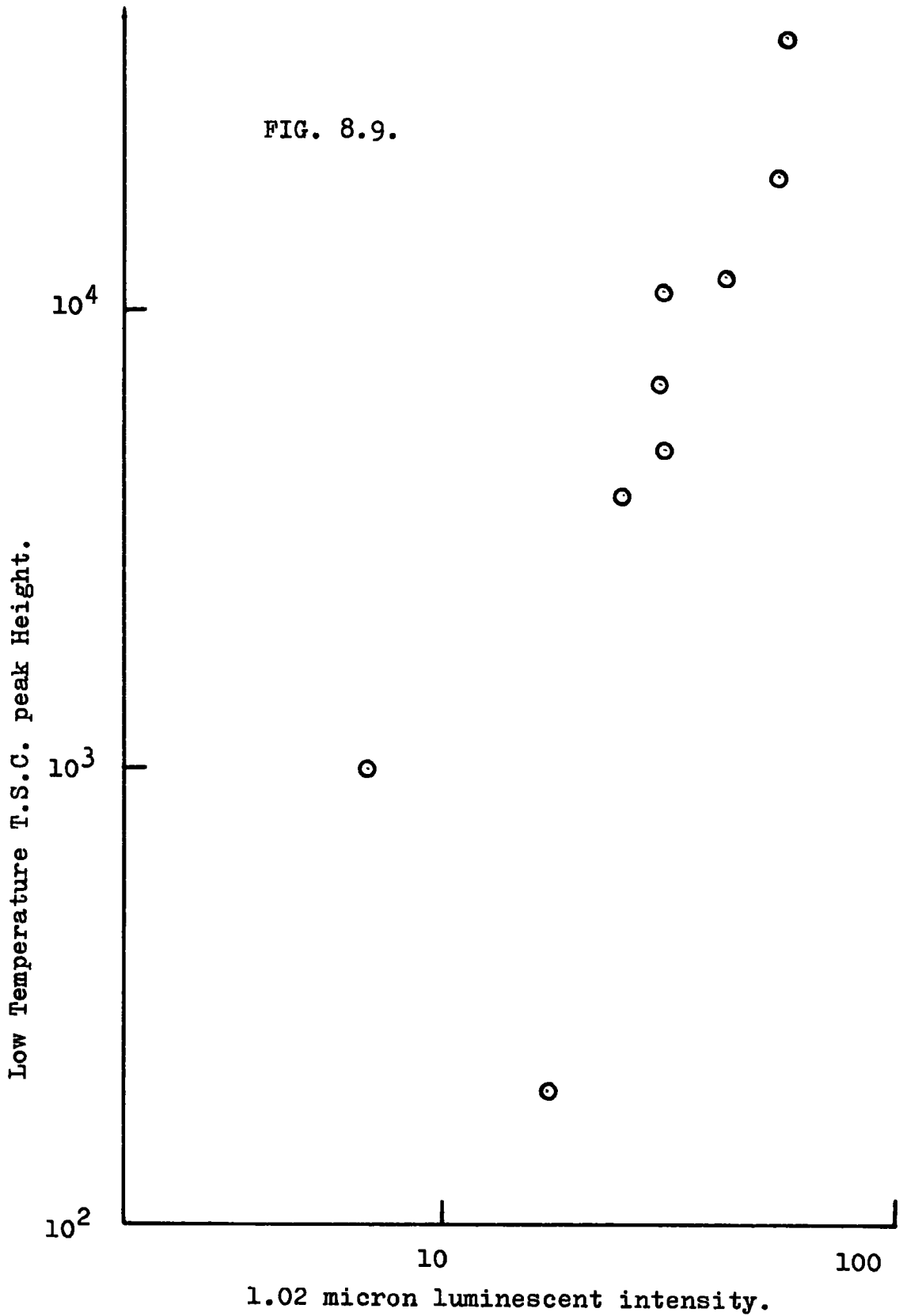
FIG. 8.8.

FIG. 8.9.

sample that corresponded to an energy depth of 0.51 eV below the conduction band. Because of the fact that the thermal depth should be less than the optical depth of a trap, there would be some difficulty in assigning this trap to the excited state of the luminescent transition. However, the inaccuracy involved in determining the trap depths from the T.S.C. data on this sample could account for this. Later samples also show this peak, and more accurate methods of measurement yield a value of trap depth of 0.48 eV. From the T.S.C. curves it can be seen that the density of these centres remains fairly constant. The centres do not seem to be involved in photochemical changes.

CHAPTER NINE

SULPHUR DOPED CRYSTALS

1. Introduction

The results described here are for a similar crystal to that used in chapter eight, i.e. a flow crystal in the form of a rod, grown at $900^{\circ}C$. The sample was, however, treated after growth by baking it for 2 hours at $600^{\circ}C$, under a saturation vapour pressure of sulphur at this temperature, which is 15 atmospheres. This is fairly light sulphur treatment, and the results for treatment at higher temperatures are given in the next chapter.

2. Thermally Stimulated Current Curves

The curves obtained are shown in figs. 9.1, 9.2 and 9.3, for the same measurement procedure as that used in chapters 7 and 8. Although these curves show an extremely complicated pattern, it should be emphasised that this was completely reproducible, provided that the same starting temperature of $390^{\circ}C$ was used, and the same procedure was adopted as that used here.

FIG. 9.1.
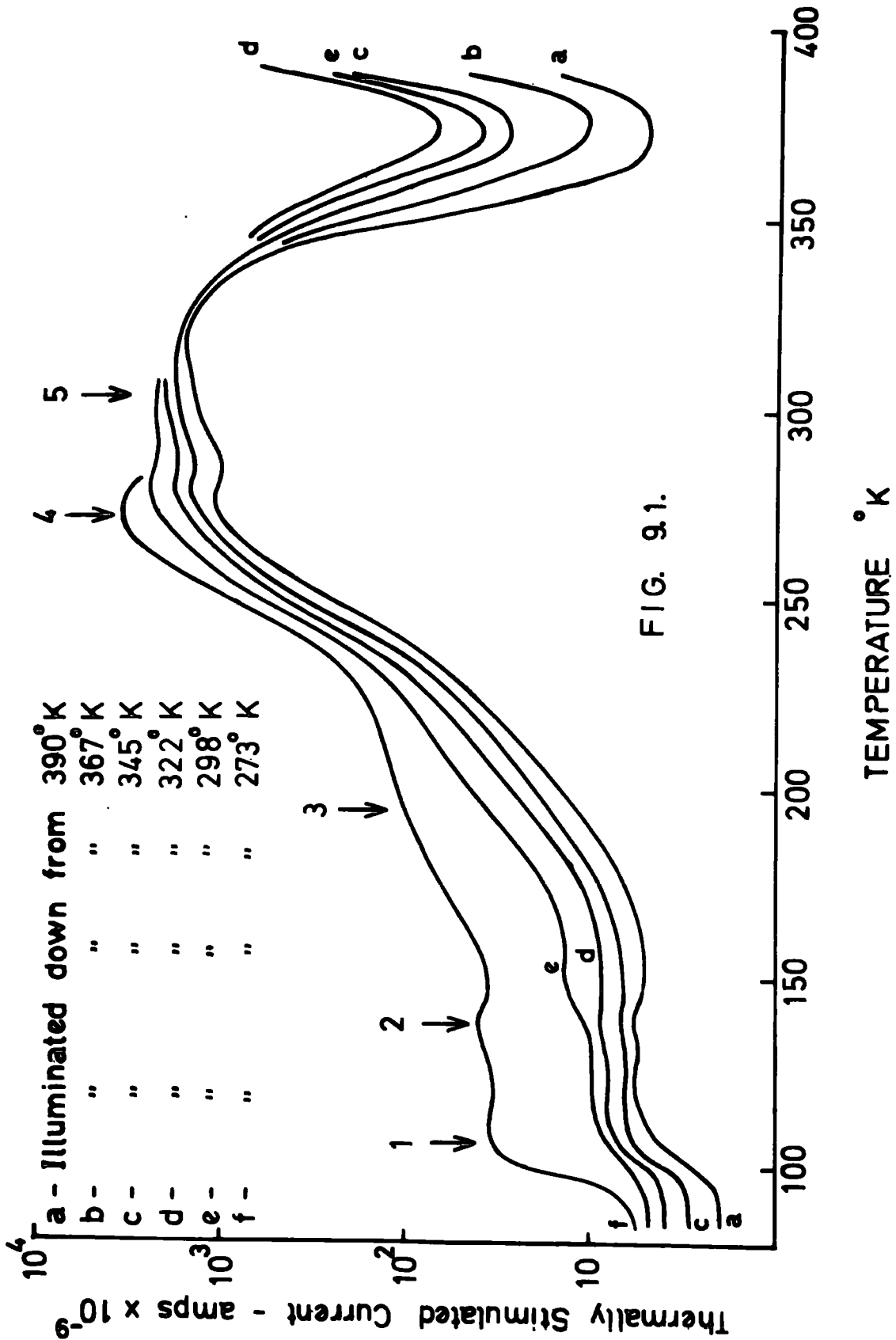
TEMPERATURE °K

Thermally Stimulated Current - amps × 10⁻⁹

a – Illuminated down from 390° K
b –   "   "   " 367° K
c –   "   "   " 345° K
d –   "   "   " 322° K
e –   "   "   " 298° K
f –   "   "   " 273° K

FIG. 9.2.

f - Illuminated down from 273°K
g -   "   "   "   246°K
h -   "   "   "   217°K
i -   "   "   "   185°K

TEMPERATURE °K

Thermally Stimulated Current - amps x 10^{-9}

FIG. 9.3.

Illuminated down from 185°K - i
149°K - j
100°K - k

Thermally Stimulated Current - amps x 10⁻⁹

TEMPERATURE °K
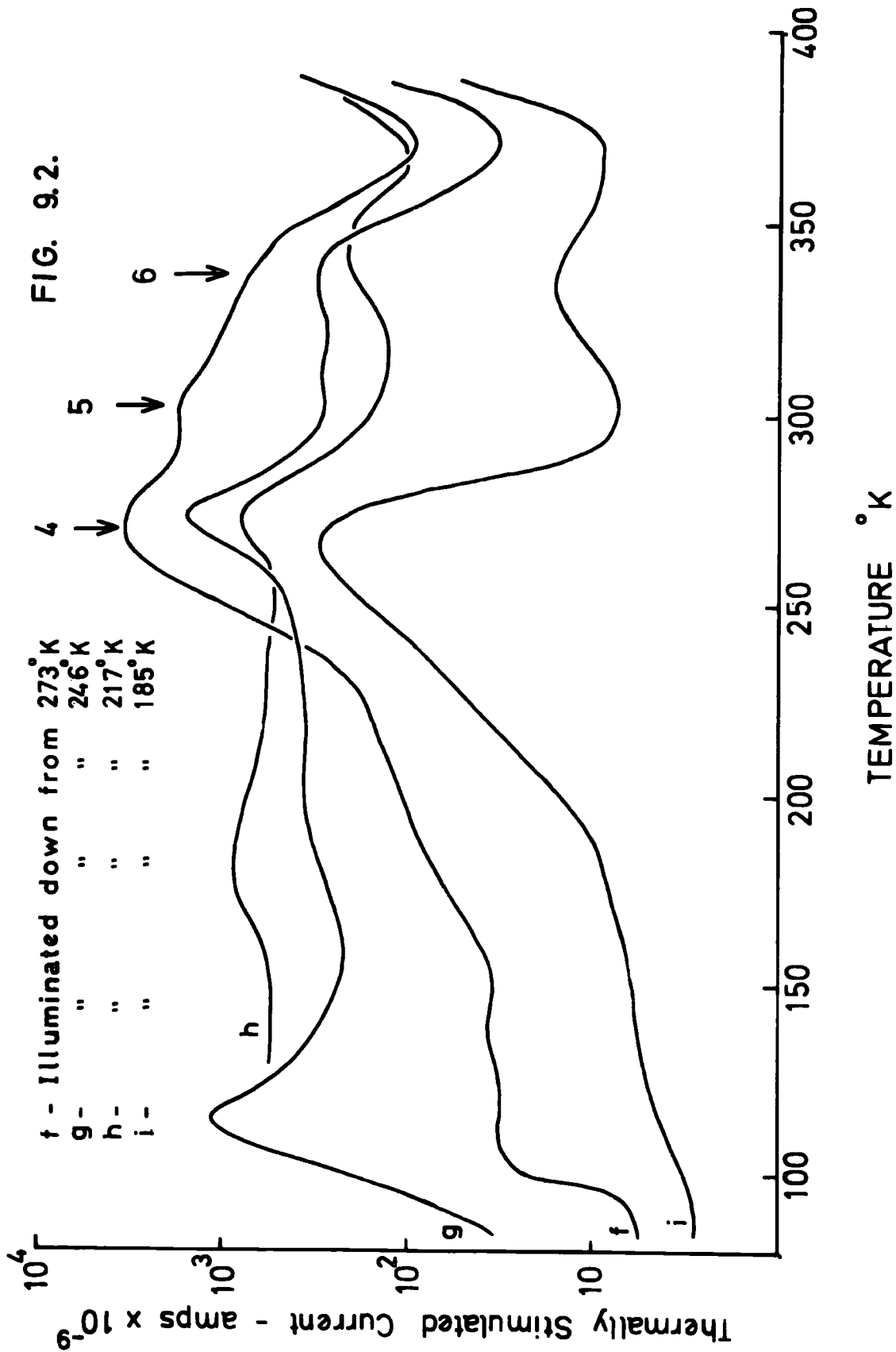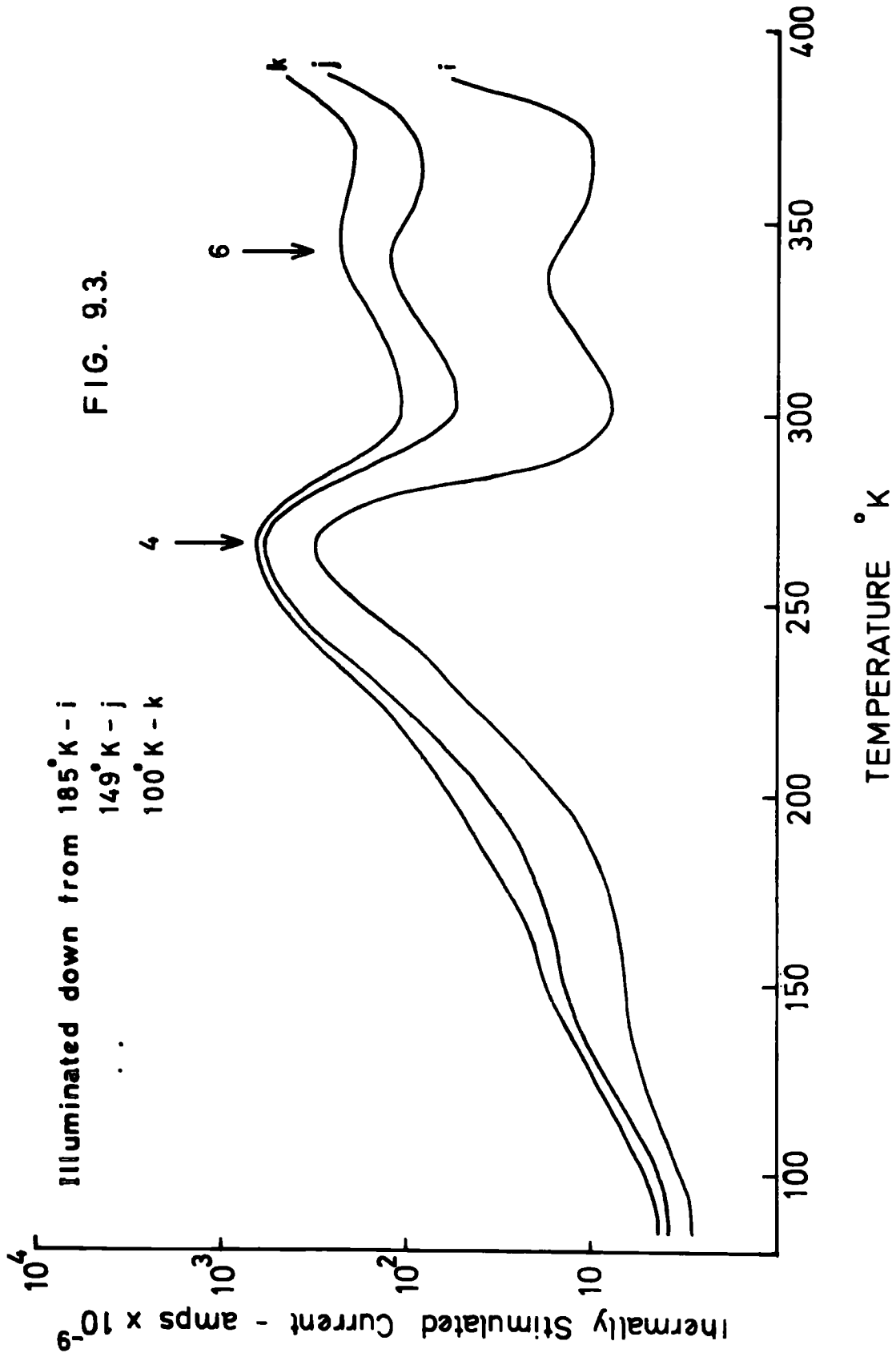
2.a. Trap Depths

Despite strong overlapping of the T.S.C. peaks, there are six maxima that can be distinguished. These are marked 1 to 6 in figs. 9.1, 9.2 and 9.3.

The traps which empty to give peaks at 108, 140 and 185°K, could not be effectively cleaned, so that the only value of trap depth obtainable by normal methods, was a value of 0.21 eV obtained for the maximum at 185°K by Garlick and Gibson's method. The technique of curve fitting could obviously not be used for these traps. However, if values of capture cross-section are assumed, then trap depths can be determined from knowledge of the temperatures at the maxima and the heating rates. The assumption that $S_T = 10^{-18} cm^2$ leads to values of E of 0.17, 0.23 and 0.32 eV for the three traps. If S_T is $10^{-19} cm^2$, then these values become 0.16, 0.20 and 0.27 eV. It is realised that there is no experimental basis for this assumption; however, the values used are reasonable for traps emptying at these temperatures, and also there is the possibility that two of these three traps are the same as those seen in the sample grown in a sealed tube (chapter 7) for which values of trap depth of 0.18 and 0.21 eV were obtained.

Trap 4, which empties to give a maximum at $270^{\circ}K$, yielded values of trap depth with a mean of 0.48 eV, although the results from several runs, using many of the methods, were quite scattered. The methods of trap analysis used were those due to Grossweiner, Luschik, Garlick and Gibson, and also the heating rate method of Hoogenstraaten. In fig. 9.4 the continuous line is the experimental result, which it can be seen, is in good agreement with the points calculated from the theoretical equation for the curve, using a value of trap depth of 0.48 eV. Calculation of trap density and capture cross-section yielded values of 3.4×10^{17} per cm^3, and $7.6 \times 10^{-19} cm^2$, respectively.

The peak marked 5, was so greatly overlapped by the other peaks that none of the standard methods of measurement could be used. Although no value of trap depth can be assigned to this centre at this stage, a T.S.C. maximum at the same temperature, showing the same behaviour, was seen in later samples. In the next chapter, the trap causing this peak is discussed further, and a trap depth is assigned to it.

Peak 6, in fig. 9.3 could be easily cleaned, so that the complete isolated curve could be obtained by thermal cleaning. The experimental curve is shown in

T.S.C. peak 4.
line – experiment
points – theory

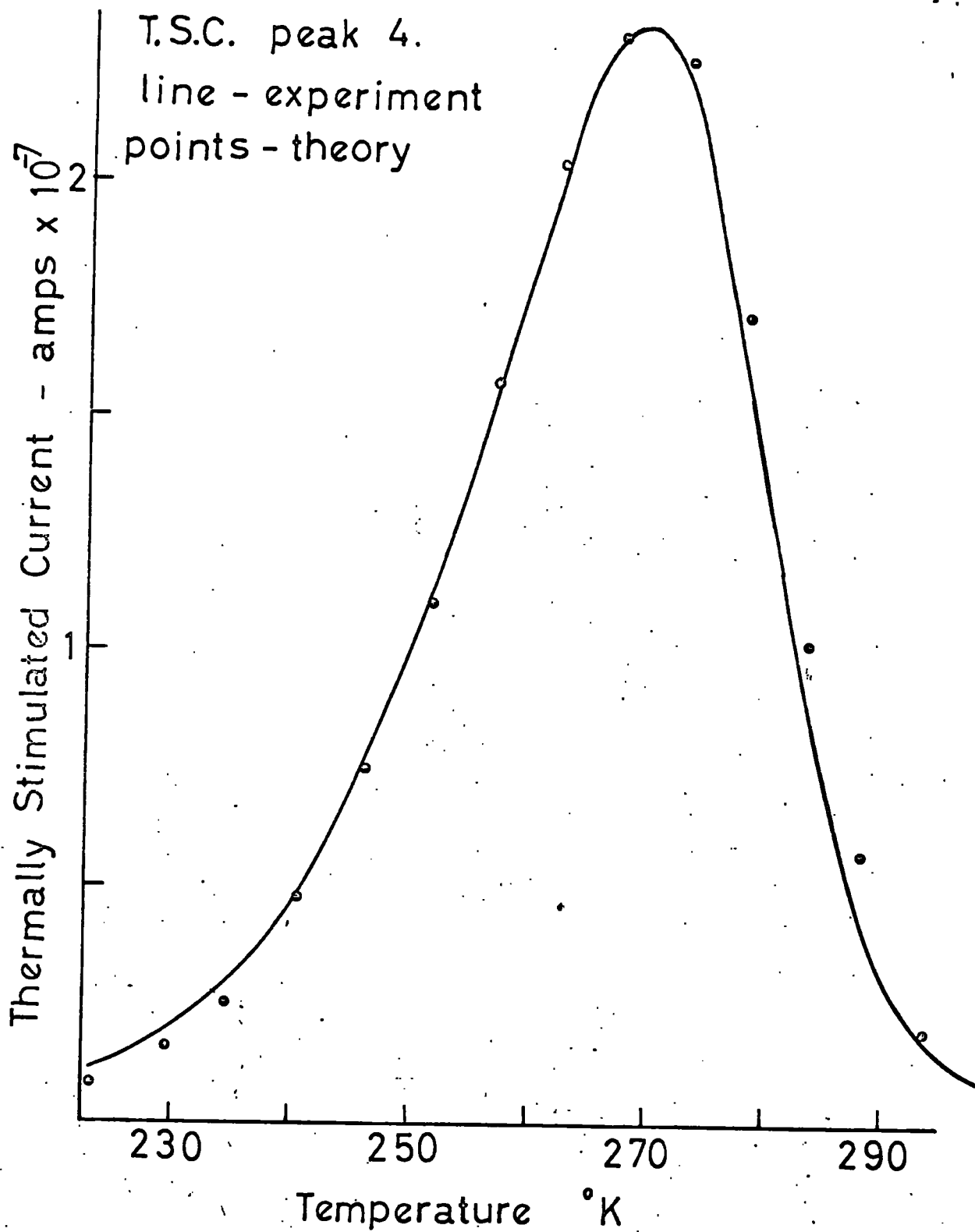Thermally Stimulated Current – amps x 10^{-7}

Temperature °K

FIG. 9.4.

fig. 9.5 as a continuous line. Again the values of
trap depth obtained from the different methods were
to some extent scattered, but these yielded an average
value of 0.64 eV. A trap at this depth has been seen
by many workers, and it is generally considered to obey
the laws of fast retrapping, so the technique of curve
fitting, using the equation derived in chapter seven,
is not applicable.

The T.S.C. curve for a trap emptying under the
conditions of fast retrapping, is described by the
equation 3.2:-

$$\sigma = \frac{N_c e \mu n_{to}}{N_t} \exp\left[-E/kT - \frac{1}{N_t \beta \tau} \int_{T_0}^{T} N_c \exp(-E/kT) dT \right]$$

Using the methods of chapter seven, this can be
rewritten as :-

$$= A \exp\left[-t + B \int_{t_0}^{t} e^{-t} . t^{\frac{1}{2}} dt \right] \qquad \text{eq. 9.1}$$

where A and B are constants, and $t = E/kT$. Again
it can be shown that the integral can be simplified,
provided that T_0 is sufficiently low, to give:-

$$\sigma = A \exp\left[-t - B e^{-t} . t^{-\frac{7}{2}} \right] \qquad \text{eq. 9.2}$$

Differentiating and equating to zero to find the
conditions at the maximum, yields a slightly different
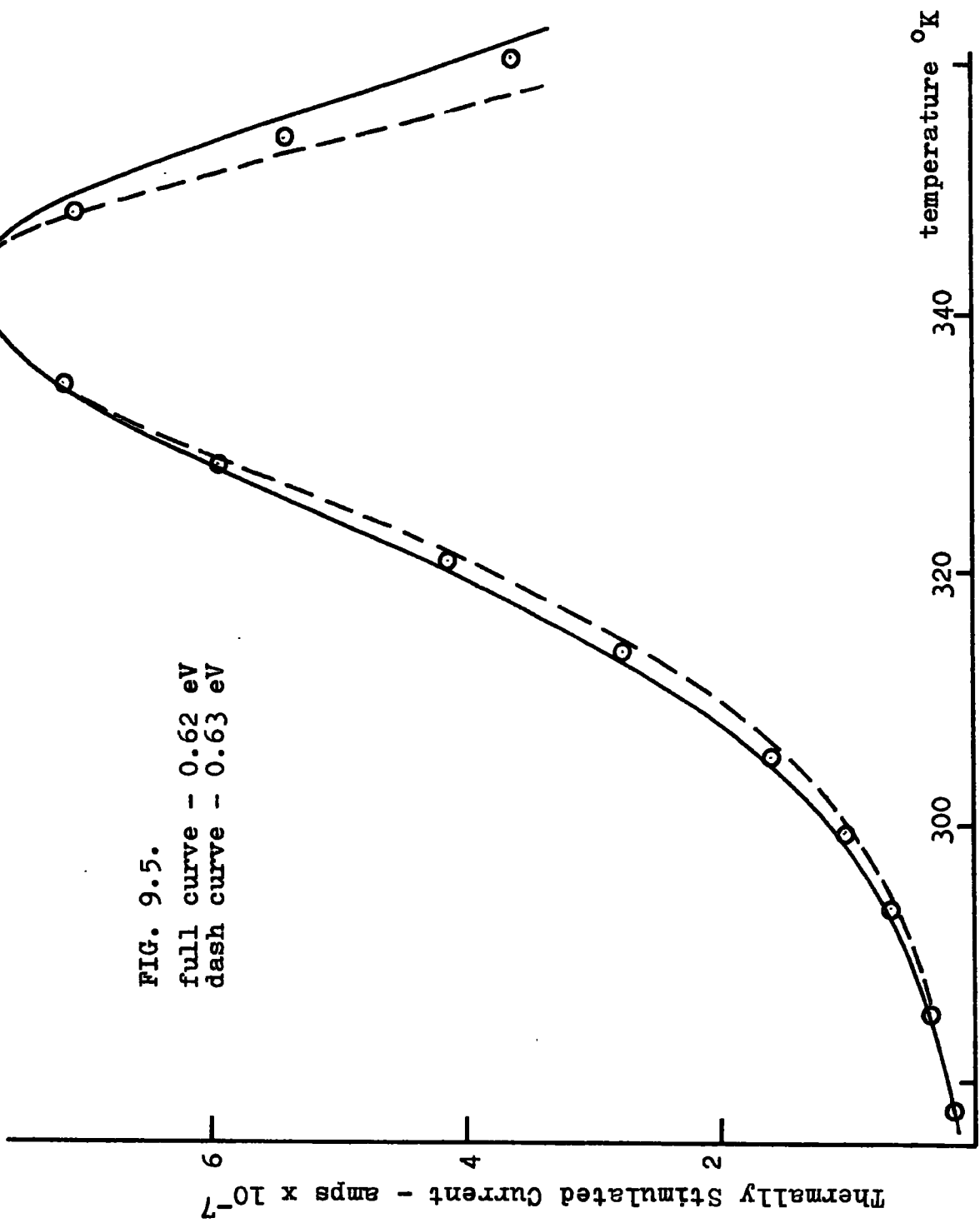equation from eq. 7.4, which is:-

FIG. 9.5.
full curve – 0.62 eV
dash curve – 0.63 eV

temperature °K

Thermally Stimulated Current – amps x 10^{-7}

$$B = \frac{e^{t*} \cdot t*}{(t*+3.5)} \qquad \text{eq. 9.3}$$

The major difference between the two equations, is that for the monomolecular case, $B = \sqrt{E}/\beta k$, and for the fast retrapping case $B = N_c E / N_t \tau \beta T*^{3/2} k^{5/2}$. In this case the value of B that best fits the experimental results can be used to obtain a value of trap density.

For the peak at $340^\circ K$, values of trap depth of 0.62 and 0.63 eV were assumed, and since the value of T* is known, the corresponding values of B were determined from eq. 9.3. These values of B were then used to calculate the theoretical curves for these two values of trap depth, using eq. 9.1. The curves are shown in fig. 9.5. It can be seen that in both cases that the leading edge of the curves fit quite well, and the experimental points lie neatly between the two curves on the falling side. To fit with the experimental curve it would be necessary to plot the curves for a trap at a depth of between 0,62 and 0.63 eV. This gives a well defined value of trap depth, and is in quite good agreement with the result obtained from the normal methods of analysis, of 0.64 eV.

3. Infra-red Luminescence.

Infra-red emission at both 1.02 and 1.6/1.8 microns was observed in this sample. Again photochemical reactions occurred, although the behaviour of the luminescent intensity was less complex than that observed from the sample discussed in chapter eight. Once again the effect of illumination at elevated temperatures was to cause an increase in the luminescent intensity, but this time the two emission bands behaved in a similar manner. In fig. 9.6 the peak heights are plotted against $1/T_r$ for both the 1.02 and 1.6/1.8 micron bands. It can be seen that both curves have a similar slope, leading to a value of activation energy of 0.1 eV for the photochemical creation of the recombination centres involved.

4. Photochemical Effects

Although the normal pattern of behaviour is observed in the infra-red luminescence spectra emitted by this sample, the associated variation in the value of z at low temperatures observed in the other samples was not seen here. Instead, the value of z showed an extremely complex behaviour. As T_r increased from 100
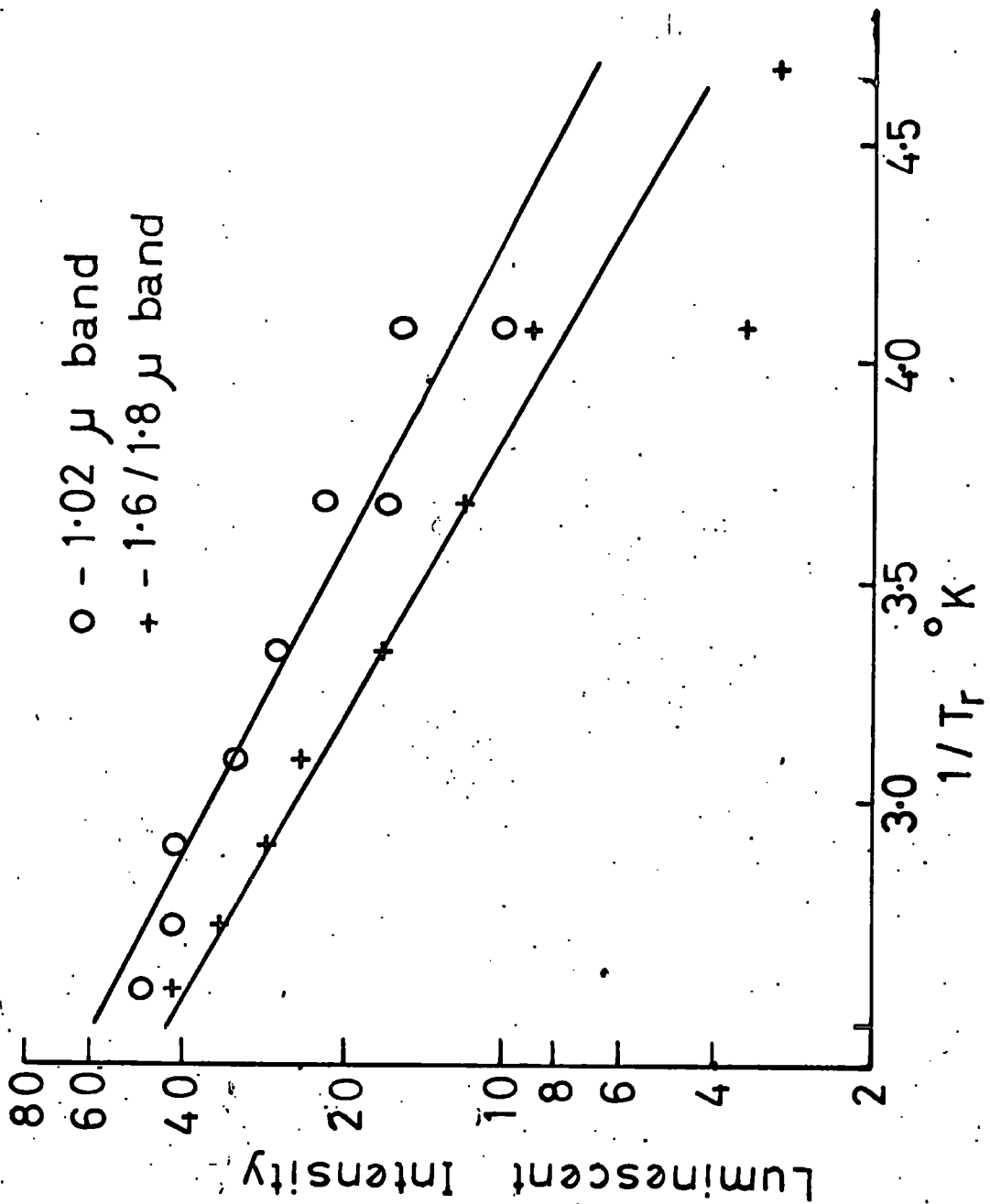
FIG. 9.6.

o - 1·02 μ band
+ - 1·6 / 1·8 μ band

Luminescent Intensity

$1 / T_r$ °K

to 185°K, the value of τ at low temperatures is seen to decrease slightly. For T_r at 217°K, τ suddenly increases by three orders of magnitude, and for T_r equal to 246°K it is seen gradually to fall again. Although the T.S.C. peaks show a complicated pattern of behaviour, it seems that only peaks 5 and 6 are involved in photochemical changes. The variations in peak height for the other maxima are due to changes in the value of electron free life time. This assumption is made because the changes in peak height of the low temperature peaks occur together, and none of the individual maxima seem to change independently. An important feature is that the photocurrent at low temperatures increased by $2\frac{1}{2}$ orders of magnitude, as the height of peak 5 increased. This provides further evidence for the postulation that the lifetime is changing by orders of magnitude.

5. Conclusions

The behaviour of the value of life time as shown by the heights of the low temperature T.S.C. peaks is difficult to explain. The gradual fall in the value of lifetime for low values of T_r (see fig. 9.3) does not seem to be associated with any changes in the trapping spectrum. For T_r around 200°K, a sudden jump

in the value of lifetime occurs which cannot be explained. As T_r is further increased the lifetime slowly falls again, but this time it is associated with the creation of the centres that cause peaks 5 and 6. It has been seen that peak 6 is caused by traps at 0.63 eV below the conduction band, that have a large capture cross-section. It could be these centres that are causing the drop in lifetime at low temperatures by acting as recombination centres.

Again in this sample, a trap at 270°K is seen. Here, however, a more accurate value of trap depth is found than that obtainable from the previous sample, and the value of 0.48 eV fits very well with the value of 0.49 eV required to explain the 1.02 micron luminescence.
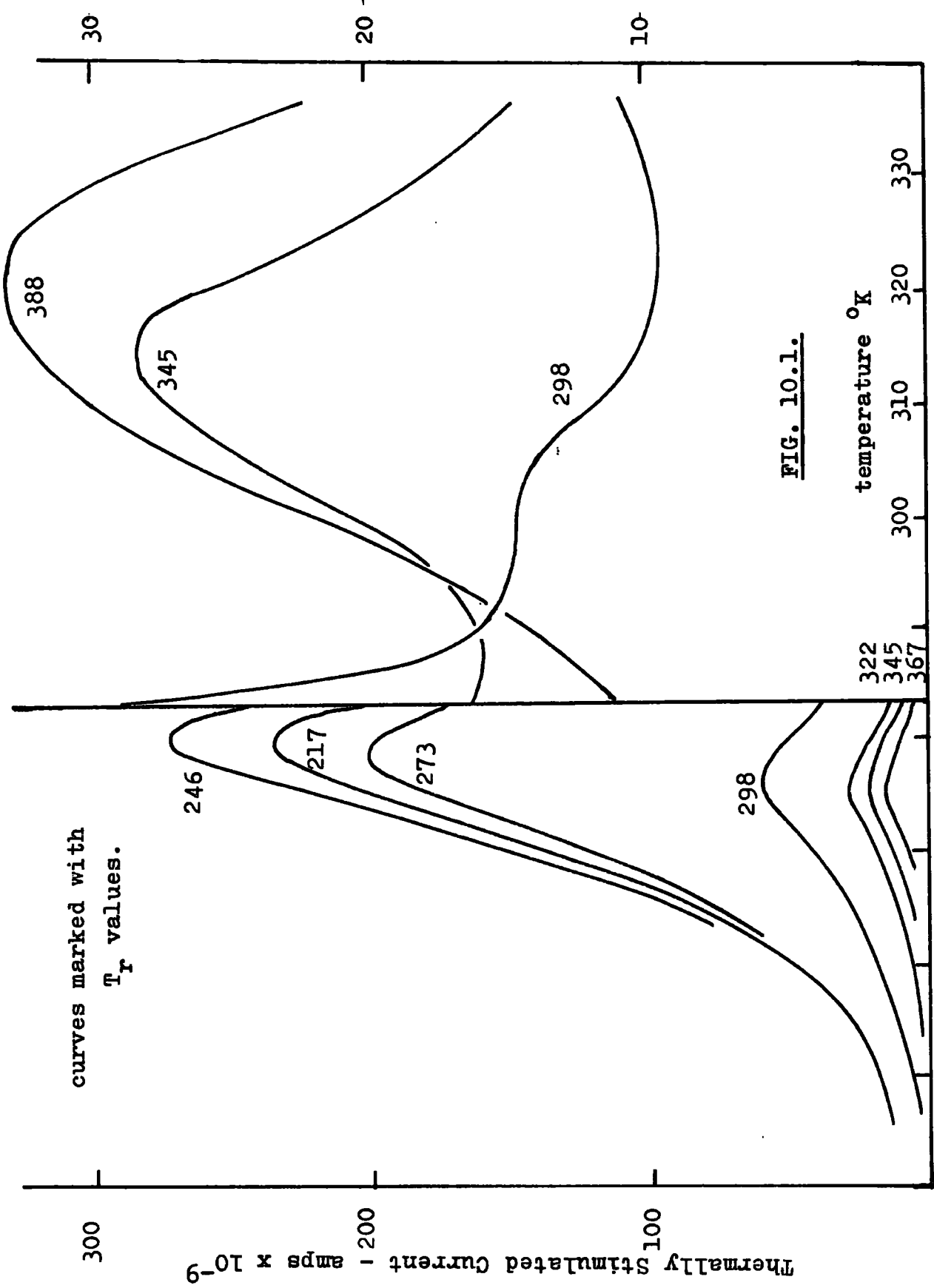
CHAPTER TEN

SULPHUR DOPED CRYSTALS II

1. Introduction

Samples from the same flow run in which the two previous crystals had been grown, were further treated under varying sulphur vapour pressures for different lengths of time. In all, crystals subjected to five different grades of treatment were used:- 1) untreated, 2) S.V.P. of sulphur at $600^{\circ}C$ (15 atmospheres) for 2 hours, 3) S.V.P. of sulphur at $650^{\circ}C$ (20 atmospheres) for 3 hours, 4) S.V.P. of sulphur $700^{\circ}C$ (27 atmospheres) for 5 hours, and 5) S.V.P. of sulphur at $700^{\circ}C$ for 24 hours. In all cases the samples were kept at the S.V.P. temperature.

2. Crystal Baked for 3 Hours under 20 ats. Sulphur

Cooling of this sample in the dark resulted in no peaks at all from the T.S.C. measurements. An essentially simila r result was obtained for values of T_r up to $185^{\circ}K$. As T_r increased further a peak at $270^{\circ}K$ began to appear which reached a maximum height for $T_r = 245^{\circ}K$. At still higher values of T_r a second peak at $330^{\circ}K$ appeared, and this showed an unusual pattern of behaviour. The T.S.C. curves for the two peaks are shown in fig. 10.1.

- 132 -

curves marked with T_r values.

FIG. 10.1.

388

345

298

246

217

273

298

322
345
367

temperature °K

Thermally Stimulated Current — amps x 10^{-9}

2.a. Peak at 330°K.

It was at first thought that two traps emptied in the temperature range 290 to 340°K because the peak was broad, and T* shifted to higher temperatures with increased temperature. Consideration of the equation for the T.S.C. curve under conditions of fast retrapping, shows that the position of the T.S.C. peak maximum depends upon the number of traps initially existing in the lattice, before any measurement is taken. The equation for the T.S.C. peak is:-

$$\sigma = \frac{N_c e^{\mu n}{}_{to}}{N_t} \exp\left[-E/kT - \frac{1}{N_t \beta \tau} \int_{T_o}^{T} N_c \exp(-E/kTdT \right]$$

<div align="right">eq. 10.1</div>

Since any change in the position of T* will involve only very small changes in N_c, this can be rewritten:-

$$\sigma = A \exp\left[-t + B\int_{t}^{to} e^{-t}/t^2 . dt \right] \qquad \text{eq. 10.2}$$

Differentiating and equating to zero gives:-

$$B = t*^2 \times e^{t*} \qquad \text{eq. 10.3}$$

$$\text{Now } B = \frac{N_c \cdot E}{N_t \beta \tau k}$$

Therefore:-

$$N_t = \frac{N_c E}{Bk} \qquad \text{eq. 10.4}$$

Thus the variations in T* could be due to changes
in the magnitude of either N_t or τ. However, since the
330°K peak increases in height as the 270°K peak falls,
it is assumed that these changes are due to variations
in N_t and not τ. Although photocurrent measurements
showed slight variations in the value of τ, they were
not sufficient to explain the shift in T*. If:-

$$N_t \propto N_{to} \, \exp(-E'/kT_r) \qquad \text{Eq. 10.5}$$

where E' is the activation energy for the creation
of these centres, then:-

$$\exp(-E'/kT_r) \propto e N_c / t*^2 . e^{t*} \beta \, \tau \qquad \text{Eq. 10.6}$$

and

$$1/T_r \propto 2 \ln t* + t* \qquad \text{Eq. 10.7}$$

The trapping level associated with the T.S.C.
curves under consideration lay at a depth of 0.63 eV
below the conduction band. Most of the measurements
that have this result came from the curve for which
$T_r = 388^\circ$K. (For lower values of T_r the curve could
not be cleaned sufficiently for its leading edge to be
obtained.) The methods used were those due to Garlick
and Gibson, Luschik, Hoogenstraaten and Bube. The
curve fitting technique was also used. The value
obtained agrees well with that obtained in chapter nine,
for a trap emptying at similar temperatures. This value

of trap depth was used to calculate the different values of t^*. A plot of $1/T_r$ against $(2 \ln t^* + t^*)$ is shown in fig. 10.2. The curve is a reasonable straight line, from which a value of $E' = 0.07$ was obtained.

There is a possibility that the differences in position of the 0.63 eV peak are due to the fact that the trap is surrounded by a potential barrier of height 0.07 eV, and so the extent to which the traps are filled depends upon T_r. However, since the height of the T.S.C. curve with its maximum at $270^\circ K$ is falling as the 0.63 eV peak rises, it is proposed that a photochemical change occurs, and that for high values of T_r, the centres causing the $270^\circ K$ peak are converted to those responsible for the 0.63 eV trap.

2.b. Peak at $270^\circ K$

The centre causing this peak was found to have a depth of 0.88 eV below the conduction band, using the heating rate methods, and the methods of Garlick and Gibson, Grossweiner and Luschik. This trapping level is the same as that causing peak 5 in the previous sample, for which no accurate value of trap depth could be given. In fig. 10.3 the experimental curve is plotted as a continuous line, and the points are from the theoretical
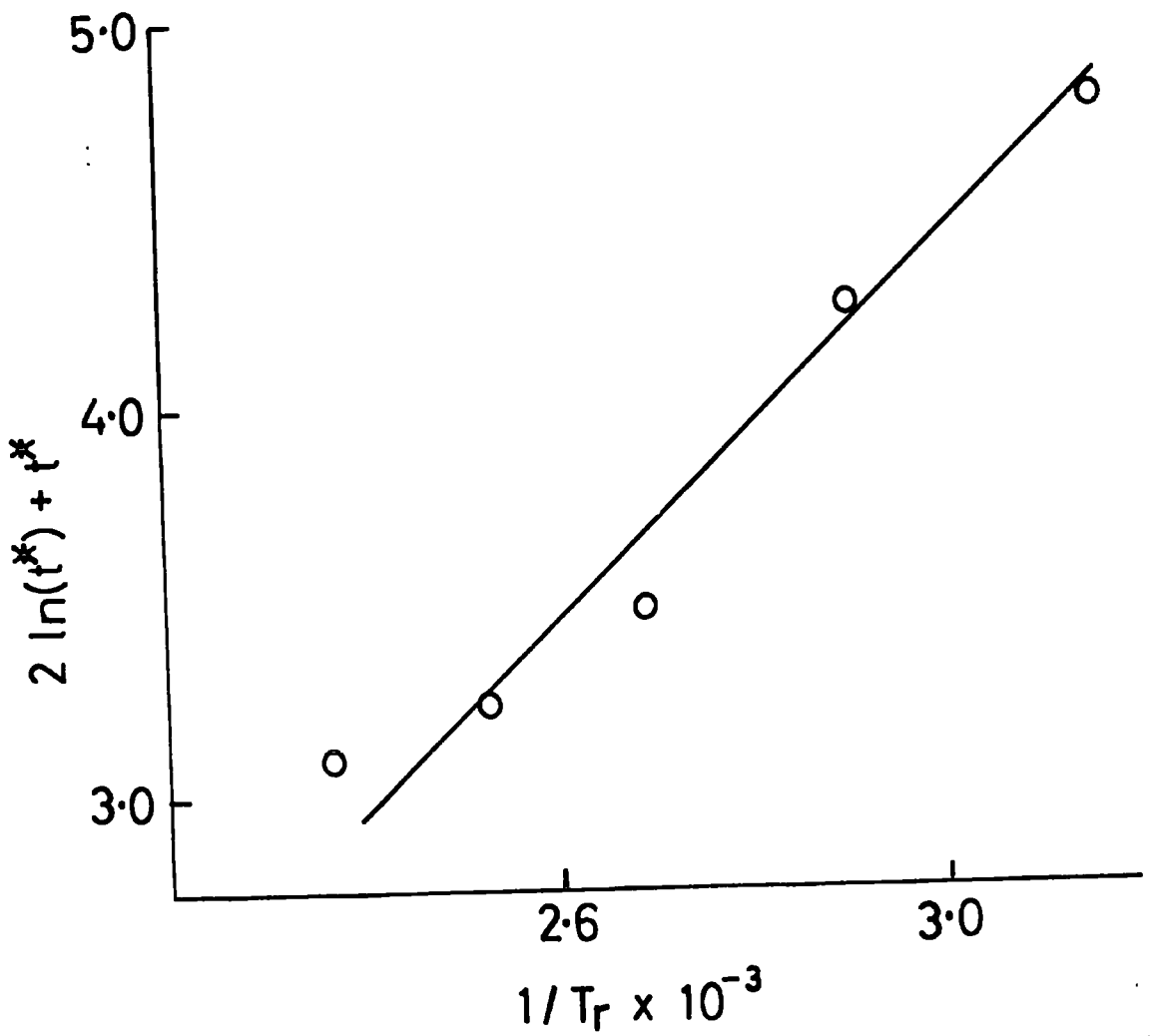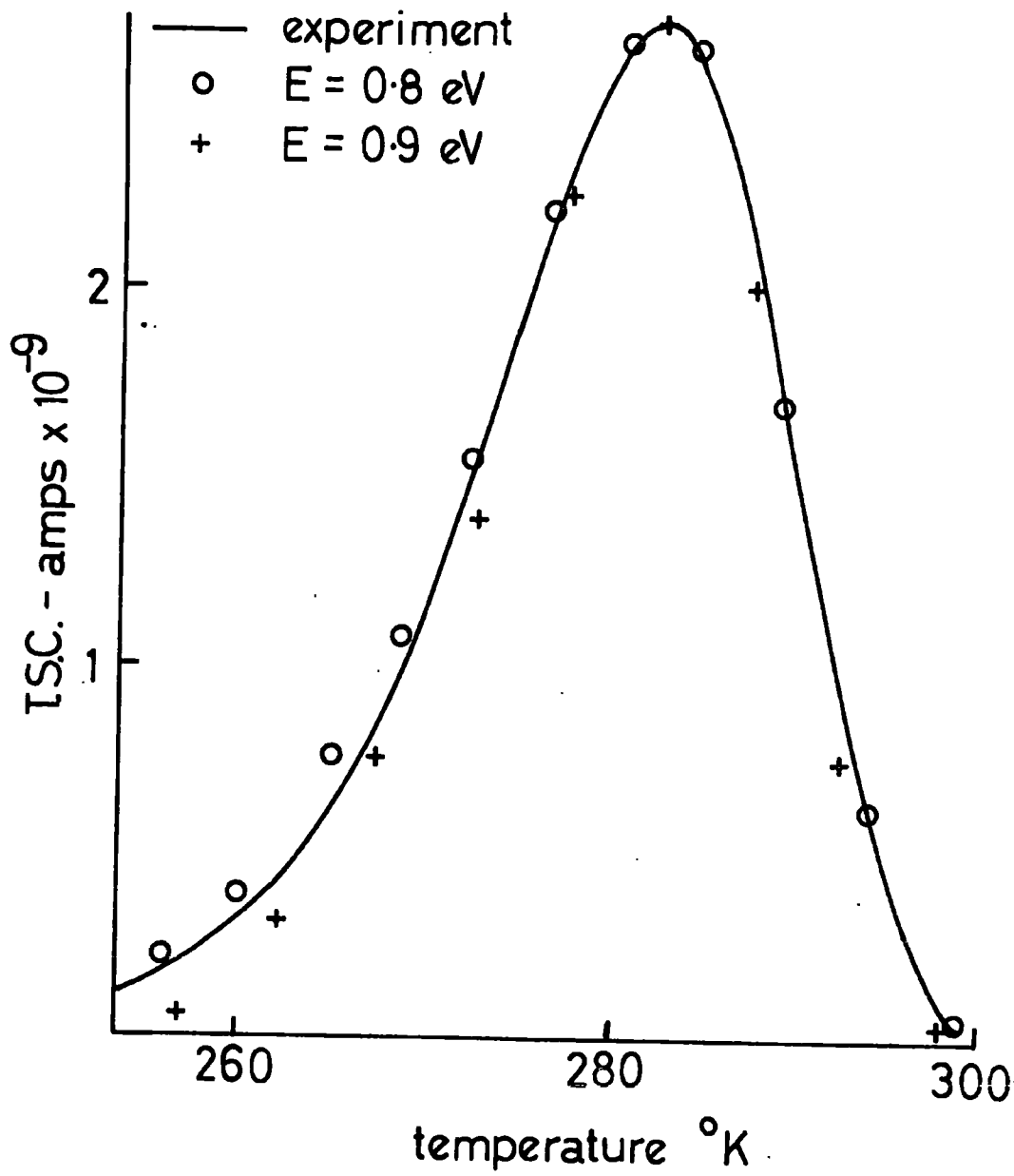
FIG. 10.2.

FIG. 10.3.

equations, using values of E = 0.8 and 0.9 eV. It can be seen that the experimental curve lies neatly between the two, so that the fit of the theoretical curves would suggest a value of E slightly lower than 0.88 eV. The trap empties under monomolecular conditions, since to obtain some sort of fit to the experimental curve from the equation of fast retrapping, would require a value of trap density of 10^{12}cm^{-3} and a value of electron . mobility of 10^5cm^2/ volt sec. which is impossibly high. The fit obtained from the monomolecular equation gives a value of $S_T = 10^{-14}$cm^2, for which value fast retrapping would be expected to occur. This must be the trap reported by Nicholas and Woods, with a depth of 0.83 eV below the conduction band. They suggested that its anomalous behaviour was due to the fact that after emptying, the trap dissociates, so that although it empties with a large cross-section, it obeys monomolecular kinetics, since it cannot capture an electron once empty. The alternative explanation proposed by Trofimenko et al., is that a potential barrier exists, surrounding the trap, so that again, once the electron has been ejected from the trap, it cannot surmount the barrier to be retrapped. This would also explain why the trap is not observed for low values of T_r, because. in this case illumination at a

high temperature is required to lift electrons over the potential barrier to fill the traps. In fig. 10.4, the logarithm of the peak height is plotted against $1/T_r$. The curve consists of two straight lines, one of positive and the other of negative slope. In this case the peak height is proportional to the density of filled centres. For high values of T_r the slope of the curve gives a value of E = 0.18 eV for the activation energy of destruction of the trapping centre. This could be the same reaction which results in the creation of the 0.63 eV trap, a process which has an activation energy of 0.09 eV, if one such centre is created from two 0.85 eV traps. Some evidence in support of this last contention is provided by the plot in fig. 10.5, where the 0.85 eV peak height is plotted against the 0.63 eV peak height. If the peak heights are proportional to the density of traps in the lattice, then it would seem to suggest that the reaction is an association of two 0.85 eV traps to form one trap at 0.63 eV deep. In fig. 10.4, the straight line of negative slope yields a value of 0.32 eV for the activation energy for the filling or creation of the 0.85 eV trap. Although it is difficult to decide between these two possibilities, it is suggested
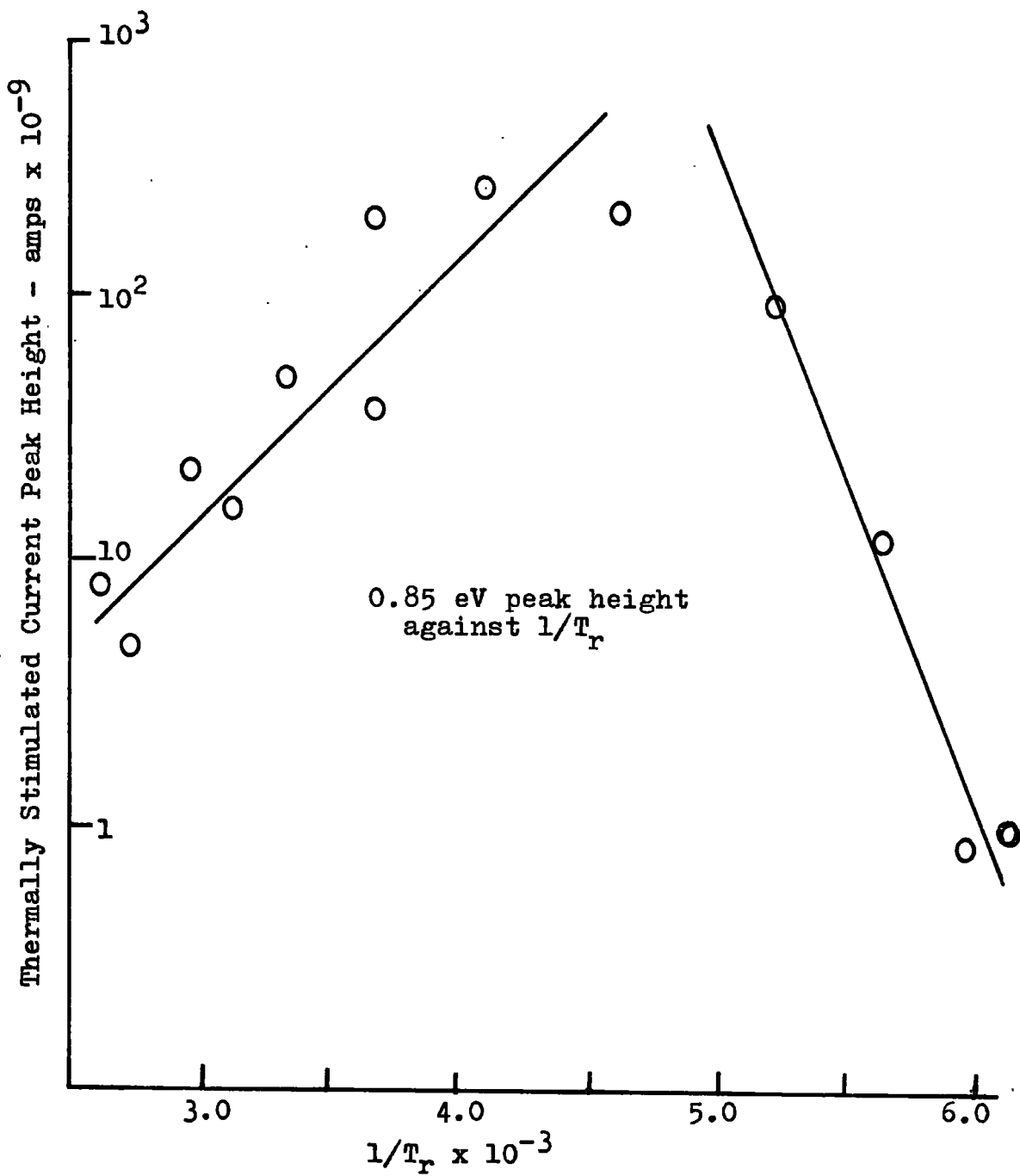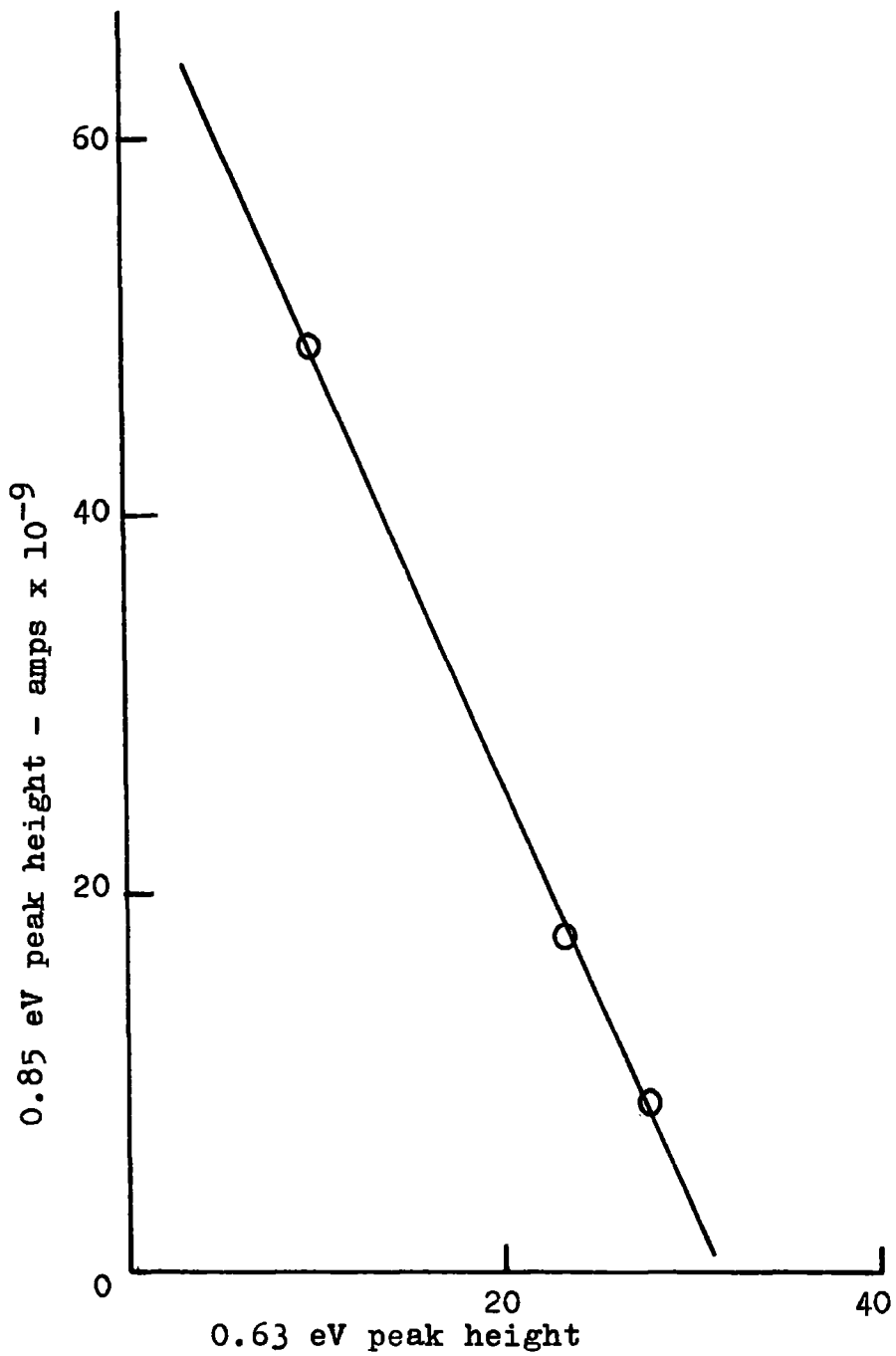
FIG. 10.4.

FIG. 10.5.

that a potential barrier surrounds this centre, rather than that it should be involved in a second type of photochemical reaction. The fact that this centre is not observed in T.S.C. measurements for low values of T_r, is probably due to the presence of a potential barrier around the trap, of height 0.32 eV.

2.c. Infra-red Luminescence

Both the bands at 1.02 and 1.6/1.8 microns were seen in this sample, although the intensity of the 1.02 micron band was less than, and the 1.6/1.8 micron band greater than the corresponding intensities for the more lightly treated samples. The behaviour of the two bands was very similar to that of the previous sample. In fig. 10.6 the maximum intensities are plotted against $1/T_r$, and values of activation energy of 0.07 and 0.08 eV were obtained from the slopes of these two curves. These are in reasonable agreement with results for the previous sample.

3. Further Sulphur Treatment

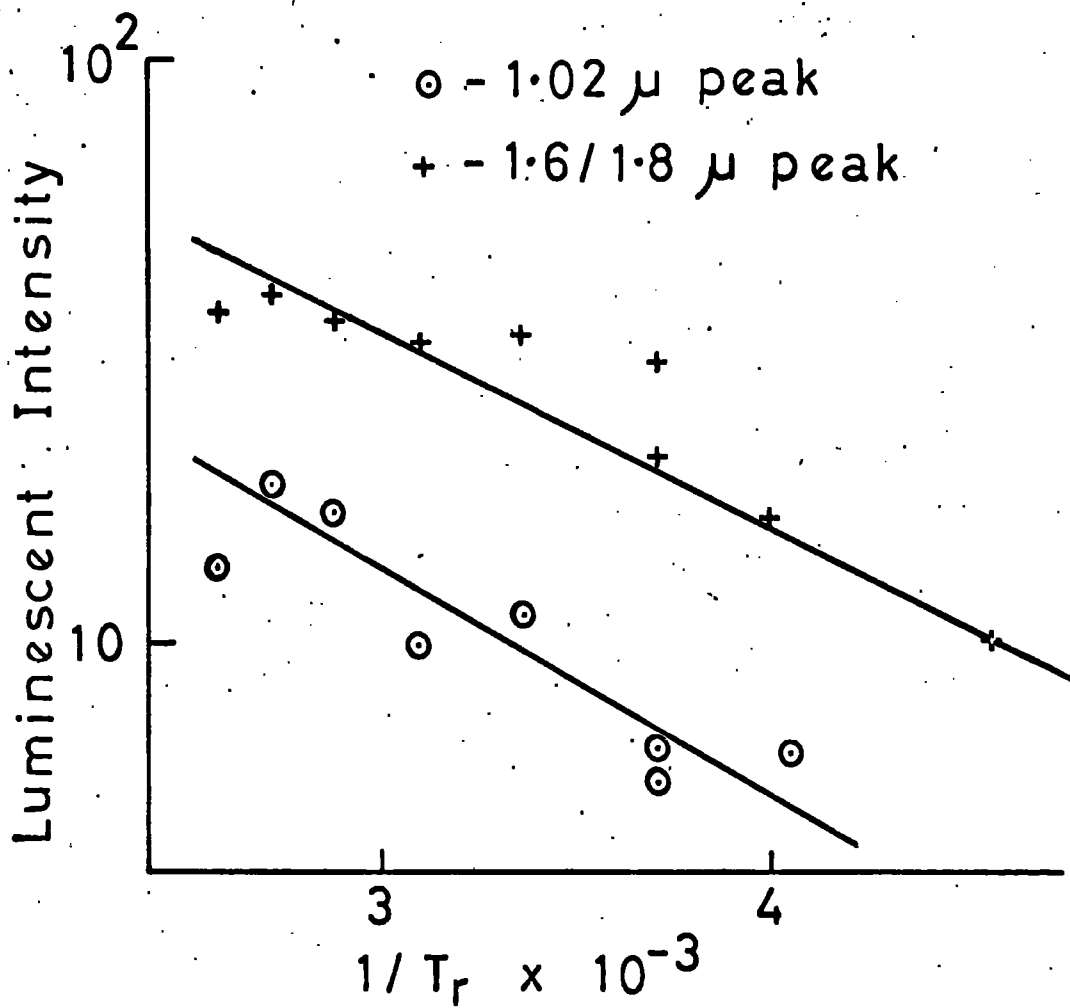The results from crystals subjected to more extensive sulphur treatment were essentially the same as those

FIG. 10. 6.

just quoted. The same two peaks occur in the T.S.C. spectra, with maxima at 280° and 330°K, and it was found that heating in increased pressures of sulphur vapour produced an increase in these peak heights. This indicates that both these centres must be associated with cadmium vacancies in some way. The potential barrier surrounding the 0.85 eV trap means that it must be negatively charged before it captures an electron. This would be the case if the centre consisted of a cadmium vacancy, or aggregate of cadmium vacancies which already contained an electron when empty. The filled trap would be effectively created by removing a Cd ion from the lattice, which would leave an entity with two negative charges. A trap at 0.63 eV is formed by the association of two of these cadmium vacancies.

The effect of sulphur treatment on the photoluminescent spectra is shown in fig. 10.7. a, b, c, d and e are the curves obtained for increasing temperature of sulphur treatment, for samples cooled in the light. It can be seen that the 1.6/1.8 micron emission increases in general up to d, and then falls again for very prolonged high temperature sulphur treatment. Because of this, it is proposed that the luminescent centre is a complex association of cadmium vacancies with sulphur
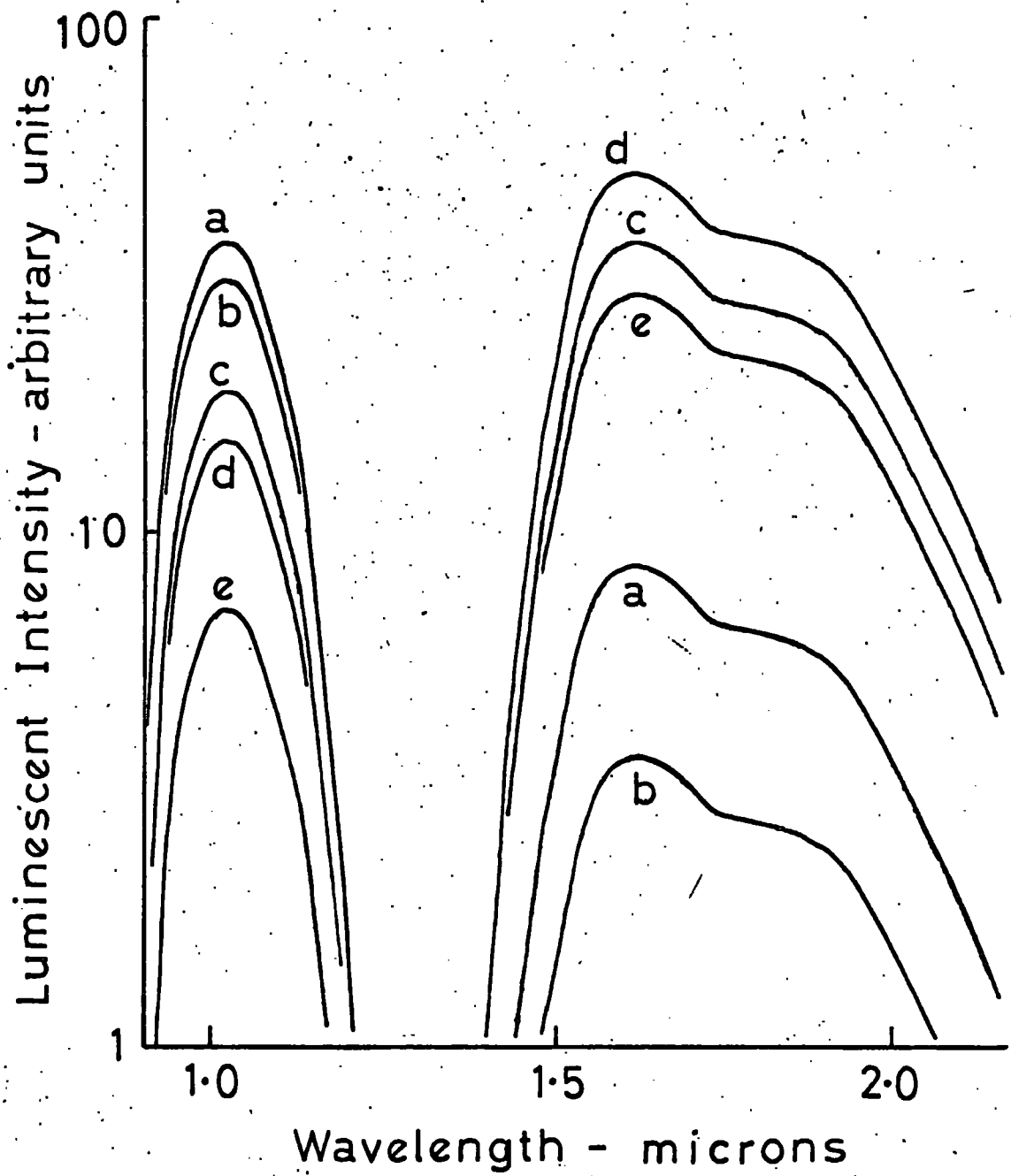
FIG. 10. 7.

vacancies. Initially the number of cadmium vacancies increases with heat treatment in increasing pressures of sulphur vapour. As a result the luminescence increases. For intense sulphur treatment, however, the number of sulphur vacancies is reduced to such an extent that insufficient of them remain to form the association that comprises this centre.

The band at 1.02 microns decreases with increased sulphur treatment. Although it is proposed that the luminescence involves the same centre as the 1.6/1.8 micron emission, this behaviour can be explained by postulating that the electron trap involved in the transition, is due to a sulphur vacancy. Increased sulphur treatment causes the number of these vacancies to decrease, with a corresponding drop in luminescence. It is suggested that the electron trap at 0.48 eV, seen in the untreated and lightly sulphur doped samples is the centre involved, because it is at the correct depth below the conduction band, and because it seems to be due to a sulphur vacancy.

4. Overshoot

When a sample is suddenly illuminated, the current through it can rise initially, reach a peak, and then fall again to a final steady value. This is the phenomenon of overshoot. The extent to which the photocurrent overshoots is determined by the temperature, and the length of time that the sample has been in the dark before illumination. This phenomenon was only observed in a single sample during the whole of this work.

The results are quoted because overshoot has been described by Mark, who concluded that it is due to photochemical adsorption (references 19 and 20, Chapter Five). No evidence for photochemical adsorption was found during this work, and it is possible that some of Mark's results could be explained in the same way as the results given here.

The crystal was a rod grown by the flow method that had subsequently been treated under a S.V.P. of sulphur at $740^{o}C$ (30 ats) for 2 hours. The T.S.C. measurements showed two peaks, at 110 and $270^{o}K$. The first was found to be at such a low temperature that no accurate determination of trap depth could be made.

The peak at 273°K gave a value of trap depth of 0.85 eV, by several of the different methods. Cooling in the light caused both peaks to appear, but for values of T_r less than 185°K, neither peak appeared. The peak at 110°K is difficult to explain, but it is suggested that the peak at 273°K is due to the same centre as that described in section 2-b, a trap at 0.85 eV, surrounded by a potential barrier.

Attempts were made to discover whether the atmosphere surrounding the sample played any part in the process, in order to test Mark's theory of photochemical adsorption; and although different curves were obtained for different atmospheres, they all show the same slope. This does not agree with the results of Mark. The differences in position of the curves (see fig. 10.9) may be due to the different atmospheres, although it is more likely that they are due to irreversible changes of some kind in the sample, caused by the prolonged baking at high temperatures that is needed in order to make measurements. The atmosphere surrounding the sample has no effect on the activation energy of the process. It is proposed that the explanation for this behaviour is that the electron trap for which a depth of 0.85 eV was determined, is

involved in the process. The phenonmenon of overshoot
can only be observed at temperatures at which the 0.85
eV can be filled. Starting in the dark, this trap is
empty at these temperatures. When the sample is
illuminated a certain photoresponse is obtained, but
as the 0.85 eV trap is surrounded by a potential barrier,
the speed at which it fills is slower than the
corresponding speed for the other traps. Thus the
photoresponse drops again as the traps gain electrons,
and remove them from the conduction band. Similarly,
the phenomenon of undershoot can be explained in the
same way, whereby this trap loses electrons more slowly
than the other centres, and so the dark current reaches
a minimum before rising again to a steady state value
when this trap is empty. Since the measurements made
determined the length of time in the dark at any
temperature which was needed for the overshoot to reach
a certain level, the activation energy obtained is the
energy for trap emptying, which is therefore the trap
depth. The sample was kept at a steady temperature,
and then illuminated. The photocurrent overshot, and
finally settled down to a steady value. The illumination
was removed and the sample left for a time t, in the dark.
Since the number of traps which empty thermally is

proportional to t, the number of traps which have to
be filled on re-illumination is also proportional to t.

If N_t is the density of the traps involved, and it
is supposed that they are all filled after the sample
has been under illumination for some time, then when
the illumination is removed at time t, the density of
filled traps n_t is changing as:-

$$- \quad \frac{dn_t}{dt} \quad = n_t \vartheta \exp(-E/kT) \qquad \text{Eq. 10.8}$$

Therefore:-

$$\log n_t = - \vartheta \exp(-E/kT)t \quad + C \qquad \text{Eq. 10.9}$$

but, $n_t = N_t$ at t = 0, therefore:-

$$\log \frac{n_t}{N_t} = \quad - \vartheta \exp(-E/kT)t \qquad \text{Eq. 10.10}$$

The density of empty traps n_e can be obtained from
this:-

$$n_e = N_t \left[1 - \exp(- \vartheta \exp(-E/kT)t \right] \qquad \text{Eq. 10.11}$$

At each temperature a value of t was determined,
such that the overshoot of the photoconductivity reached
a value twice as high as the final steady state value.
See fig. 10.8. At higher temperatures, traps will
empty faster, and so t will be shorter. The result of
this method of measurement is that the value of n_e is
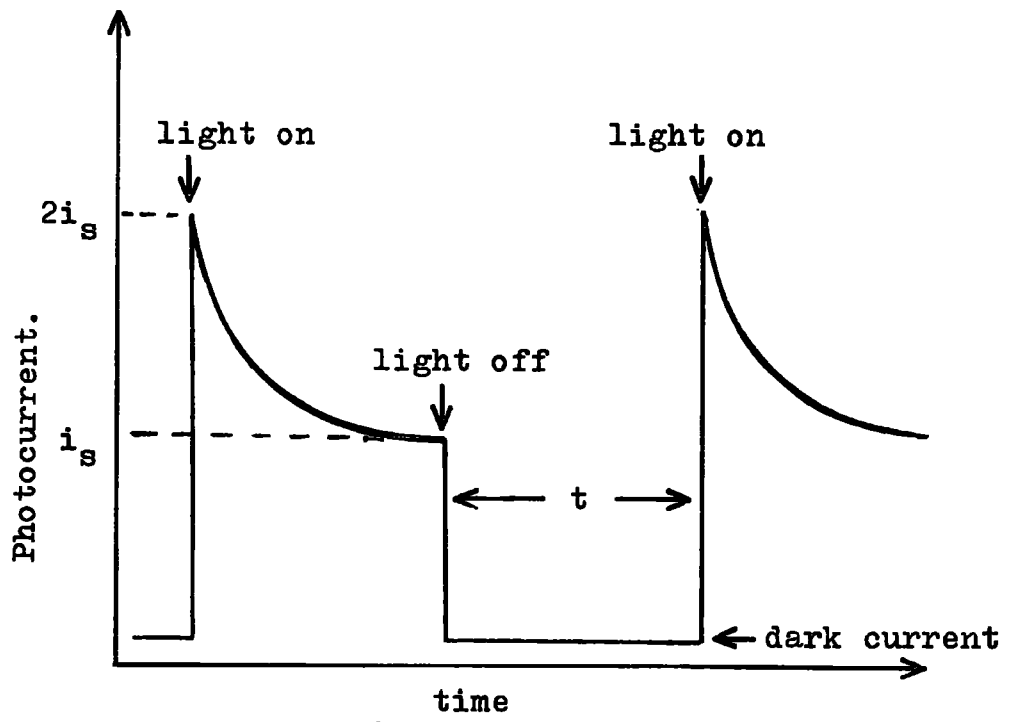being kept effectively constant. Therefore, from

FIG. 10.8.

Eq. 10.11:-

$$\left[\nu \exp(-E/kT)t \right] \quad \text{must be a constant, and}$$

therefore:-

$$t \propto \exp(E/kT) \qquad\qquad \text{Eq. 10.12}$$

A plot of $\log(t)$ against $1/T$, has a positive slope, from which a value of the trap depth can be obtained. The four curves in fig. 10.9 all yield a value of trap depth of 0.82 eV. The two determinations of trap depth for this centre agree very well, and provide good evidence for the correctness of the explanation of overshoot. If undershoot had been measured, it is suggested that the activation energy obtained would have been the barrier height, i.e. 0.35 eV. Unfortunately, the sample had such a high resistance, that the measuring equipment could not determine the value of dark current, and so no undershoot measurements could be made.

FIG. 10.9.

time t - in seconds

1/T °K x 10⁻³

O — air
● — backing pump
+ — diffusion pump
X — argon
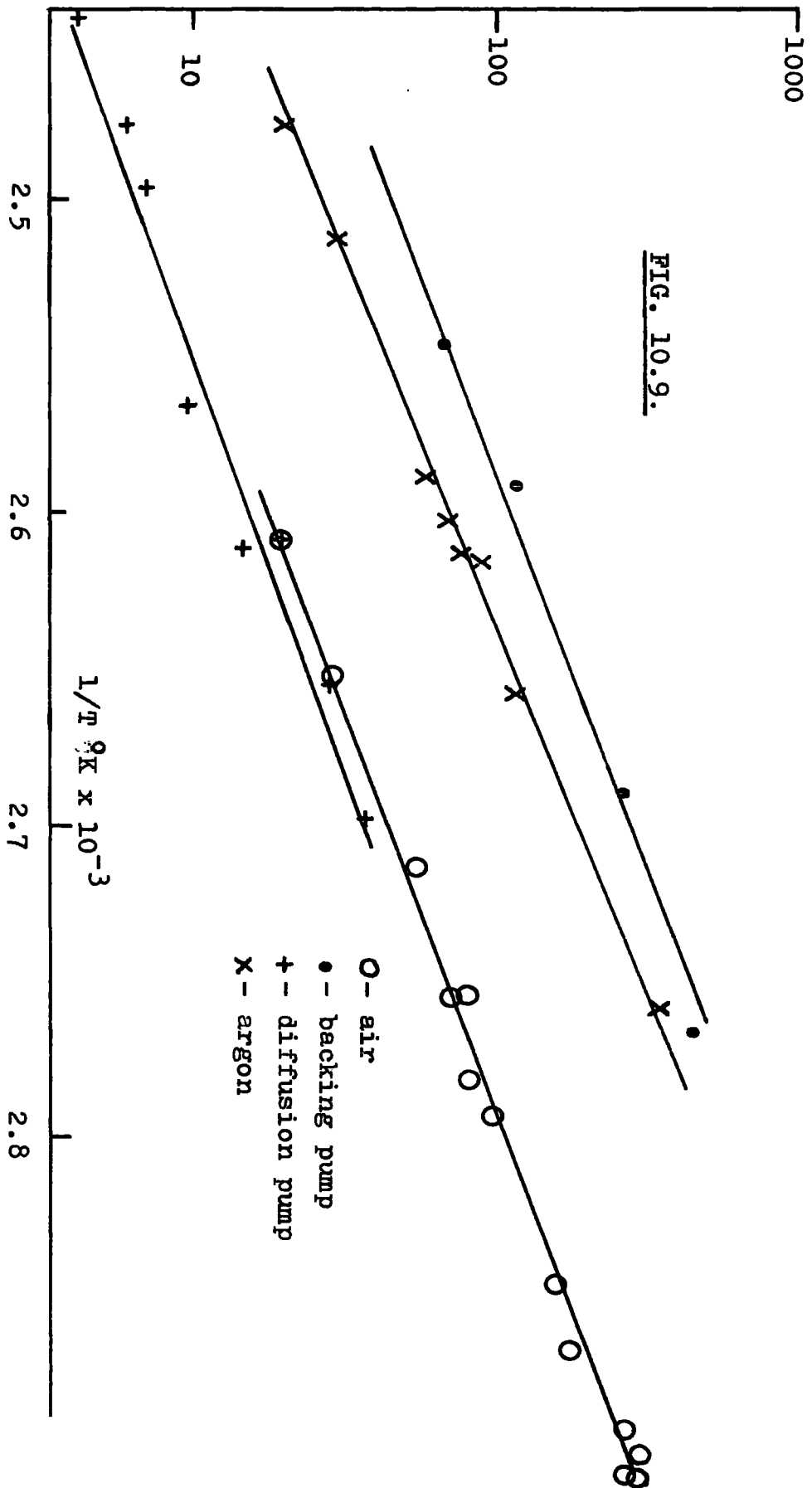
CHAPTER ELEVEN

DISCUSSION

1. Introduction

The conclusions that can be drawn from this work are basically twofold. The use of the technique of curve fitting has helped to provide more accurate values of trap depth, and it has also helped to show up and to explain some of the shortcomings of the other standard methods of T.S.C. curve analysis. The second result of this work has been an explanation of the extremely complicated patterns that can occur in measurements of T.S.C. and luminescence in cadmium sulphide.

2. The Curve Fitting Technique

The basic advantage of this method of curve fitting is that it allows determination of more accurate values of trap depth. It is virtually an extension of the method of Garlick and Gibson, one of the most reliable standard methods. The modified equations for the curves, eqs. 7.3 and 9.2, can both be simplified to give :-

$$\sigma = A \exp(-E/kT)$$

for the leading edges. This is the equation of Garlick and Gibson. The curve fitting technique extends this

equation to allow use to be made of the whole curve.
Most of the other methods are less accurate than that
of Garlick and Gibson because they rely upon measurements
from only one or two points on the curve. Because it
uses all the experimental points on a curve, the method
also gives more accurate values of trap densities and
capture cross-sections. The main inaccuracy in the
method lies in the approximation made in the series,
eq. 7.2.a, to obtain a usable value of the integral
inside the exponential term. This inaccuracy can easily
be overcome, however, by taking an extra term or two in
the series, without greatly complicating the mathematics.

The method helped to explain the anomalously high
values of trap depth found for some of the low
temperature traps. It showed that insufficiently low
starting temperature would not affect the form of the
curve, and would only give erroneous values of trap
density. The explanation for these odd results is most
probably the non-linear heating rates at temperatures
just above the starting point. By assuming a variation
of heating rate, β proportional to $(T - T_o)$, it was
found possible to obtain an extremely good fit to the
curve. This was, in fact, useless for measurement
purposes, because no value of the constant of

proportionality in the above assumption could be found, and there is, of course, only empirical reasoning to support the possibility of this kind of behaviour. It did show, however, that this kind of mechanism is the most likely to be the reason for the anomalous curves.

Another cause of inaccuracy could be the assumption that the trap capture cross-section S_T, is proportional to T^{-2}. To test this, values of S_T proportional to T^{-1} and T^{-3} were tried for several curves. The differences between the two curves were so slight that they could not be seen on a graph. This showed that over the range of a single peak, any changes in S_T are unimportant compared with changes that occur in $\exp(-E/kT)$.

A trap at a depth of around 0.3 eV has been reported by several workers, whilst others have found no trace of its existence. The application of the technique of curve fitting has not proved that it does not exist, but it has shown how values of 0.3 eV can be obtained for trap depth, when in fact, such a trap does not exist. The method allowed two closely overlapping peaks to be analysed, because the leading edge of one and the falling side of the other could be seen. A check could be obtained on the results, because addition of the two theoretical curves allowed comparison with the experimental curve.

The method of curve fitting showed that the 0.85 eV trap must empty under monomolecular conditions, although it has a large capture cross-section, around $10^{-14} cm^2$. The theoretical curve for the fast retrapping case could be made to fit the curve, but it would have required a very small value of N_t, of about $10^{12} cm^{-3}$, as defined by the constant B. Since N_t is also involved in the constant A, it would also have required a value of mobility ludicrously high to obtain a fit. The value of 0.85 eV was obtained for trap depth, because this method of anlysis takes into account the shape of the curve, as well as the position of the maximum. Methods which do not do this, such as that due to Bube, give values around 0.5 eV for this trap.

A trap at around 0.63 eV has been reported by many workers. Its position in the temperature scale has varied enormously from author to author, and sometimes from sample to sample for the same author. Values of T^* for this peak have ranged from 300 to $400^{o}K$. This has sometimes led to confusion, since it was not known for sure whether two sets of results could refer to the same centre or not. For the monomolecular case the value of T^* depends only upon

the heating rate for a given type of centre. For the
fast retrapping case, the position of the maximum
also depends upon trap density. It has been shown
here how the differences in trap density can cause
large differences in the value of T*, and how it is
possible for one type of centre to empty at such a
range of different temperatures. A factor of 2 in
the trap density has been shown to cause a change
in the value of T* of 20°K.

Use of the above methods, and a selection of the
other methods outlined in chapter three, has given
trap depths of $<$ 0.2, 0.18, 0.21 eV and a double
trap at 0.39 and 0.42 eV for the boule crystal. The
flow crystals showed a number of low temperature
peaks that could not be analysed, and peaks at 290
and 330°K. These gave trap depths of 0.51 and 0.62
eV. Lightly sulphur doped samples showed T.S.C.
maxima that yielded trap depths of 0.48 and 0.62 eV,
as well as a range of peaks at low temperatures and
a maximum at 270°K for which a trap depth could not
be obtained. Increased intensity of sulphur doping
caused all the T.S.C. peaks to disappear except for
the 0.62 eV trap, and the peak at 290°K, that was
found to be due to a trap at a depth of 0.85 eV.

3. Photochemical Effects

The infra-red luminescence measurements have shown peaks at 1.02 microns and a double peak at 1.6 and 1.8 microns. A further peak at 0.78 is often seen in CdS, but the equipment used here could not detect it, because its sensitivity fell off very rapidly below 1 micron. A stated in chapter four, Bryant and Cox have shown that the 1.02 micron emission is due to an electron transition from a trap at 0.5 eV below the conduction band, to a recombination centre 0.7 eV above the valence band. The 1.6/1.8 micron emission is due to transitions from this recombination centre to the various valence bands. A trap at 0.48 eV below the conduction band was found in untreated and lightly doped samples. It was not found in the more heavily sulphur doped crystals. Since the 1.02 micron emission was also only seen in the untreated and lightly doped samples, it is suggested that this T.S.C. peak is caused by the same centre as that involved in the 1.02 micron emission. It also seems probable that sulphur vacancies are involved in this centre. The 1.6/1.8 micron emission increased in intensity with increased sulphur doping, except for extreme treatment, when the

intensity fell again. This suggests that the centres are basically composed of one or more cadmium vacancies, but that these are in some way associated with sulphur vacancies, to account for the falling-off in intensity for extreme sulphur treatment. These centres must be near to sulphur vacancies in order to account for the 1.02 micron emission arising from the transition from sulphur vacancies to these centres.

Throughout the results there has been correlation between the behaviour of the 1.6/1.8 micron emission and that of the sensitising recombination centres and reasonable agreement has been found between the values of energy of creation obtained for the two centres. Although these sensitising centres have not been accurately located in cadmium sulphide, Bube has suggested that they lie between 0.7 and 1.0 eV above the valence band. It is proposed that the infra-red emission and the sensitising effect are due to the same centre, and as stated before, this is composed of a cadmium vacancy associated with a sulphur vacancy.

It is suggested that the boule crystals are cadmium rich, since they showed no signs of the 0.62 and 0.84 eV traps that were found in sulphur rich crystals. They are in some way essentially different from the flow

crystals, because, although cadmium rich, they showed
no trace of the 0.48 eV trap and the associated 1.02
micron luminescence. It is not known what this
difference is.

Results from the flow crystal, Chapters 8, 9 and
10, suggest that the 0.62 eV trap can be created from
the sensitising or emission centres, and sulphur doped
crystals have shown that it can be formed from the 0.84
eV trap. The agreement between the values of activation
energy are strong evidence for the contention that the
luminescent and sensitising centres are identical. The
suggested distribution of centres to explain the
results is shown in fig. 11.1. The 0.62 eV centre is
an association of two cadmium vacancies, that dissociate
under illumination above 270°K (see fig. 10.1) to form
two 0.84 eV traps. The 0.84 eV centre is also
surrounded by a potential barrier 0.3 eV high, that
does not allow it to be filled below 200°K. This
potential barrier is also supposed to be the reason for
the phenomenon of overshoot that is sometimes observed,
since good agreement is obtained between the trap
depths calculated from T.S.C. date and overshoot
measurements. The potential barrier could be due to
the cadmium vacancy already having one electron attached

conduction band

0·35 eV

0·84 eV

Cd vac.

—0·62 eV

2Cd vac.

—0·18eV —0·21eV —0·39eV
0·42eV

—0·48eV

1·02μ emission
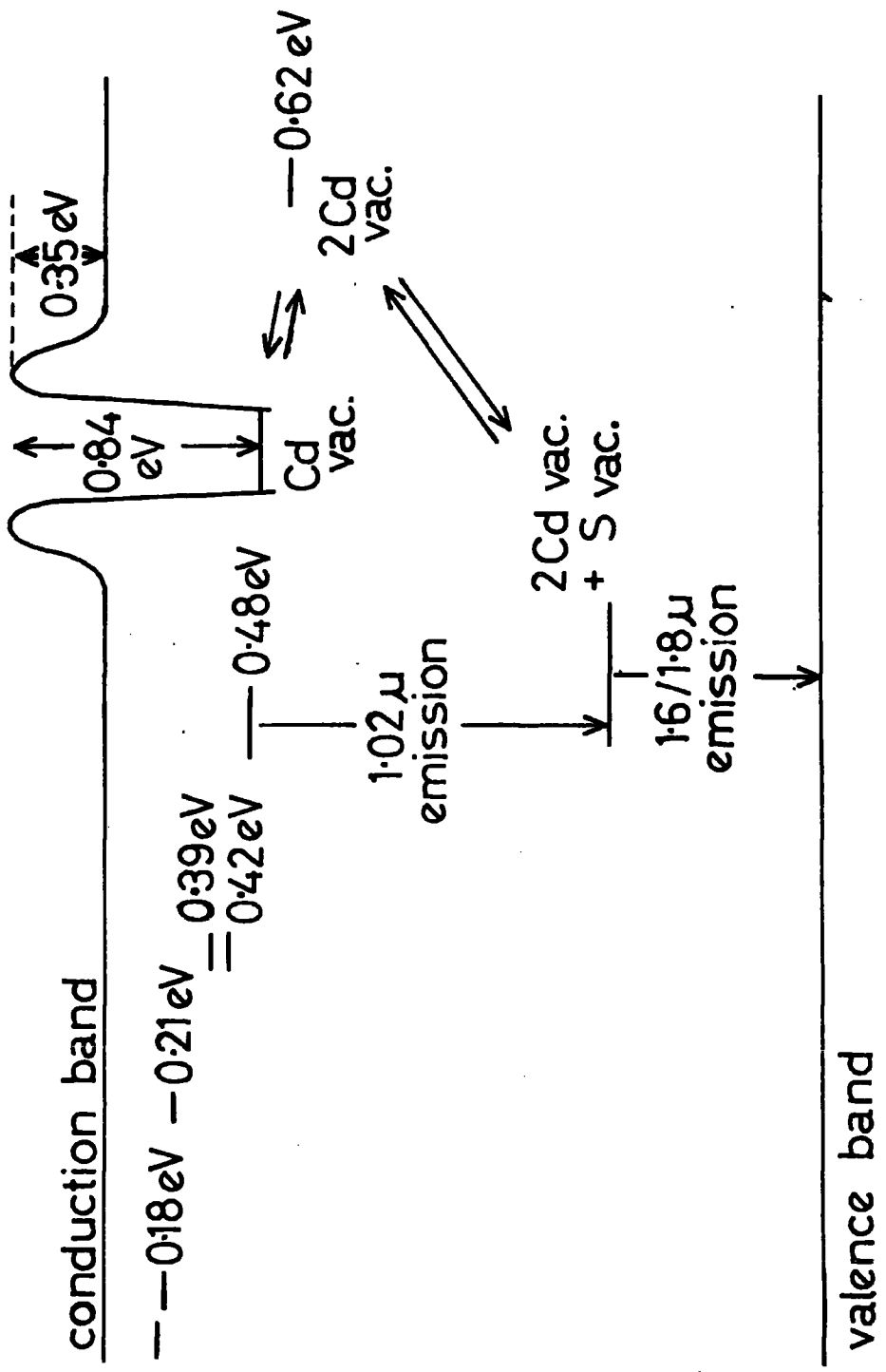
2Cd vac. + S vac.

1·6/1·8μ emission

valence band

FIG. 11.1.

to it and the 0.84 eV trap arises from its ability
to trap a second electron.

A diagram of the suggested forbidden gap is shown
in fig. 11.1. A series of shallow traps exist for
which depths of 0.18, 0.21, 0.39 and 0.42 eV have
been determined. These are supposed to be due to
sulphur vacancies since they are only found in cadmium
rich samples. The centres do not take part in
photochemical reations. A trap at 0.48 eV below the
conduction band is found, which is again due to a
sulphur vacancy. This is the top level from which the
1.02 micron emission arises. These centres must be
near to the 1.6/1.8 micron emission centres for the
1.02 micron emission to occur, and it is found that
associations between cadmium and sulphur vacancies
occur to form centres giving the 1.6/1.8 micron emission.
This association does not affect the ability of the
sulphur vacancy to act as a 0.48 eV trap. The 1.6/1.8
micron emission band and the sensitising centres are
identical, and consist of two cadmium vacancies
associated with a sulphur vacancy. It exists 0.7 eV
above the valence band, which is the correct level for
the infra-red luminescence and also agrees with the
position of the sensitising centres suggested by Bube.
(Reference 3, Chapter 5.). The two cadmium vacancies

are dissociated from the sulphur by baking in the dark, and these give the trap at 0.62 eV. The process can be reversed by illuminating at high temperature. Both processes have an activation energy somewhere in the range 0.1 to 0.3 eV. In extreme cases of sulphur doping, where insufficient sulphur vacancies exist for the many sensitising centres to occur, illumination at high temperatures can cause the 0.62 eV trap to dissociate even further to form the 0.84 eV trap. This consists of a single cadmium vacancy, and thus two such centres are formed from one 0.62 eV trap. The 0.84 eV trap is surrounded by a potential barrier of height 0.35 eV. With all these possibilities of photochemical reaction, and the existence of potential barriers surrounding centres, it is not surprising that very complicated and semmingly meaningless results can be obtained from T.S.C. and infra-red luminescent measurements. It has been shown here, however, how some sense can be obtained from such results, if one appreciates the various reactions that can occur.

4. Future Work

More accurate values of activation energy for the photochemical effects could be obtained, if a cryostat

were built that could be cooled and kept at any T_r for a known length of time, rather than, as at present, cooling through a value of T_r.

The infra-red emission at 0.78 microns is obviously of importance, since it is supposed to be due to electron transitions from the conduction band to the same centre that causes the 1.6/1.8 micron emission. This could give further information on the behaviour of this centre and also help to confirm the results obtained so far.

One strange aspect of this work is that the boule crystal, which is supposed to be cadmium rich, does not show any electron trap at 0.48 eV, and does not emit at 1.02 microns. This may be due to a basic difference between boule and flow crystals. This is worth investigating further since high resistivity boule crystals are becoming more readily available.

Although no evidence was found here of the effect of ambient atmosphere on the results, it has been suggested that many of the traps could be due to surface states rather than bulk defects. It would be useful to extend the work to ultra high vacuum in order to check on this possibility.

Useful work could be done in correlating T.S.C. measurements with electron spin resonance studies. Preliminary studies by other workers have found broad bands that suggest the existence of cadmium vacancy complexes at 0.7 eV above the valence band. If confirmed, these would be further support for the results given here.